THE THERMAL REGIME OF MACKENZIE DELTA LAKES AND CHANNELS

Timothy Peter Ensom

A thesis submitted to the
Faculty of Graduate Studies and Research
in partial fulfillment of the
requirements for the degree of

Master of Science

in

Physical Geography

Carleton University
Ottawa, Ontario

Your file Votre référence
ISBN: 978-0-494-79603-0
Our file Notre référence
ISBN: 978-0-494-79603-0

ABSTRACT

Thirteen channels and 17 lakes distributed throughout the Mackenzie Delta were instrumented with data loggers to determine mean annual basal water temperature (MAWT) for the period June 2009–June 2010. Average MAWTs for perched lakes, channels, and connected lakes were 5.5°C, 4.6°C, and 3.4°C respectively. Spatial variability of MAWT in the delta was less than 4.0°C. Perched lake MAWT was greater in the forest than in the tundra, while connected lake and channel MAWT were consistent across treeline. Distinct thermal regimes were observed for perched and connected lakes. The width distribution of Mackenzie Delta lakes and channels was determined using a geographic information system. MAWT and mean annual ground temperature for the delta were used in steady-state thermal models to determine critical lake and channel width for through talik occurrence. It is estimated that 60% of delta lakes and nearly the entire channel network maintain taliks through permafrost.

ACKNOWLEDGEMENTS

This thesis has benefited enormously from decades of exceptional field science conducted in the Mackenzie Delta region, and from the wisdom of northerners who know it intimately. I am grateful to my supervisor Dr. Chris Burn – Carleton University NSERC Northern Research Chair – for the confidence he has shown in me and the extensive academic and financial support he has extended to me. I have been fortunate to hold an NSERC Northern Research Internship with Indian and Northern Affairs Canada (INAC) in Yellowknife, and receive the support of Dr. Steve Kokelj and colleagues.

I would like to acknowledge the generous support of the INAC Northern Scientific Training Program and Carleton University's Naida Waite Scholarship, Michal Hare Fellowship, and Graduate Travel and Research Bursary. The Aurora Research Institute's Inuvik Research Centre provided invaluable field support and introduced me to many Canadian researchers involved in a breadth of fascinating research projects.

The Mackenzie Delta is vast, dynamic, and intricate. My research assistants Graham Gilbert and Andrew Thoms were a source of reason, vigilance, and good humour for each of the 8,000 kilometres we logged by motorboat. I am also grateful to Dr. Sean Carey, Peter Morse, Kumari Karunaratne, Pascale Roy-Leveille, Dr. Sharon Smith, Dr. Derek Mueller, Stephen Dunbar, Stefan Goodman, Douglas Esagok, Leonard Joe, Mike Palmer, Julian Kanigan, Stan Yee, Dr. John Stone, Trevor Porter, Natalie Pressburger, Elsie Clement, Peter Cott, Larry Greenland, Michelle Cote, Richard Webster, Tom Carter, William Hurst, Don Ross, and the Aklavik Hunters and Trappers Committee. Maps herein are based on those by Christine Earl.

I am so fortunate for the support of my family and Sophie Desaulniers.

TABLE OF CONTENTS

LIST OF TABLES

LIST OF FIGURES

LIST OF APPENDICES

CHAPTER 1: INTRODUCTION

1.1 Introduction

The purpose of this research is to understand the thermal regime of lakes and channels in the Mackenzie Delta, Northwest Territories (NWT). The thermal regime of water bodies is an important control on ground temperature and hence permafrost configuration (Brown et al., 1964). In the Mackenzie Delta, thousands of lakes and an intricate channel network maintain taliks which may penetrate permafrost (Mackay, 1963; Smith, 1976). Given the renewed interest in hydrocarbon resource development in the delta, an understanding of permafrost configuration around delta channels and lakes is essential for the development of linear infrastructure, particularly pipelines, in the region. Using delta channel and lake-bottom temperatures recorded from June 2009 through June 2010, this thesis presents the mean annual basal water temperature (MAWT) and spatial variability in thermal regime of delta water bodies. MAWTs are used to predict the pervasiveness of through taliks in the delta.

1.2 The Mackenzie Delta

The Mackenzie Delta, over 13,000 km^2 in area (Fig. 1.1), is the second largest delta in the Arctic after the Lena Delta in Siberia. It is a postglacial feature, into which sediment from the Mackenzie and Peel River basins is deposited, and contains over 49,000 lakes and a complex network of channels (Emmerton et al., 2007). These water bodies, which cover 40% of the delta surface and have mean annual basal temperatures above 0°C, alter the configuration of permafrost from what would be expected at this latitude. The

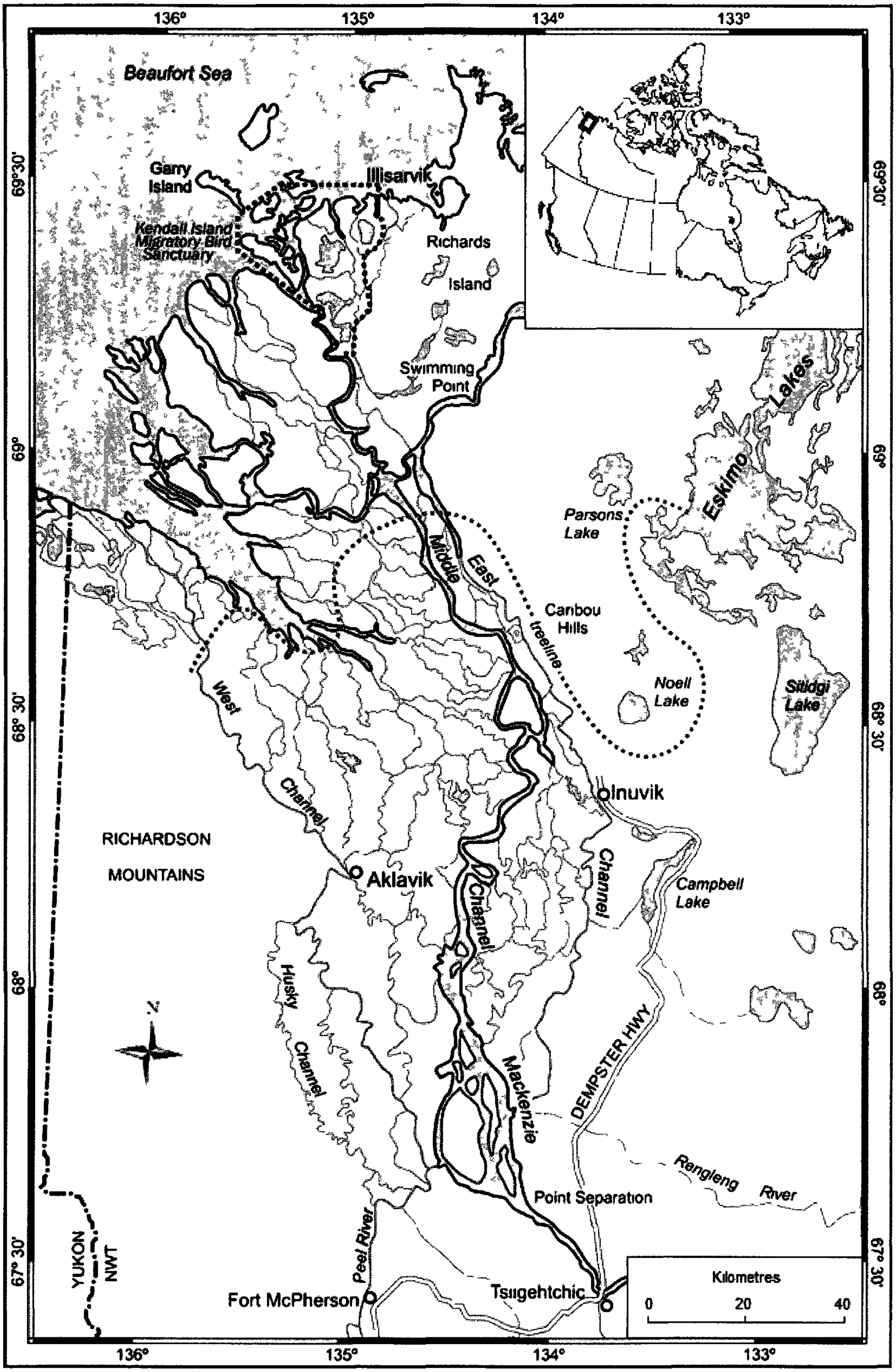

Figure 1.1. The Mackenzie Delta, NWT. The location is shown on the inset map. Adapted from Burn and Kokelj (2009, Fig. 1).

delta is bordered by the Richardson Mountains to the west and rolling uplands to the east. Two distinct ecological regions – taiga forest and tundra – exist in the delta and are delineated by treeline as shown in Fig. 1.1. The delta is an ecologically sensitive environment because nutrient supply to the floodplain is dependant on flooding hydrology (Lesack et al., 1998). As a productive Arctic aquatic ecosystem, the delta provides habitat for numerous fish, mammals, and migratory birds (Squires et al., 2009).

1.3 Thermal Regimes of Northern Lakes and Rivers

There is limited information available on the thermal characteristics of northern water bodies. Arctic lakes have an annual temperature cycle whose general form is illustrated in Fig. 1.2. Water at the margins of lakes may freeze to the bottom. Lakes in the Mackenzie Delta typically do not freeze to the bottom, and maximum ice thickness is generally 0.6–1.5 m (Marsh, 1998). Water temperature data for rivers and channels of the delta region are quite limited. The closest Canadian site for which data are available is the Stewart River near Mayo, Yukon. The thermal regime of the Stewart River is shown in Fig. 1.3. Water temperature falls to 0°C in the winter, yet the water remains unfrozen due to turbulence. Channels in the Mackenzie Delta generally have ice cover between mid-October and early June, and shallow channels may freeze to the bottom (Burn and Kokelj, 2009).

1.4 Ground Thermal Regime

The influence of surface water on underlying ground temperatures in permafrost environments has been described by several researchers (Mackay, 1963; Smith, 1976;

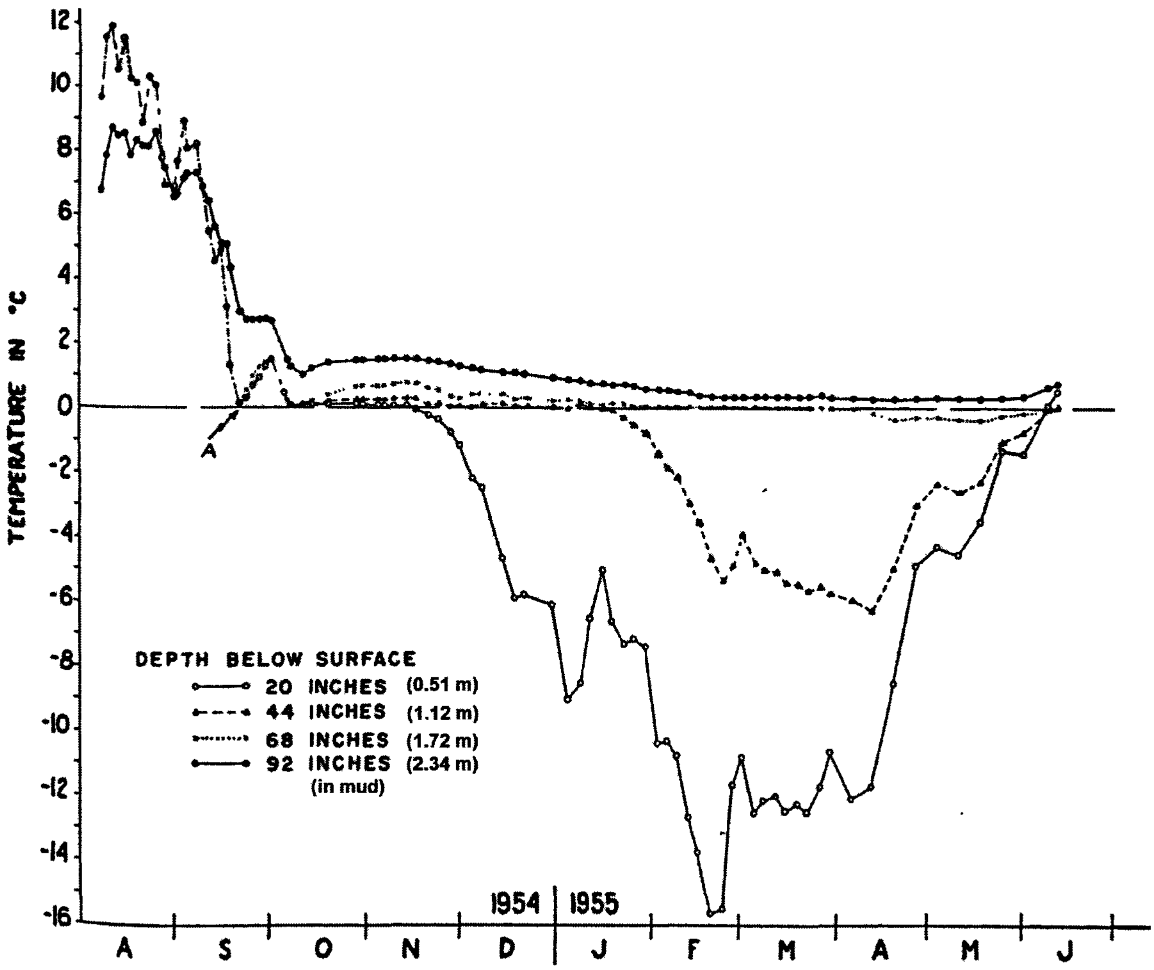

Figure 1.2. Annual temperature cycle for Imikpuk Lake near Barrow, Alaska. Source: Brewer (1958, Fig. 6).

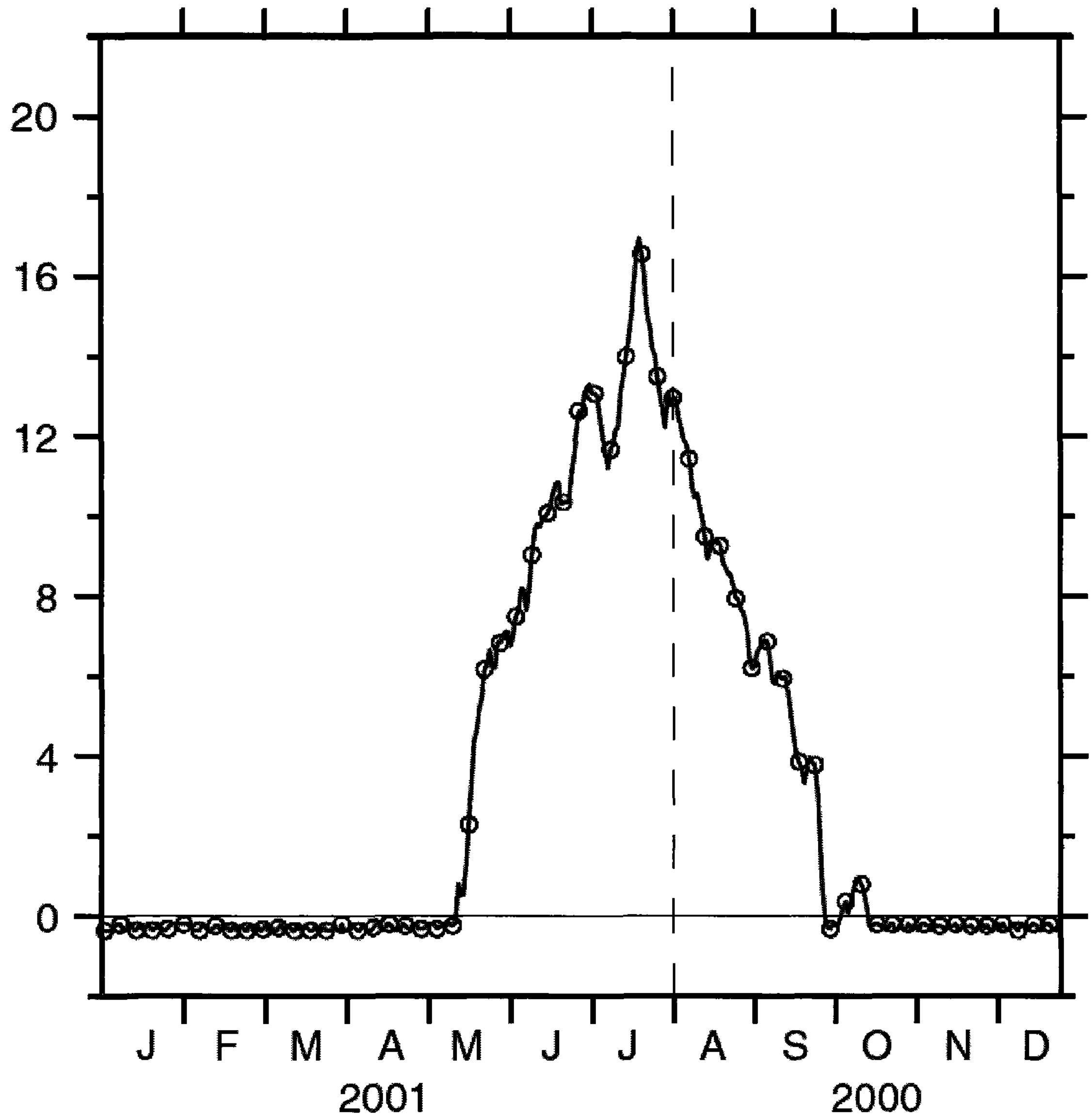

Figure 1.3. Annual temperature cycle (°C) of Stewart River at Mayo, YT, 1 August 2000–31 July 2001. Source: Burn (2003, Fig. 4).

Burn, 2002). Water bodies with mean annual basal temperatures above 0°C maintain taliks, or thaw bulbs beneath them. Talik configuration beneath and around a water body is controlled by the size, bathymetry, and basal temperature of the channel or lake. Figure 1.4 illustrates talik dependence on lake bathymetry in the outer Mackenzie Delta. Steady-state models, applied by several researchers in the delta (Smith, 1976; Burn, 2002; Kanigan et al., 2009) permit estimates of the ground temperature field when mean annual ground surface temperature and that of an overlying lake or channel bed are known. Transient thermal models have been developed to describe the migration of taliks beneath shifting channels in the Mackenzie Delta (Smith 1976), and changes to talik configuration at the margins of lakes (Kokelj et al. 2009).

1.5 Objectives and Hypothesis

The objectives of this thesis are to:

1) determine annual and summer thermal regimes for water bodies throughout the delta;

2) determine the spatial variability of thermal regime;

3) explain observed temporal variability in water bodies' thermal regimes;

4) estimate the pervasiveness of through taliks in the delta using observed MAWTs.

It is hypothesized that spatial variability in the thermal regime of delta water bodies exists on the basis of ecological region (taiga forest vs. tundra) and on the basis of water body type (channels vs. lakes). Three specific hypotheses follow.

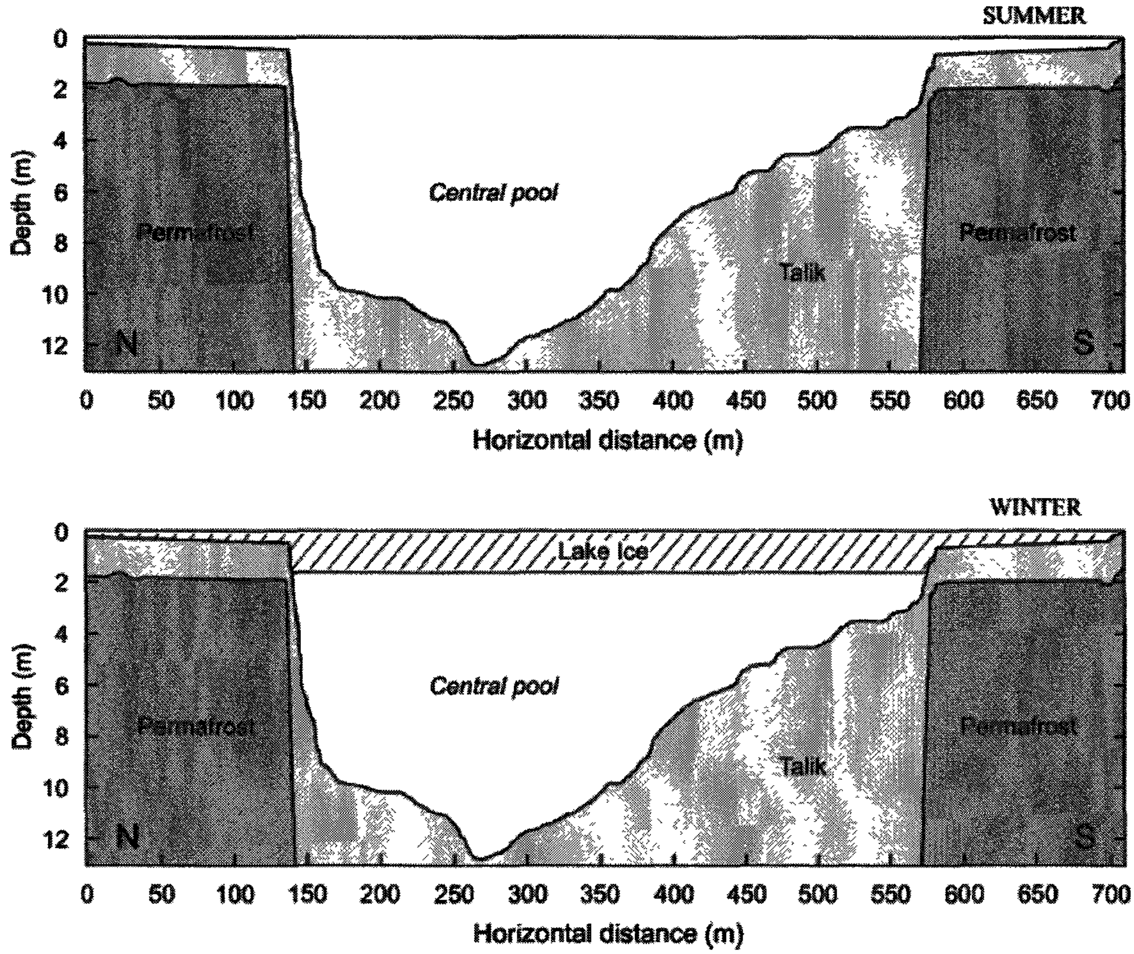

Figure 1.4. Cross-section of Todd Lake, Richards Island, showing ice cover, littoral terraces, central pool, and permafrost configuration. Source: Burn (2005, Fig. 2).

The MAWT of water bodies in the tundra region of the delta is expected to be lower than that of water bodies in the forested region of the delta. This hypothesis is based on the results of research in adjacent uplands comparing thermal regimes of lakes in forest and tundra ecological regions (Burn, 2005). This research is discussed in Chapter 2.

The MAWT of channels is expected to be lower than that of lakes in the delta. This hypothesis is based on the above-zero basal water temperature observed to persist through winter in Arctic lakes (Brewer, 1958; Burn, 2005), and the 0°C basal water temperature observed to persist during the period of ice cover in a northern river (Fig. 1.3) (Burn, 2003).

Spatial variability in MAWT is expected to be lower among channels than among lakes. This hypothesis is based on the connectivity of the delta channel network.

1.6 Methods

For the measurement of thermal regime, 13 channel sites and 17 lakes distributed throughout the Mackenzie Delta were selected using 1:50,000 and 1:250,000 National Topographic Series maps. Examination of late summer 1:30,000 aerial photographs enabled the selection of lakes either (1) visibly connected to or (2) disconnected from the channel network (perched lakes). Miniature data loggers were weighted to each channel and lake bed at the deepest location possible in mid-June 2009, and attached to shore by cable for retrieval. At the time of logger deployment, a coarse bathymetric survey was conducted at each lake and channel site. Temperature profiles were measured in the central water column and horizontally along the bed at each channel site to assess thermal consistency. Thermal profiles were measured at an additional 21 channel sites occasionally through the summer to investigate spatial variations in thermal regime. In early- to mid-August 2009, channel logger installations were modified to better withstand winter ice formation and spring breakup. Winter temperature records for each study lake and six of the channel sites were obtained in June 2010 with the removal of temperature loggers and additional materials from study sites.

1.7 Thesis Structure

This thesis is presented in six chapters. Chapter Two reviews scientific knowledge of the thermal regime of northern lakes and rivers, and discusses the nature and modelling of ground thermal regime. Chapter Three provides a discussion of the physical geography of the Mackenzie Delta and outlines research methods. Chapters Four and Five present results for the summer and annual thermal regimes of Mackenzie Delta water bodies, respectively. Chapter Five also discusses the likely influence of water bodies' measured MAWT on permafrost configuration in the delta, and makes estimates of the prevalence of through taliks. Chapter Six reviews the findings of the research, and suggests directions and opportunities for future related research.

CHAPTER 2: GROUND AND WATER-BOTTOM THERMAL REGIMES IN NORTHERN CANADA

2.1 Thermal Regime of Northern Lakes

Lakes have received more attention than rivers in investigations of thermal regime of northern water bodies. Arctic lakes have a distinctive annual temperature cycle, in which the growth and melt of surface ice are significant events (Welch and Bergmann, 1985). Figure 1.2 provides an illustration of the annual thermal regime of a lake near Barrow, northern Alaska. At that site, ice formation (early October) is accompanied by the onset of basal water warming after the steady decline in basal temperature during autumn. Ice breakup occurs as near-surface water temperatures rise above 0°C in early June (Brewer, 1958).

Lake ice in the Mackenzie Delta generally melts between early- and mid-June (Marsh and Bigras, 1988). In the outer Mackenzie Delta, ice melt has been observed between mid-June and early July (Burn, 2002). The disappearance of ice decreases the albedo of the lake surface and permits wind-driven convection of lake water. This leads to a rapid increase in lake temperature and a transition from stratified to isothermal conditions (Burn, 2002). Abundant insolation around the time of the summer solstice contributes to this rapid temperature increase (Brewer, 1958), so that maximum summer water temperatures are generally observed in late July or early August. Brewer (1958) observed that water was isothermal vertically and horizontally during the ice-free period in study lakes approximately 2.3 m deep, and that temperature fluctuated throughout the water column in response to short-term changes in air temperature. He also noted that the diurnal cycle appeared to induce a temperature fluctuation of 1–2°C.

Following the formation of the ice cover, generally in early October in the outer Mackenzie Delta (Burn, 2002), the thermal regime begins to differ according to depth. This is referred to as thermal stratification. Basal water temperature has been observed to increase by up to 2°C (Brewer, 1958) immediately following ice formation. This is most likely due to the cessation of surface heat loss to air by convection and evaporation, and the continued influx of solar radiation through the ice prior to the accumulation of snow. Figure 2.1 illustrates how water nearer the lake-bottom maintains a stable temperature slightly above 0°C during the period of ice cover. The slight increase in lake-bottom temperatures over winter at the bottom of the lake's central pool occurs as a result of the ongoing release of stored heat by lakebed sediments (Brewer, 1958; Burn, 2002). In contrast, middle and surface layers of the lake cool until late winter. While thermal stratification beneath ice cover may be pronounced during winter (Cott 2007, p. 72), it has been suggested that some degree of circulation may persist (Welch and Bergmann, 1985). In lakes where winter water temperature is below 4°C (the temperature of maximum density) at all depths, water immediately above the lake bed may warm slightly as it receives heat from the lake-bottom. The resulting increase in density causes the water to sink downslope. Water at maximum depth is displaced upwards, and water immediately beneath the ice is moved laterally shoreward. Figure 2.2 illustrates this model of midwinter circulation and the winter thermal structure of a lake (Welch and Bergmann, 1985).

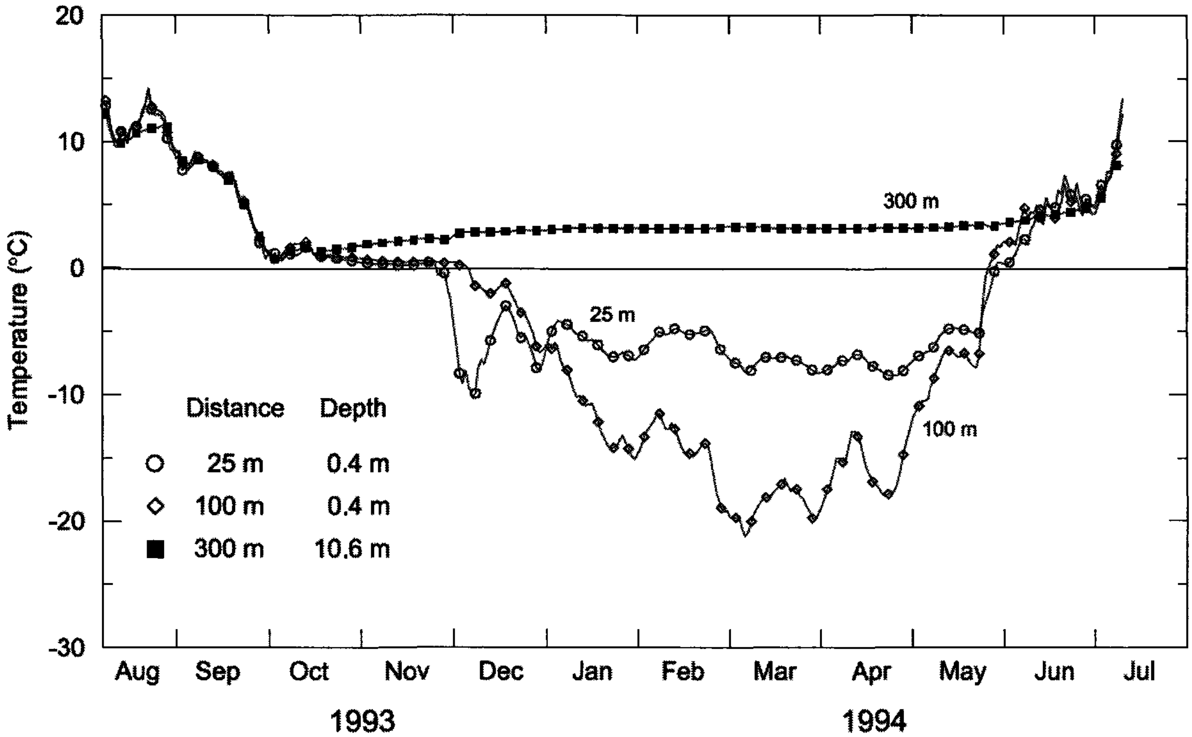

Figure 2.1. Lake-bottom temperatures (6 August 1993–3 July 1994) on a littoral terrace (depth 0.4 m) and central pool of Todd Lake, Richards Island, NWT. The terrace location at 25 m from shore has significantly greater snow accumulation. Source: Burn (2002, Fig. 5).

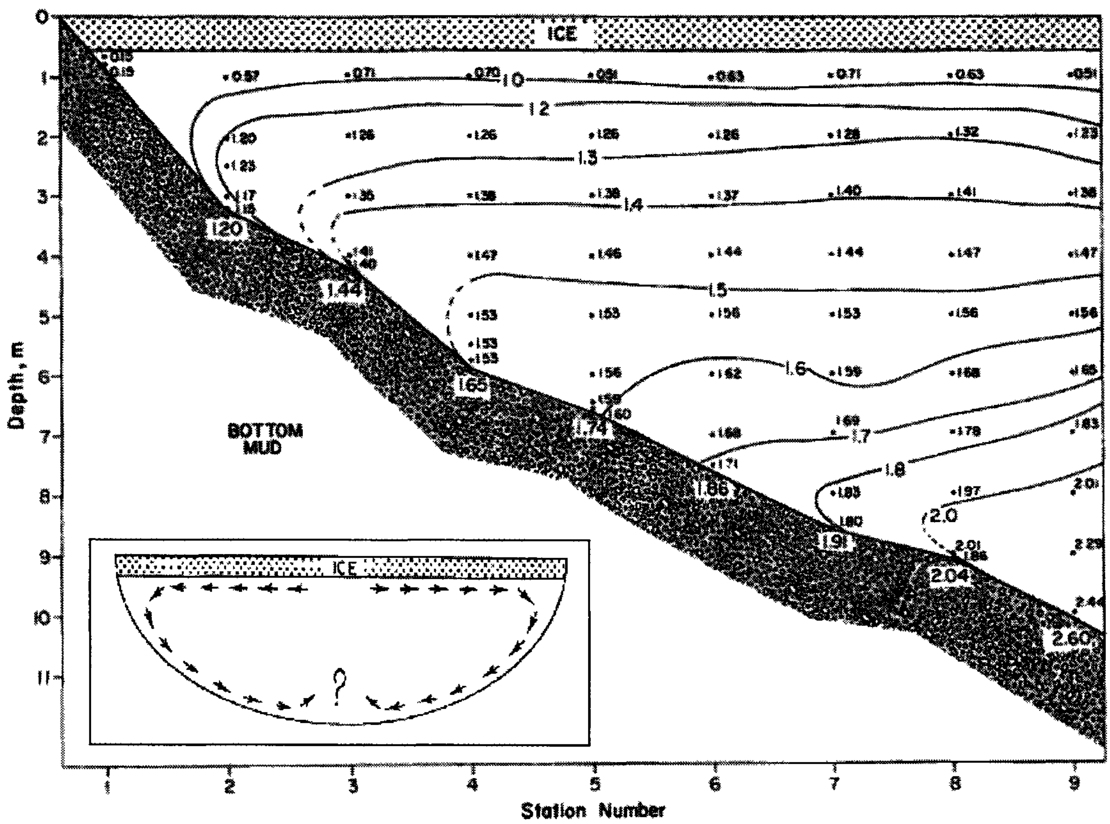

Figure 2.2. Isotherms in Methane North Lake, NWT. Temperatures in shaded area are for mud at 2 cm depth. Inset shows flow inferred by authors. Source: Welch and Bergmann (1985, Figs. 3 and 10).

Average maximum lake ice thickness measured by Burn (2002) between 1992 and 2001 for a tundra lake in the outer Mackenzie Delta was 167 cm. The characteristic thickness of ice and bathymetry of a tundra lake, which may consist of a deep central pool and marginal terrace (Brewer, 1958; Burn, 2002), may mean that ice freezes to a substantial proportion of the lake-bottom. In some cases, snow accumulation may provide insulation and reduce temperature variability within or beneath the ice at the lake margins. Temperatures at the tundra lake site 25 m from shore in Fig. 2.1 were moderated by snow cover on the ice, whereas relatively little snow accumulated at the site 100 m from shore. Maximum ice thickness for a taiga lake near Inuvik, NWT, is generally less than 1 m. This is primarily due to greater accumulation of snow on the ice surface than occurs on tundra lakes (Burn, 2005).

Figure 2.3 illustrates the observed relation between water depth and mean annual lake-bottom temperature for Todd Lake on Richards Island in the outer Mackenzie Delta area. For locations in the central pool where water remains unfrozen through winter, Burn (2002) reported mean annual water temperatures of 3.7°C, 4.3°C, and 4.8°C for depths of 9.7 m, 10.0 m, and 10.6 m, respectively. Mackay (1963) estimated mean annual lake-bottom temperatures in the central pool to be >2°C. For September 1954–September 1955, Brewer (1958) determined the mean annual water temperature at 8 ft. (2.4 m) depth in a coastal lake near Barrow, Alaska to be 1.8°C. The mean annual bottom temperature of a lake in the taiga forest near Inuvik is approximately 2°C warmer than that of Todd Lake (Burn, 2005). This likely results from the earlier disappearance of ice from the taiga lake, due to thinner ice cover. The earlier warming of taiga lakes in spring is apparent in Fig. 2.4, which compares the lake-bottom thermal regimes of Andrew Lake

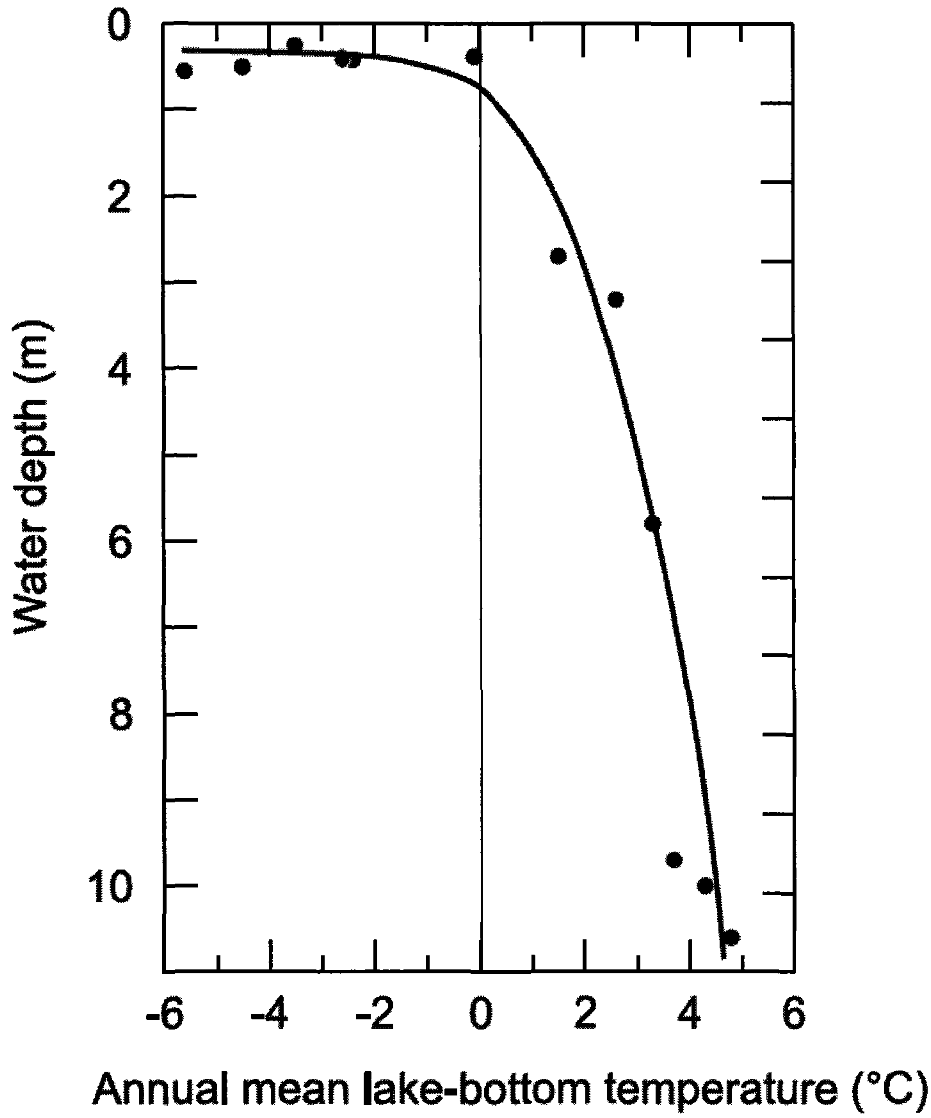

Figure 2.3. Annual mean lake-bottom temperature at various depths in Todd Lake, Richards Island, NWT. Measurements were collected in 1993–1996 by a data logger connected to thermistor cables strung out from shore. Source: Burn (2002, Fig. 9).

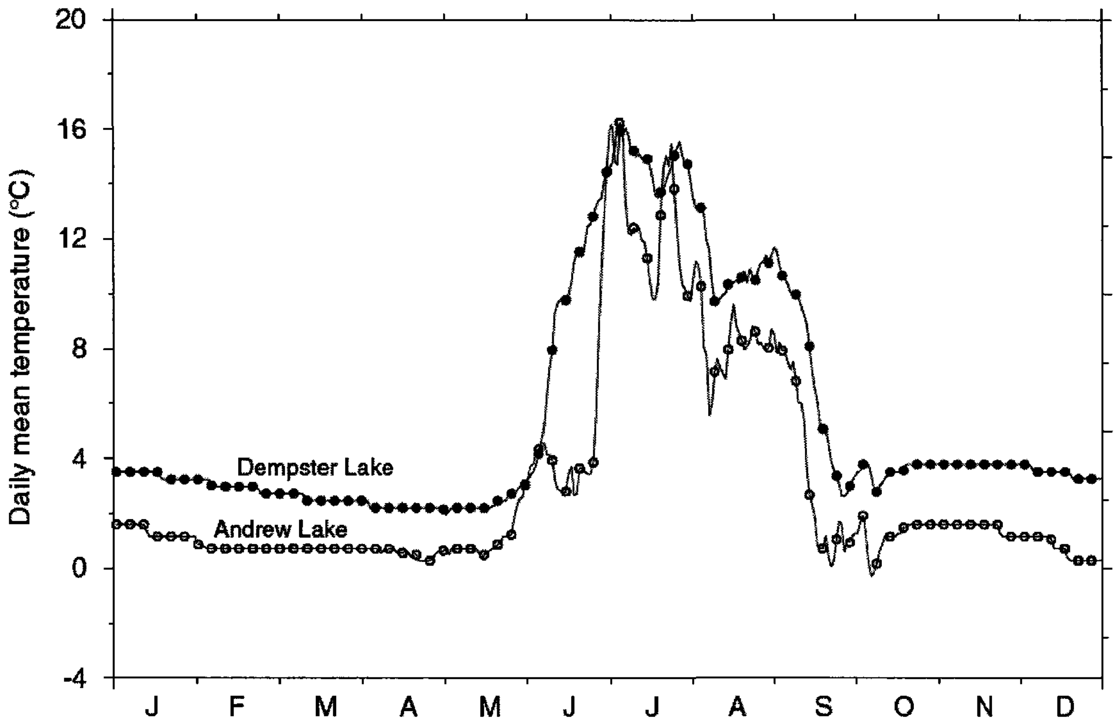

Figure 2.4. Daily mean lake-bottom temperatures for 2003 at 4 m water depth in the central pool of a tundra lake (Andrew Lake) on Richards Island, NWT, and from 3 m depth in a taiga lake near Inuvik, NWT (Dempster Lake). Mean annual temperatures for Andrew and Dempster lakes were 3.1°C and 5.6°C, respectively. Symbols for daily data are plotted every 5 days for clarity. Source: Burn (2005, Fig. 10).

(tundra) and Dempster Lake (taiga). These two ecological regions are home to the lakes of the outer and main portions of the Mackenzie Delta, respectively.

As suggested in the preceding discussion, the thermal regime of tundra lakes is better known than that of lakes in the taiga forest. Treeline delineates two distinct ecological regions within the delta, as on adjacent uplands. On the basis of ecological region (tundra, forest) alone, the potential for two distinct delta lake thermal regime types must be considered.

2.2 Thermal Regime of Northern Rivers

Northern rivers generally follow an annual temperature cycle and remain near 0°C throughout the winter (Burn, 2003; Caissie, 2006). River morphology and solar insolation may have particular influence on thermal regime, especially in the case of relatively shallow or braided river systems (Caissie, 2006). Spatial and temporal river heat distribution is dependant on a variety of factors including climate, bed sediment type, riparian features, flow characteristics, groundwater exchanges, channel morphology, and the connectivity of local surface water features (Webb et al., 2008). The thermal regime within Mackenzie Delta channels has not been described to the same extent as for Arctic lakes. Brosten et al. (2006) suggest that temperature may be highest in the thalweg – the deepest and fastest-flowing portion of a stream. This is based on observations of greater permafrost thaw depth beneath this portion of streambeds. While few temperature records for Mackenzie Delta channel waters are available, Smith (1976) presents monthly measurements and/or estimates for a major distributary channel within the Mackenzie Delta for 1967–1970. The annual thermal regime of the Stewart River, YK, has been determined by Burn (2003) and is illustrated in Fig. 1.3 (p. 5). Between October and May, river bed water temperature is near 0°C but unfrozen. Water temperature ascends sharply to its peak in late July, and then descends rapidly.

2.3 Permafrost and Ground Thermal Regime

The ground thermal regime depends on regional climate, soil properties, and local surface conditions. Permafrost exists if the ground temperature is at or below 0°C for two or more years (Associate Committee on Geotechnical Research, 1988). Figure 2.5 illustrates the temperature profile and thermal envelope in permafrost at equilibrium. The geothermal gradient – the rate at which ground temperature increases with depth due to heat emission from the earth's interior – is indicated. Mean annual ground temperature (MAGT) is obtained at the depth of zero annual amplitude.

Soil properties are of fundamental importance to the movement and storage of heat in the ground, and hence ground temperature. These properties include soil density, mineral composition, organic content, moisture (vapour, water, and ice) content, and temperature (Williams and Smith, 1989). Together they determine the thermal conductivity λ (W m^{-1} K^{-1}) and heat capacity c (J kg^{-1} K^{-1}) of a material. Values of λ and c have been reported for the northeastern Mackenzie Delta by Smith (1976), who noted that alluvium consisted of silt and fine sand with little variation in grain size among 50 samples from three sites. Geotechnical properties of Mackenzie Delta soils and their associations with sediment deposition rate, elevation, and vegetation community were described by Kokelj and Burn (2005). It is likely that little spatial variability in sediment composition exists in the delta,

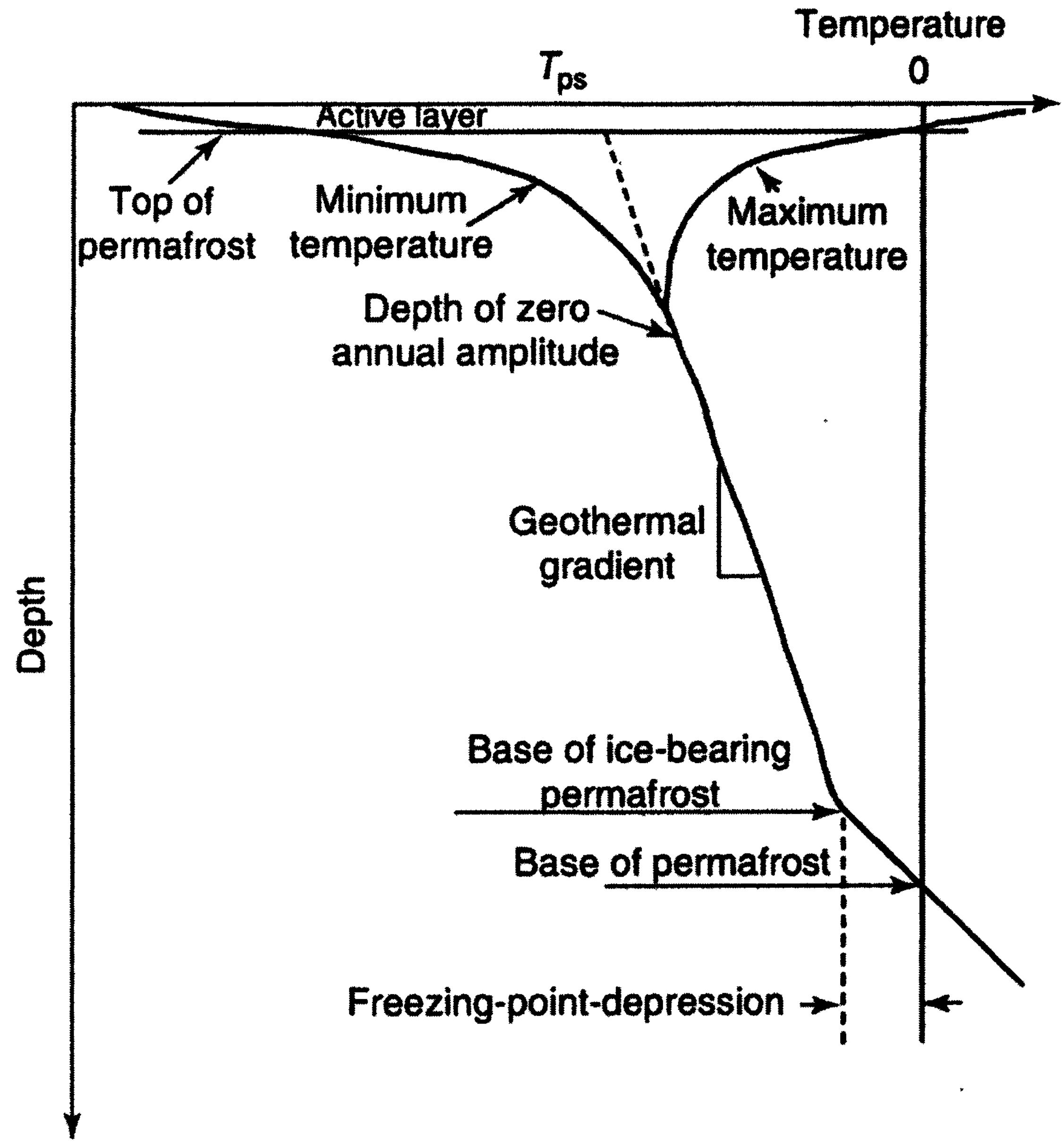

Figure 2.5. Schematic temperature profiles in permafrost illustrating annual maximum and minimum temperatures (thermal envelope). T_{ps} is annual mean permafrost surface temperature. Mean annual ground temperature is equivalent to temperature at depth of zero annual amplitude. Source: Burn and Osterkamp (2003, Fig. 1).

as river and channel turbulence ensure a homogeneous sediment supply and a migrating depositional history. Soil thermal properties are therefore likely to be relatively consistent spatially in a delta environment such as the Mackenzie.

Surface features which disturb the climate-imposed ground thermal regime include surface vegetation, winter snow cover, and water bodies such as channels and lakes (Smith 1976, p. 12). All such features modify the surface energy balance. The influences of vegetation community and snow cover on ground thermal regime are outlined in this section. The Mackenzie Delta itself has provided a good environment for the study of the influence of vegetation on ground thermal regime, as it is home to several distinctive vegetation communities. Kanigan et al. (2009) investigated the four principal spruce forest communities south of treeline in the delta and their influence on ground temperature. In increasing age of succession, these include a spruce/alder-bearberry (SAB) community dominated by alder and bearberry ground-level vegetation, closed-canopy (CSF) and open-canopy (OSF) spruce/feathermoss communities characterized by feathermoss ground cover, and an open-canopy spruce/crowberry-lichen (SCL) community (Kanigan et al., 2009). Figure 2.6 illustrates these four communities. Table 2.1 presents MAGT at two depths for each vegetation community, plus the annual temperature range. The CSF community, with the thickest canopy and therefore the thinnest snow cover, showed the lowest mean annual near-surface ground temperature. The vegetation community in the earliest successional stage, SAB, showed a MAGT significantly higher than that of the other three vegetation communities. Although the SAB and CSF communities have thin organic layers and thick active layers, they present the warmest and coldest MAGT among the vegetation communities due to

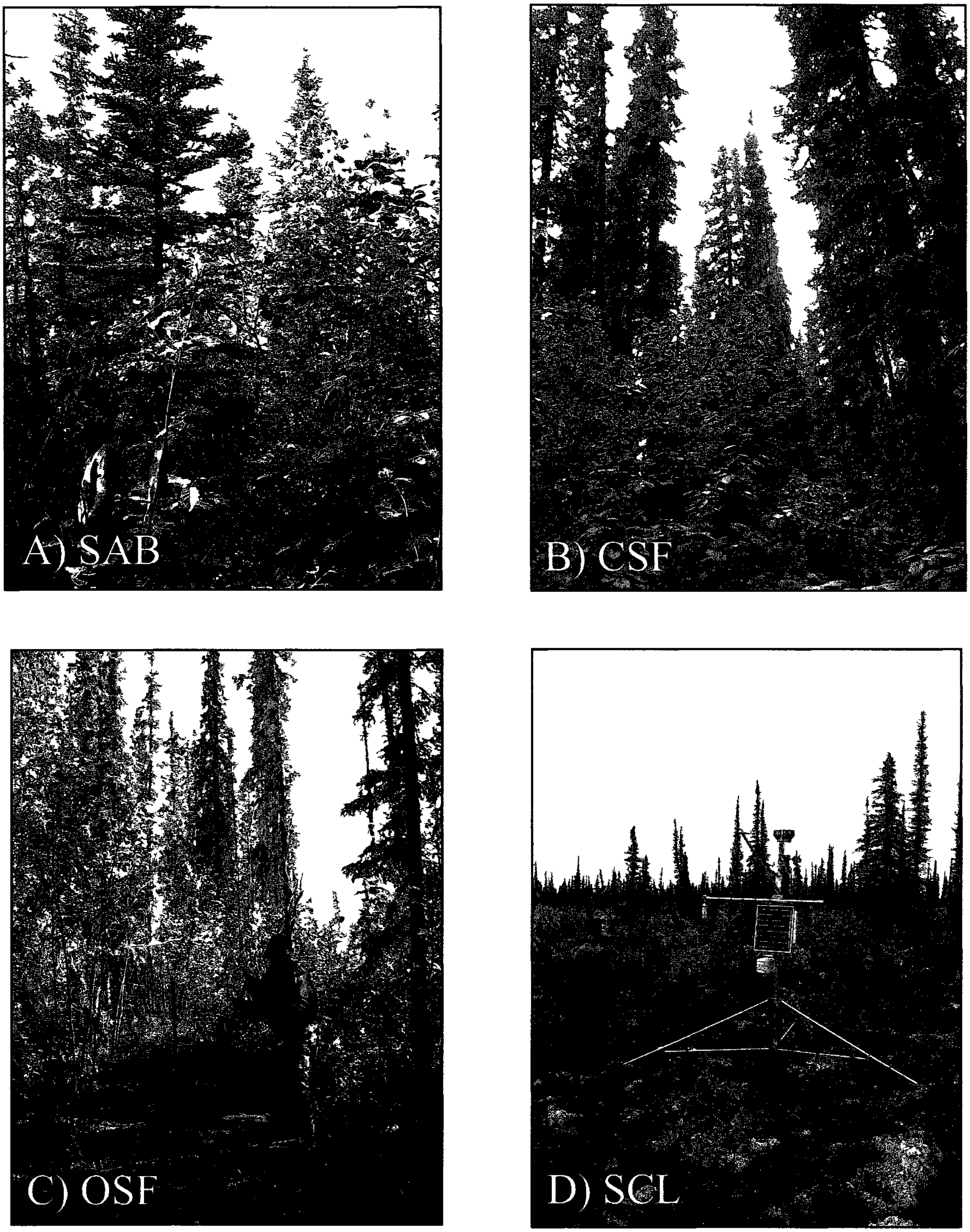

Figure 2.6. Spruce forest communities: A) spruce/alder-bearberry (SAB), B) closed spruce-feathermoss (CSF), C) open/spruce-feathermoss (OSF) and D) spruce/crowberry-lichen (SCL). Source: Kanigan et al. (2009, Fig. 3).

Table 2.1. Mean annual temperature at 1 m depth for 1 September 2003 to 31 August 2004 for three different spruce forest sites near Inuvik, mean 20 m ground temperatures at the same sites, and the range of 20 m ground temperatures measured at all instrumented sites in the Mackenzie Delta, April 2007. Reproduced from Kanigan et al. (2009, Table 2).

Depth	SAB	CSF	OSF	SCL
1 m	-1.0 (n=1)	-4.4 (n=1)	---	-2.1 (n=1)
20 m	-1.1 (n=3)	-2.3 (n=8)	-2.0 (n=9)	-2.1 (n=6)
Range at 20 m	0.6 to -1.5 (n=3)	-1.9 to -2.9 (n=8)	-1.6 to -2.9 (n=9)	-1.7 to -2.7 (n=6)

characteristically thick and thin snow covers, respectively (Kanigan et al., 2009). SAB communities are characterized by flooding every 5–10 years, and support stands of age generally <250 years. CSF and subsequent successional communities develop with increases in elevation and decreases in flood frequency, and support stands of older trees (250–450 years) which promote the development of a surface organic layer. Kanigan et al. (2009) note that ground temperature variability is small within forest communities.

On an aggrading point-bar (or slip-off slope), a general decrease in MAGT was observed by Smith (1976) as distance from the channel increased. Nguyen et al. (2009) provided an illustration of characteristic vegetation succession on a Mackenzie Delta point-bar (Fig. 2.7). While mean annual air temperature (MAAT) was -9°C to -10°C, mean annual surface temperature (MAST) ranged from -1.0°C to -1.5°C on bare ground, and was -3.0°C and -4.2°C in areas of willow/alder and spruce, respectively (Smith, 1975). On slip-off slopes, variations in snow accumulation produce greater MAGT variations than those resulting from vegetation cover alone (Smith, 1975). Surface temperatures were found to differ by up to 20°C where snow depths ranged from 4 to 110 cm. Ground temperatures at 1 m depth, within 12 m of one another, differed by up to 6°C in mid-winter where a variable snowpack existed (Smith, 1975).

Tundra ground temperatures are lower than in nearby regions south of treeline (Burn and Kokelj, 2009), due primarily to deeper snow occurring in forested regions. The taiga forest canopy is thin enough to permit snow accumulation on the ground, yet provides requisite shelter from wind which reduces the snow depth on tundra. As Fig. 2.8 illustrates, this is the case both within the Mackenzie Delta and on the adjacent uplands.

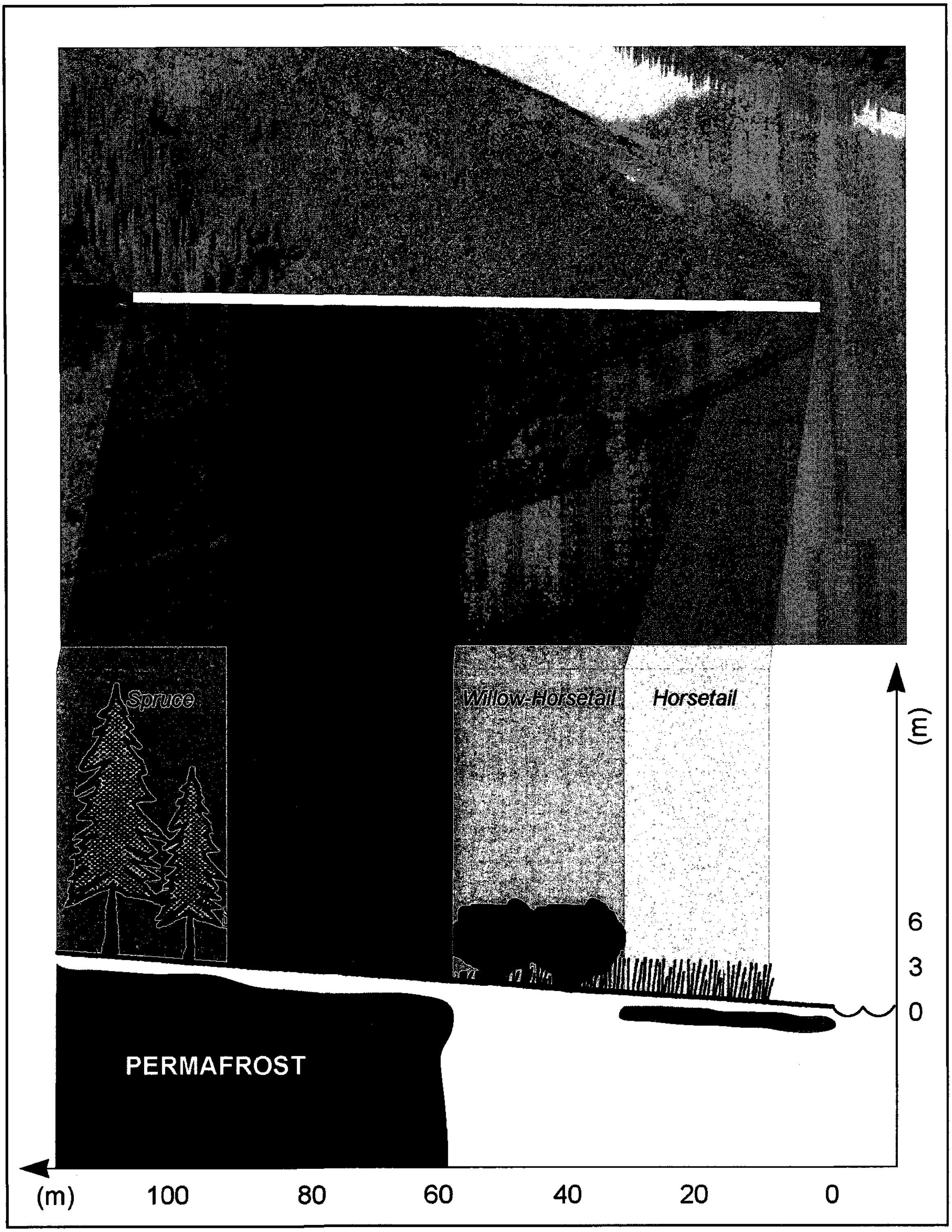

Figure 2.7. Vegetation succession on a point-bar in the Mackenzie Delta. Source: Nguyen et al. (2009, Fig. 2).

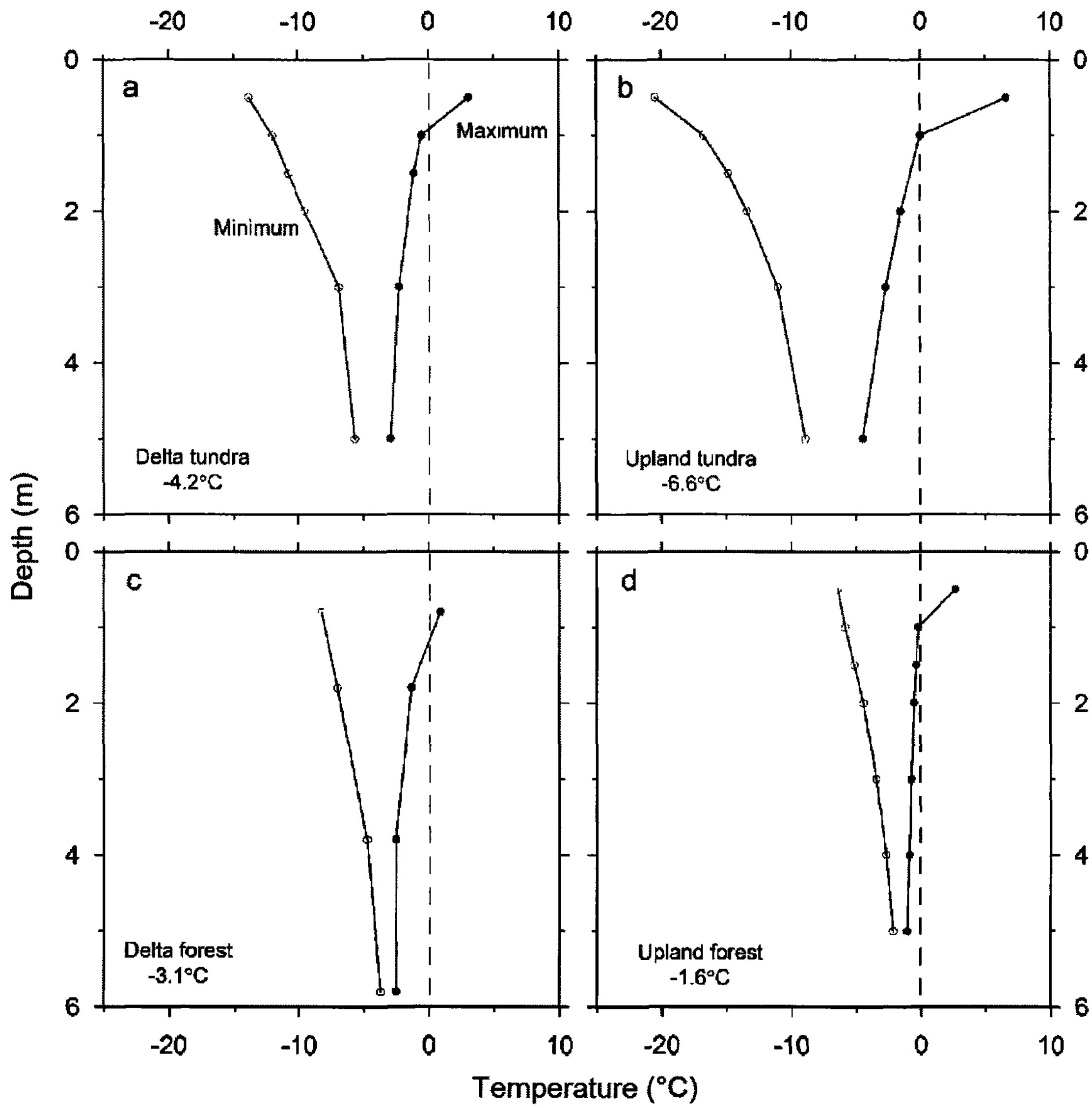

Figure 2.8. Thermal envelopes to depths of 5.8 m for upland and delta environments in the coastal western Canadian Arctic both north and south of treeline. Source: Burn and Kokelj (2009, Fig. 8).

This figure provides an illustration of thermal envelopes for tundra and forest in both upland and delta regions. Mackay (1974) showed that MAGT is distinctly higher in the delta than on adjacent uplands. The following section discusses the primary cause of the modified ground thermal regime in the delta.

2.4 Influence of Surface Water Bodies on Ground Thermal Regime

At high latitudes, water bodies create the greatest local departure from climate-induced ground thermal regimes (Lachenbruch et al., 1962). This is primarily due to the high heat capacity of water, the fact that ice and snow cover on water bodies reduce heat loss during winter (Smith, 1976), and the latent heat transfer required for the freezing and thawing of lake ice. Lakes which are deeper than maximum winter ice thickness retain mean annual basal temperatures above 0°C. At NRC Lake in the eastern Mackenzie Delta, Brown et al. (1964) observed that ground temperatures in a borehole established adjacent to the lake were approximately 1°F (0.56°C) higher than approximately 400 ft. (122 m) further away from the lake. Through probing along transects perpendicular to the shore of Todd Lake, Burn (2002) described the permafrost configuration beneath the shallow terraces around the margins of this tundra lake in the outer Mackenzie Delta (Fig. 2.9). Mean active layer depths beyond 20 m from shore were 136 cm and 140 cm for the north and south terraces, respectively. At the terrace edges (the perimeter of the central pool of the lake), a steep boundary of frozen ground was inferred from drilling. At Todd Lake, where maximum winter ice thickness is on average 1.67 m (Burn, 2002), a water depth of approximately 1 m corresponds with the edge of permafrost. Burn (2002) observed that this is consistent with an estimate by Mackay (1992) that permafrost would

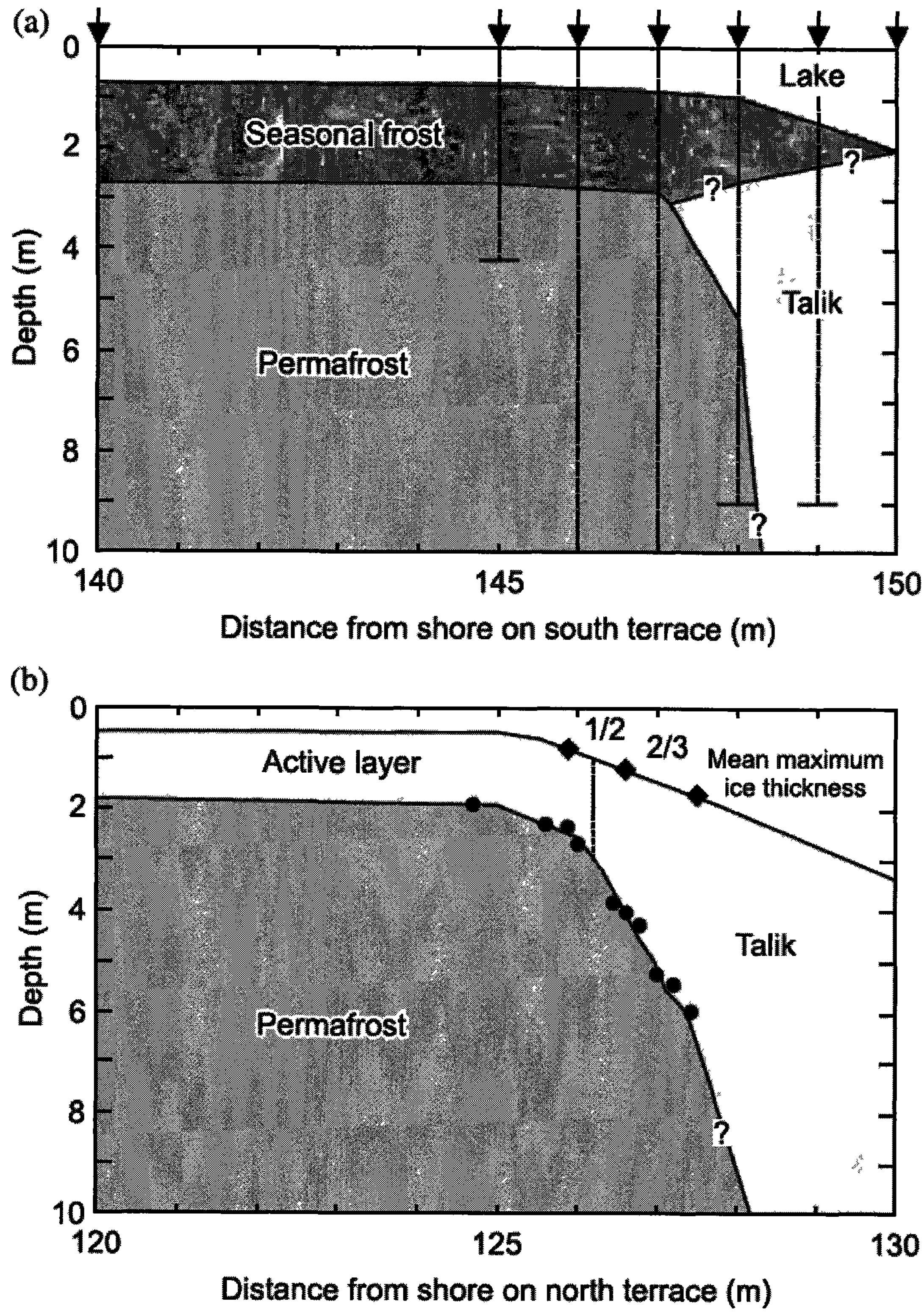

Figure 2.9. Configuration of permafrost at the edge of littoral terraces on the (a) south and (b) north side of Todd Lake, delineated by water-jet drilling (Burn 2002, Fig. 11).

not occur beneath water deeper than two thirds of the maximum winter ice thickness. Lake Illisarvik, 300 m wide by 600 m long, and 3 m deep with no littoral terraces, maintained a talik of depth 32 m beneath its centre prior to its drainage (Mackay, 1997).

While modelling ground thermal regime is the subject of the following section, field-verified relations developed by Mackay (1963) permit the definition of the critical radius beyond which a lake will maintain a "through talik" which penetrates permafrost. Also defined is the maximum possible talik depth for lake radii less than this critical value. For a shallow circular lake with no terraces and a mean annual water temperature of 2°C, the critical radius and maximum talik depth are 215 m and 155 m, respectively. For a deep terrace-free lake of mean annual water temperature 4°C, critical radius decreases to 180 m and maximum talik depth extends to approximately 175 m (Burn, 2002).

Thermal effects from rivers have not been investigated to the same extent as for lakes (Smith, 1976), and few basal temperature data are available from rivers. Departures from climate-induced MAGT have been observed around channels in the Mackenzie Delta. Smith (1976, Table 6) reports that ground temperature at 9 m depth decreased with distance from a channel on a slip-off slope at a site in the east-central delta. The application of heat conduction models by Smith (1976) identified a relation between talik depth and channel width in agreement (± 0.5°C) with observed values. A channel of approximate width ≥70 m is expected to maintain a through talik (Fig. 2.10).

Comparisons have also been made of MAGT between the cut-bank and slip-off slope, at a location where a major distributary channel is undergoing lateral migration. Table 2.2 shows ground temperature over a range of depths at similar distances from the channel on

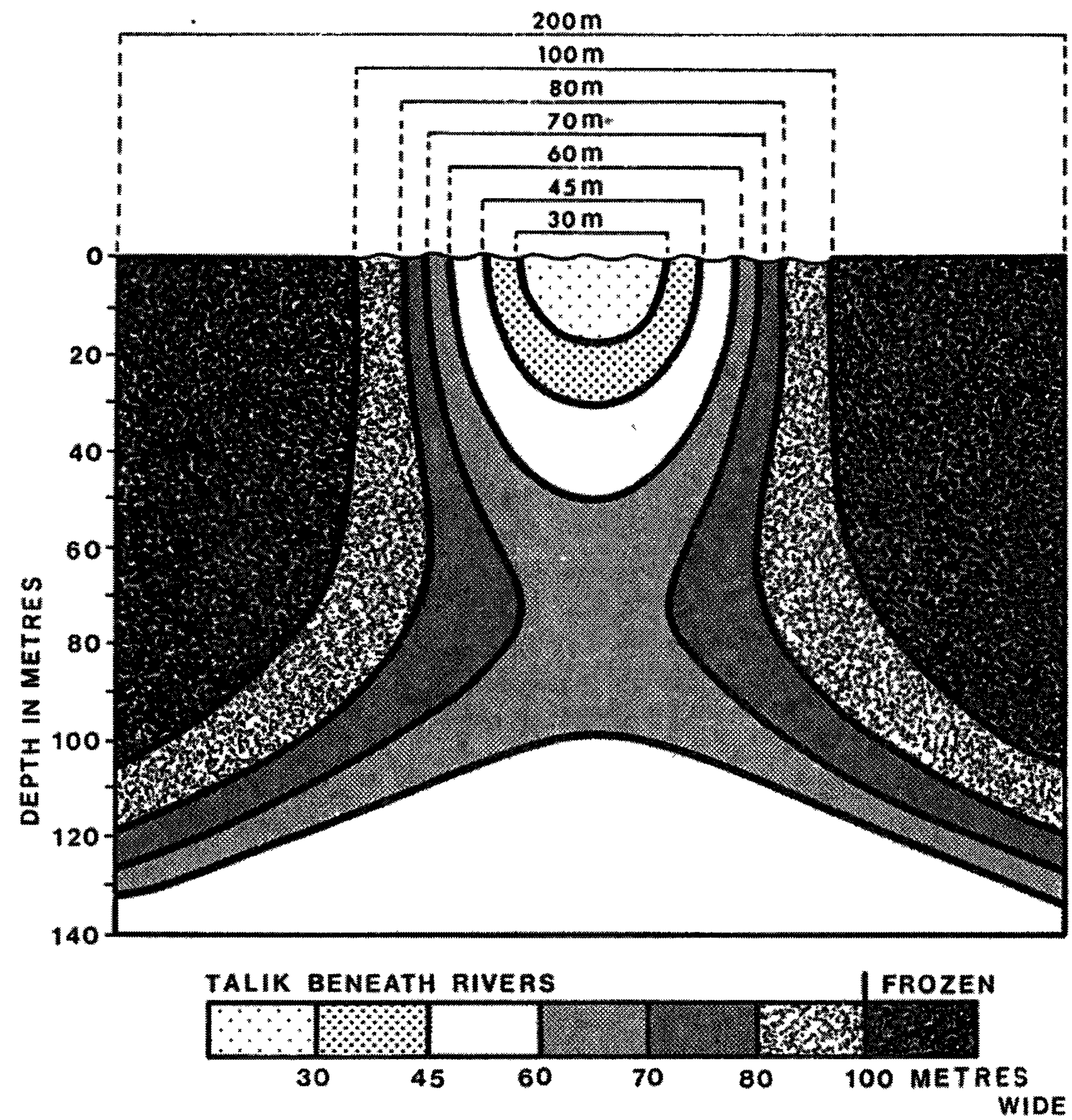

Figure 2.10. Steady-state permafrost configuration under rivers. Source: Smith (1976, Fig. 11).

Table 2.2. Ground temperatures beneath a cut-bank and slip-off slope. Distance to channel is 36 and 35 m, respectively. Reproduced from Smith (1976, Table 4).

Depth (m)	Cut-bank (°C)	Slip-off (°C)
6	-3.6	-0.5
9	-3.3	0.0
12	-3.0	0.2
15	-2.7	0.4
20	-2.4	0.7

opposite banks. Slip-off slope ground temperatures generally exceeded cut-bank temperatures by over 3°C, due to gradual thermal re-equilibration as the distance from the water body increases and related vegetation succession occurs. The permafrost table was observed to fall steeply beneath the cut-bank (Smith, 1976) and to aggrade beneath the slip-off slope in a wedge-shaped configuration as illustrated in Fig. 2.11. The absence of permafrost beneath the early successional stage of vegetation on the slip-off slope results from the accumulation of a snowbank amid the willows.

2.5 Modelling Ground Thermal Regime

In locations where no major thermal disturbance from water bodies or other surface cover exists, the ground temperature profile (Fig. 2.5) can be represented by:

$$T_z = T_g + z/I \qquad (1)$$

where T_z is temperature (°C) at depth z (m), T_g is the mean annual ground surface temperature (°C), and I is the geothermal gradient (m°C^{-1}; Lachenbruch, 1957). Equations developed to estimate ground temperature at or near locations of thermal disturbance combine a form of Equation 1 with an additional term estimating the degree of thermal disturbance at the point of interest. Smith (1976. Eq. 1) presents a solution developed by Lachenbruch (1957) for the thermal disturbance Θ in the ground, at a point of interest of location x,y, depth z, and at time t, created by the presence of one or more nearby temperature disturbances at the surface:

$$\Theta(x,y,z,t) = (T_d\text{-}T_s)\ {}_0\Sigma^{360}\ \sigma/360\ \{[1/(1+(R_1/z)^2)^{1/2}] \cdot \mathrm{erfc}[(z^2+R_1^2)^{1/2}/(2(\alpha t)^{1/2})]$$
$$- [1/(1+(R_2/z)^2)^{1/2}] \cdot \mathrm{erfc}[(z^2+R_2^2)^{1/2}/(2(\alpha t)^{1/2})]\} \qquad (2)$$

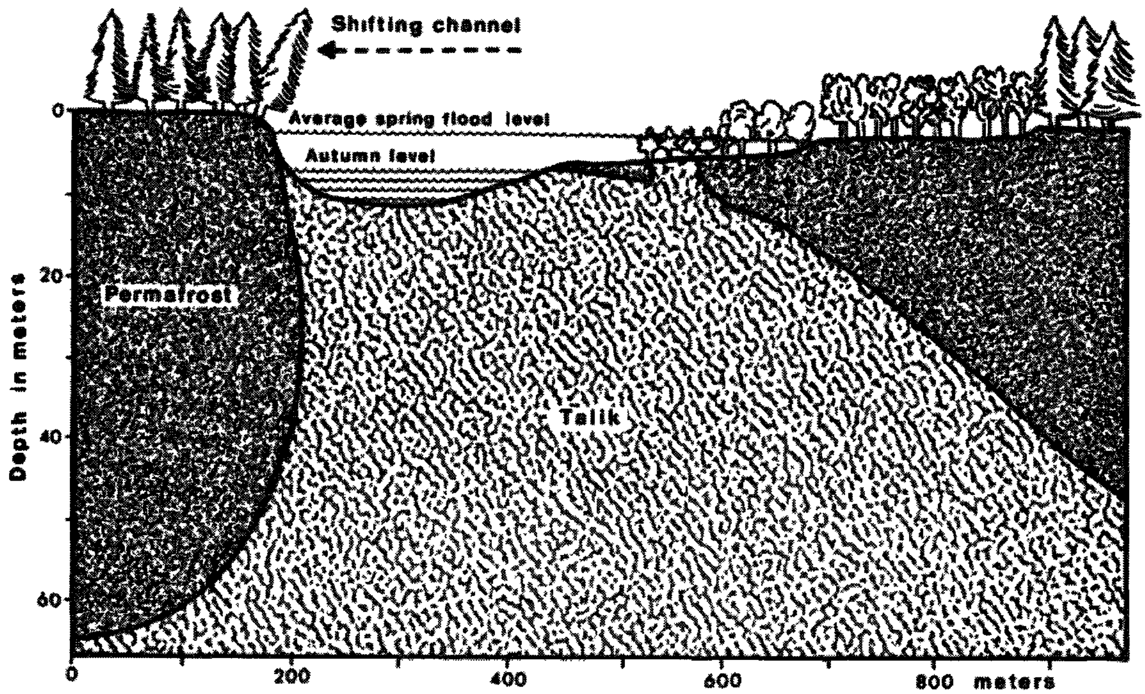

Figure 2.11. Cross-section through a shifting channel area. Source: Smith (1976, Fig. 9).

The variables T_d and T_s are the mean annual temperatures of the disturbed surface (i.e. lake basal temperature) and the undisturbed ground surface, respectively. The symbol σ is the extent, in degrees, to which a region of disturbed surface temperature surrounds the point of interest (Fig. 2.12). R_1 and R_2 are the distances between the point of interest and the nearest and farthest extents, respectively, of each region of disturbed surface. erfc is the complimentary error function (Lachenbruch, 1957). The $\Theta(x,y,z,t)$ term is therefore an integration of thermal modifications, from disturbances from one or more nearby sources, to ground temperature at a point of interest. It may be used in the following equation (Smith 1976, Eq. 2) to determine temperature T at any point in the ground at location x,y, depth z, and time t:

$$T(x,y,z,t) = \Theta(x,y,z,t) + \{T(x,y,0,t) + Gg \cdot z\} \tag{3}$$

where $T(x,y,0,t)$ is the mean annual ground surface temperature, and Gg is the earth's geothermal gradient (expressed as the reciprocal of I in Equation 1). The term in { } is therefore equivalent to the right side of Equation 1. If the point of interest lies within the region of disturbed surface temperature (i.e. beneath a lake), and if steady-state conditions – whereby the lake has been in the same position for a long time – are assumed, Brown et al. (1964) show a simplified version of Equation 2 (presented as Eq. 3 in Smith, 1976):

$$\Theta(x,y,z) = (T_d\text{-}T_s)\ {}_0\Sigma^{360}\, \sigma/360\ \{[1/(1+(R_1/z)^2)^{1/2}] - [1/(1+(R_2/z)^2)^{1/2}]\} \tag{4}$$

In this case, R_1 is set to 0 and R_2 is the radius of the water body or thermal disturbance. Mackay (1962, Eq. 7) presents a similar equation, which provided estimates of talik depth

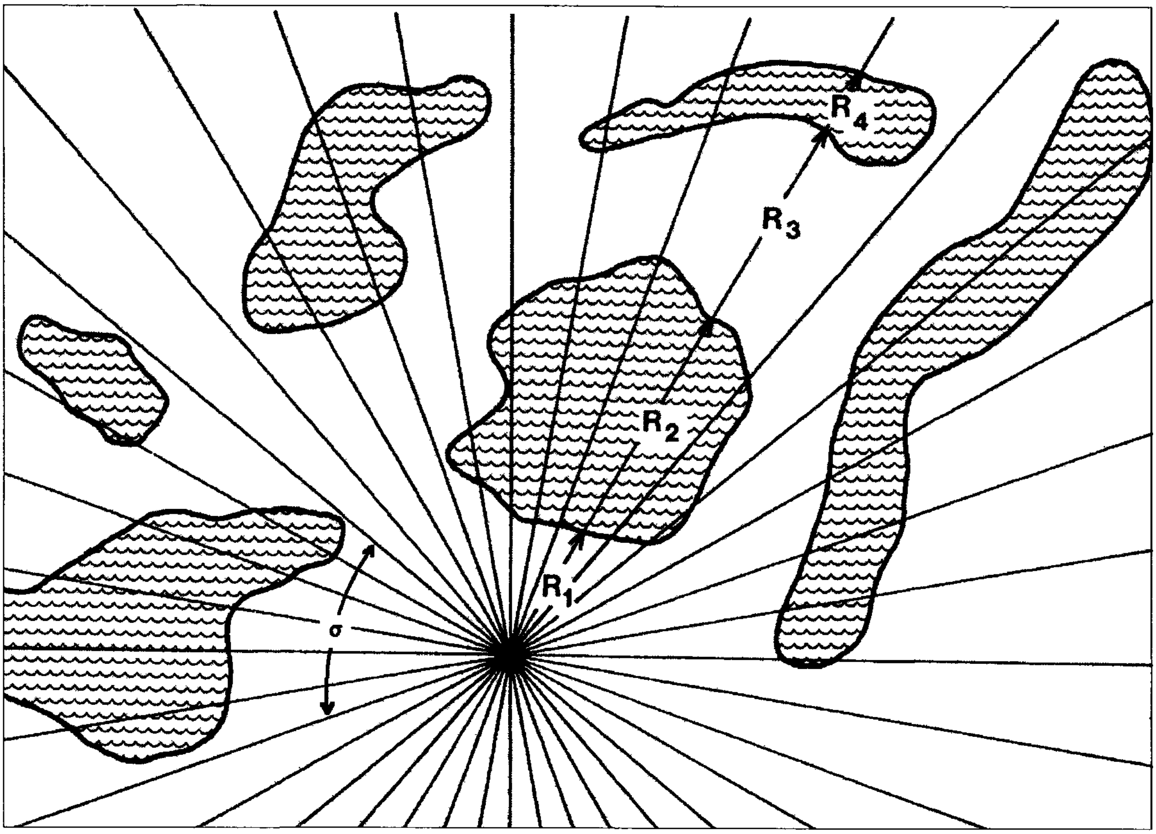

Figure 2.12. Illustration of terms employed in Equation 2, with respect to a point of interest (modified from Smith, 1976, Fig. 10).

consistant with those observed beneath Lake Illisarvik as discussed in the previous section. This equation permits estimates of ground temperature T_z beneath the centre of circular lakes:

$$T_z = T_g + z/I + (T_p - T_g)[1\text{-}(z/(z^2 + R_p^2)^{1/2}] \qquad (5)$$

Variables are as defined in Equation 1, and T_p and R_p are pool temperature and radius, respectively. As this equation applies to lakes without terraces, R_p simply refers to lake radius.

Ground temperature beneath strip-shaped disturbances such as channels and elongate lakes may be estimated, under steady-state conditions, using an equation developed by Werenskiold (1953) and Smith (1976, Eq. 7), and presented in the form below by Burn (2002, Eq. 4):

$$T_z = T_g + z/I + (T_p - T_g)/\pi[2\tan^{-1}(H_p/z)] \qquad (6)$$

where H_p is the half-width of the disturbance. A variant of this equation is the basis for Fig. 2.10, developed by Smith (1976).

Equations 3 and 4 were applied by Smith (1976) to calculate the temperature field beneath a traverse line in the east-central delta. A Gg of 2.5°C/100 m was used, and values for T_d of 3.2°C and 4.0°C were taken to be representative of mean annual lake and river temperature, respectively. Along the traverse, ground temperatures were measured at three sites in boreholes up to 30 m deep, and predicted ground temperatures were within 0.2°C of those observed. This temperature field, shown in Fig. 2.13,

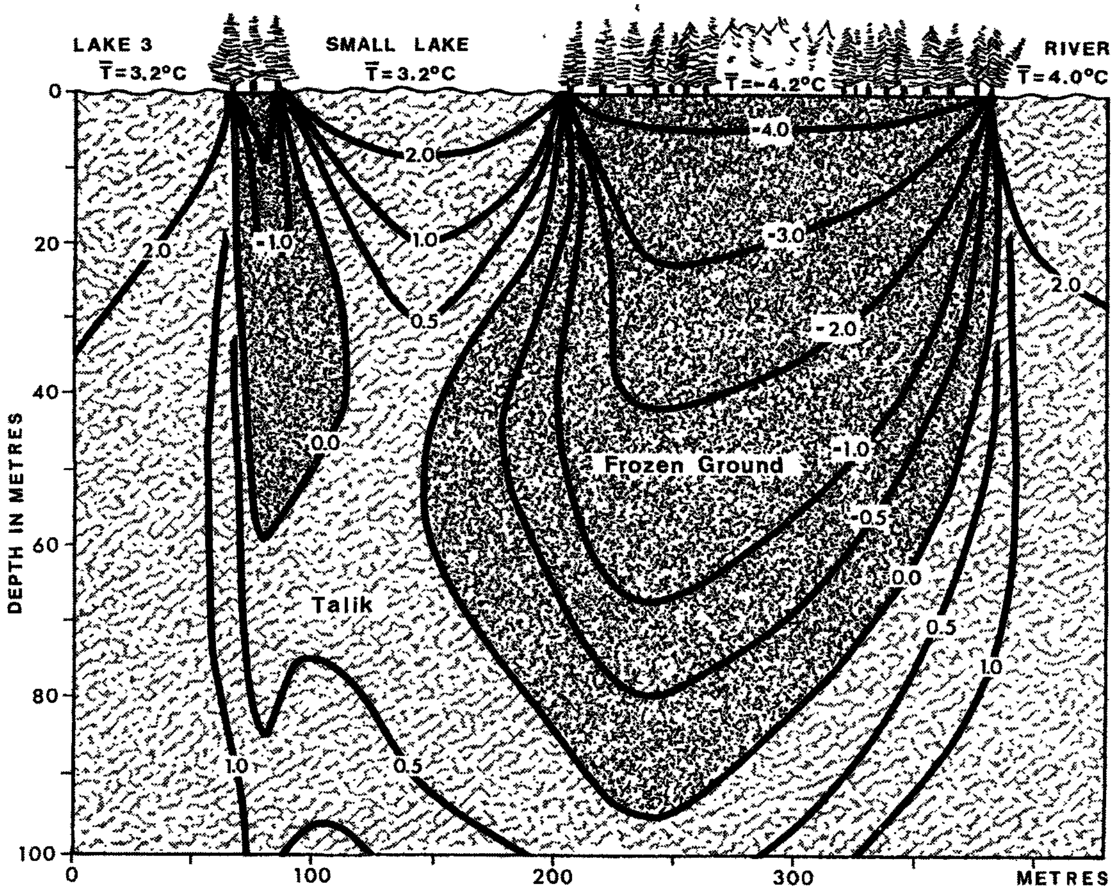

Figure 2.13. Temperature field calculated beneath a traverse line. Source: Smith (1976, Fig. 14).

therefore provides a good illustration of ground temperature field and permafrost configuration beneath proximal lakes in the Mackenzie Delta. As mentioned, where steady-state conditions apply, Equation 6 has produced estimates of ground temperature proximal to a channel in good agreement with field measurements (Smith, 1976).

In environments like the Mackenzie Delta, numerous surface water bodies likely influence ground temperature at any given point. Kanigan et al. (2008, Eq.2) present a modification of Equation 6 which may be applied in determining the ground temperature field at some position between a lake and channel:

$$T_z = T_w + z/I + [(T_g - T_w)/\pi][\tan^{-1}(H_{p1}/z) + \tan^{-1}(H_{p2}/z)] \qquad (7)$$

where T_w is mean annual water temperature °C, H_{p1} is the distance (m) from the lake to the point of interest, and H_{p2} is the distance from the point of interest to the channel. Application of this equation showed that, within the delta, the influence of a water body on ground temperature is greatest within 200 m, and becomes negligible (equivalent to the 0.1°C resolution of temperature instrumentation) beyond approximately 750 m.

The formulae above permit the calculation of exact temperatures or temperature disturbances at known locations within a fixed geometry under steady-state conditions. These analytical techniques are relatively simple to apply, however they assume spatial and temporal homogeneity to an extent which is seldom the case in the environment being modelled. While thermal conditions such as geothermal gradient and thermal conductivity may be reasonably spatially consistent in a delta environment, boundary conditions such as MAWT and MAGT are likely to change over time, as is the physical geometry of the setting where a temperature field is to be determined. Assumptions must be made when analytical methods are applied in these settings, and these are discussed in relation to the results obtained through the use of steady-state models in this research.

CHAPTER 3: STUDY AREA AND METHODS

3.1 The Mackenzie Delta

3.1.1 Introduction

The Mackenzie Delta (Fig. 1.1), with an area of over 13,000 km^2, is the world's second-largest Arctic delta (Burn and Kokelj, 2009). The delta floodplain is covered by numerous lakes and an intricate channel network, and consists of permafrost-influenced silt and sand covered by spruce, alder, willow, and birch (Emmerton et al., 2007). Treeline traverses the delta, and the outer delta is an aggrading landscape characterized by sedge wetland. The region supports a diversity of plants, fish, and wildlife, and is important for waterfowl staging (Mackenzie River Basin Committee, 1981).

3.1.2 Physiography and Geomorphology

The Mackenzie Delta occupies the northernmost extent of the Interior Plains of North America. It is bounded to the west by the Richardson Mountains which form the northern extension of the Cordillera, to the northeast by the Tuktoyaktuk Coastlands, and to the east by the Anderson Plain (Fig. 1.1). Its formation began following the retreat of the Laurentide ice sheet from the area about 13,000 BP (Duk-Rodkin and Lemmen, 2000). The alluvial delta is composed of a layer of sediment (70–80 m thick approximately 5 km west of Inuvik) overlying bedrock that receives approximately 43 Mt of sediment from the Mackenzie and Peel rivers each year. An additional 85 Mt is deposited annually offshore (Marsh, 1998). There are a few rocky outcrops in the east and southeast portions of the delta, the highest being about 30 m above the delta plain (Burn and Kokelj, 2009). Beneath delta sediments, Wisconsinian glacial till covers clastic and carbonate sedimentary bedrock. The ongoing lateral migration of channels forms cut-bank and point-bar features throughout the delta (Gill, 1972).

3.1.3 Climate

The climate of the Mackenzie Delta region is bounded by conditions at Fort McPherson and Tuktoyaktuk (Burn and Kokelj, 2009), and is illustrated in Fig 3.1 using 1971–2000 climate normal air temperature and precipitation at Inuvik. Air temperatures near the coast are typically lower due to the persistence of sea ice in the spring, and the contrast in albedo between tundra (0.75) and boreal forest (0.3) (Burn and Kokelj, 2009). Coastal conditions are drier than those inland. Fort McPherson has an average snow depth of 0.7 m at the end of February, twice that of Tuktoyaktuk. Month-end climate normal snow depth is also given for Inuvik in Fig. 3.1. Monthly air temperature, precipitation, and final snow depth for the June 2009–May 2010 study period are also given in Fig. 3.1. During the study period, winter temperatures were above normal while summer and autumn temperatures were approximately normal. The study period was drier than normal, aside from the late summer (2009) and early spring (2010).

Since the end of the Wisconsinian glaciation, the climate of the Mackenzie Delta region has shown several distinct phases. The cold, dry glacial climate gradually warmed by 10,000 BP. Temperatures were greatest during the early Holocene, 10,000–6,000 BP (Ritchie, 1985), and treeline advanced to the present position of the coast. Since 6,000 BP, regional climate has cooled and vegetation communities have stabilized. Over the past four decades, however, the climate of the western Arctic has shown warming at an unprecedented rate. While mean annual air temperature at Inuvik was -9.5°C and stable

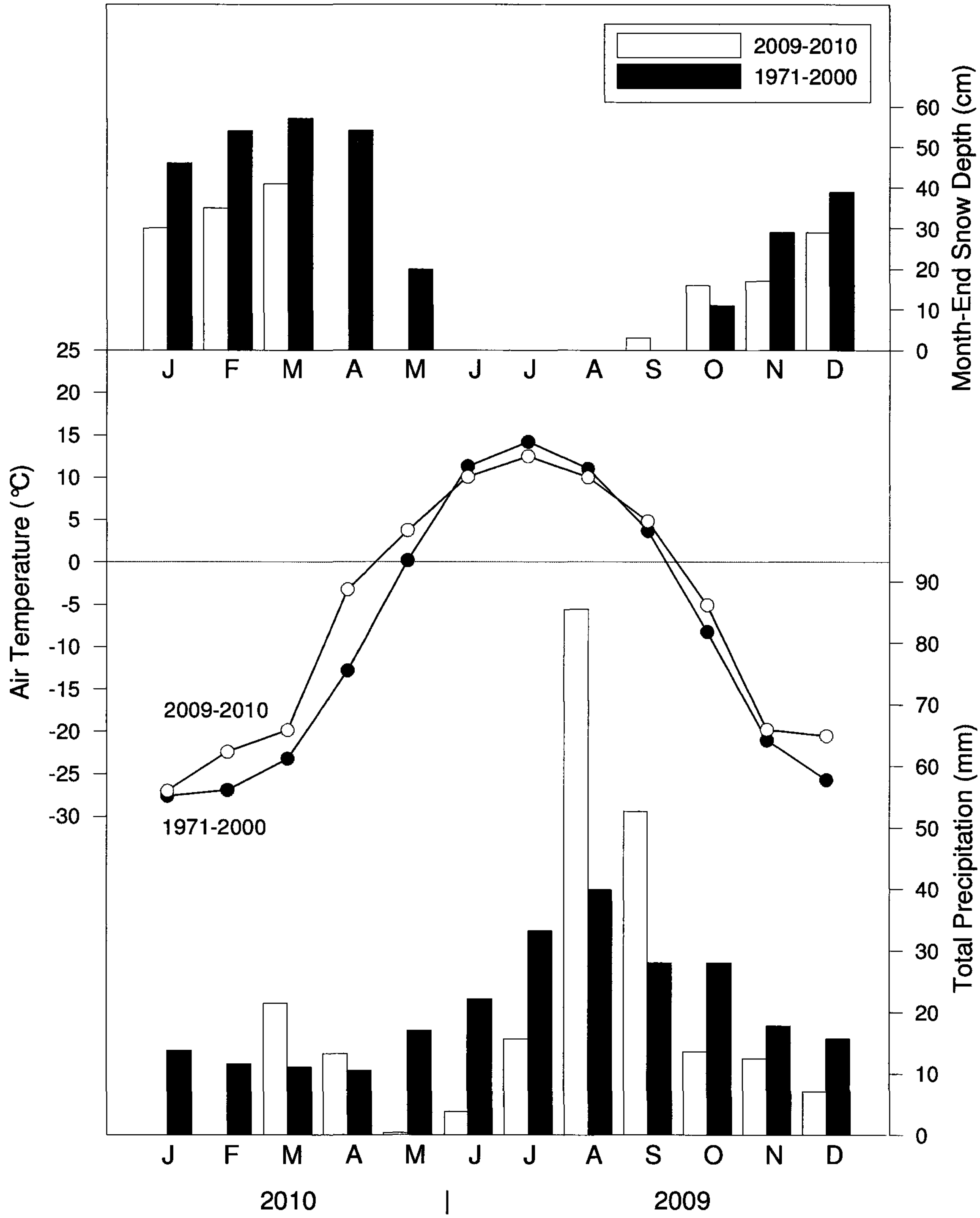

Figure 3.1. Climate normal (1971–2000) and study period (June 2009–May 2010) air temperature, precipitation, and snow depth at Inuvik, NWT. Absent columns indicate measured values of 0 for month-end snow depth, and unavailable data for total precipitation. Environment Canada data are available at http://www.climate.weatheroffice.gc.ca/climateData/dailydata_e.html?Prov=XX&timeframe=2&StationID=41883&Day=1&Month=2&Year=2010&cmdB1=Go

between 1926 (the start of the period of record) and 1969, it has climbed approximately 0.75°C each decade since 1970 (Burn and Kokelj, 2009). For this period, the rate of increase of mean seasonal temperature is greatest for winter (1.1°C per decade).

3.1.4 Hydrology

The Mackenzie Delta receives over 55 km^3 of water annually as discharge (Emmerton et al. 2007). The 1,787,000 km^2 Mackenzie basin, comprising nearly 20% of Canada's land area, contributes about 90% of this volume via the Mackenzie River. The Peel River and other inputs comprise the remaining 10% (Bigras, 1990; Emmerton et al., 2007).

The hydrology of the Mackenzie Delta is characterized by the annual spring flood in late May or early June (Fig. 3.2). At Inuvik, peak spring water level in the East Channel typically exceeds the late summer mean water level by over 4 m (Marsh and Hey, 1989). The principal driver of the spring flood is snow melt, completed in only a few weeks due to the abundance of solar insolation (Burn and Kokelj, 2009). Ice jams may cause extreme flooding in some regions of the delta, though not in every year. Through the summer, base flow is maintained by contributions from reservoirs such as Great Slave and Great Bear lakes, and frontal precipitation is the primary control on the hydrograph (Burn and Kokelj, 2009). During winter, the freeze-through of relatively small distal channels increases flow through the main channels of the delta (Burn, 1995). Late summer ocean storm surges may elevate water levels up to and beyond Point Separation, and can inundate the outer delta. Figure 3.2 shows daily mean East Channel water level at Inuvik and the 1985 hydrograph which includes the highest spring flood level on record. The 2009 hydrograph is included, indicating that water levels during the summer

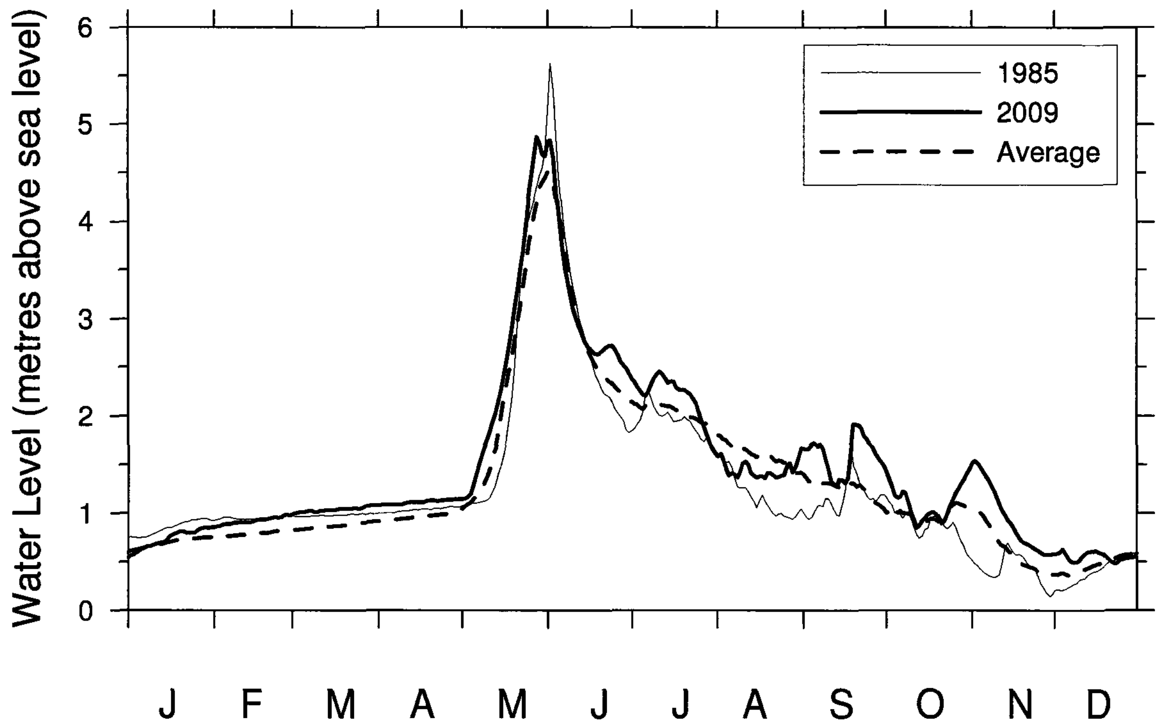

Figure 3.2. Daily mean water level of the Mackenzie River (East Channel) at Inuvik (Station 10LC002). The heavy solid line is 2009, and the light solid line is the year of highest spring peak on record (1985). The dashed line is the average level taken from the eight complete records available for the past 25 years (1985–1988, 2002, 2006, 2007, 2009). Datum is mean sea level at Tuktoyaktuk, NWT. Water Survey of Canada data are available at www.wsc.ec.gc.ca/hydat/H20/index_e.cfm?cname=main_e.cfm.

and early winter of the study period are generally representative of normal conditions.

The Mackenzie Delta contains 49,046 lakes (Emmerton et al., 2007), which are estimated to contain 5.4 km^3 of water during the post-flood period of summer. Lakes cover 15–30% of the area of the southern delta, 30–50% of the middle delta, and <30% of the delta north of treeline (Mackay, 1963). The annual hydrograph is the primary control on the hydrology of delta lakes, which are refilled by spring flooding and then lose water through evaporation and drawdown from connected channels for the remainder of the open-water period (Bigras, 1990). When measured at low water, few delta lakes exceed 10 feet (3.05 m) in depth (Mackay, 1963).

Delta lakes may be classified according to the frequency with which they flood. This depends upon the maximum elevation of the deepest portion of the distributary channel thalweg connecting the lake to the channel network, or, if no connecting channel is present, the lowest elevation of the levee between the lake and channel (Marsh and Hey, 1989). Mackay (1963) classified the delta into three subregions on the basis of sill elevation, as shown in Fig. 3.3. Bigras (1990) classified delta lakes as "connected" or "perched". Connected lakes (also termed "no-closure", Marsh and Hey 1989) are joined to the delta channel network by well-defined distributary channels which remain water-filled from spring break-up to autumn freeze-up. This permits the continual exchange of water between the lake and channel network through the open-water period. Perched lakes may be further defined as "high-closure", "low-closure", or entirely disconnected. High-closure lakes, due to their relatively high sill elevations and the flooding regime of the delta, do not flood annually in the spring, and never later in the summer. Low-closure

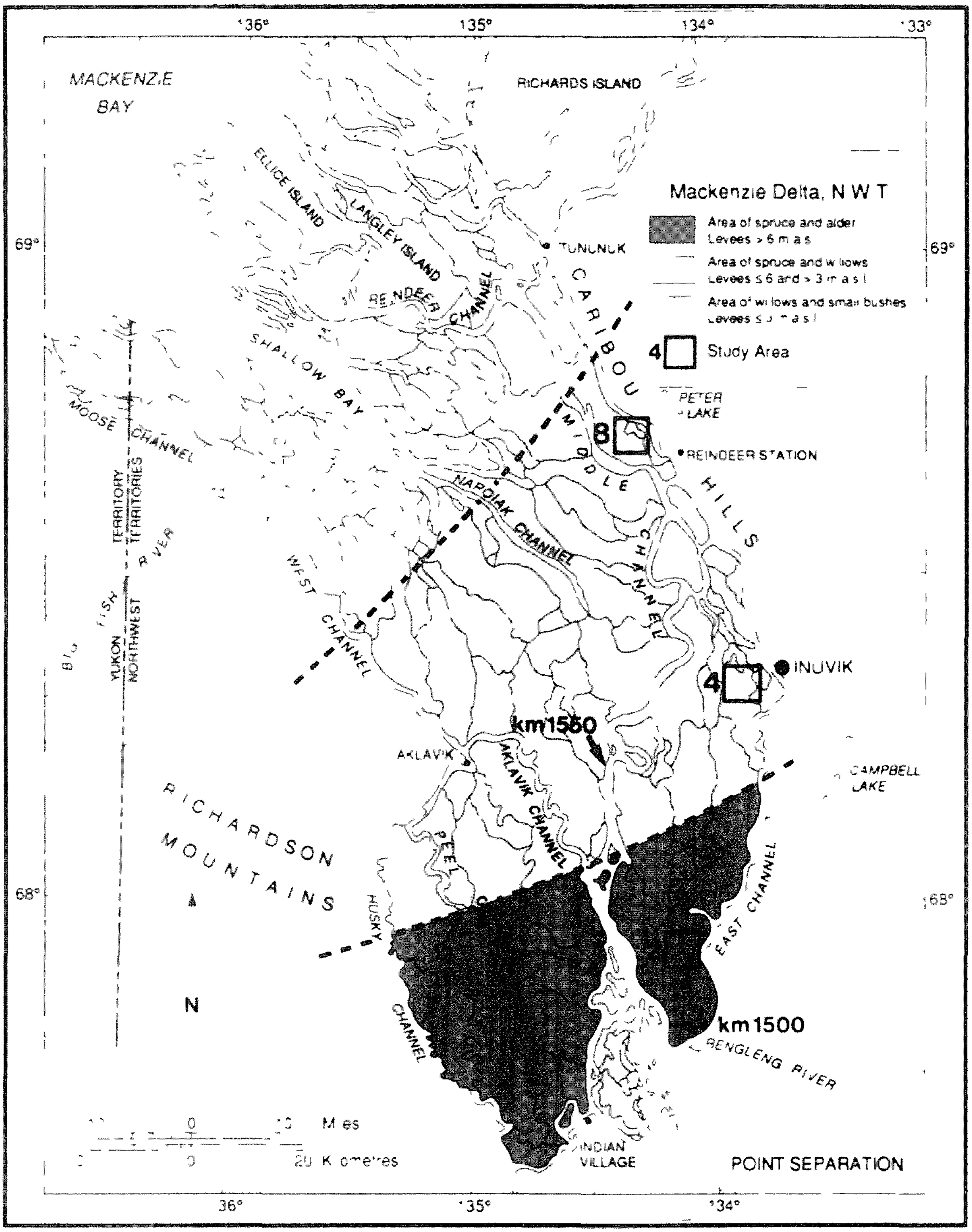

Figure 3.3. Zones of typical levee or sill elevation for Mackenzie Delta lakes. Source: Bigras (1990, Fig. 1), based on Mackay (1963).

lakes do flood annually in the spring, but are then cut off from the channel network for at least a brief period later in the summer (Marsh and Hey, 1989). High- and low-closure lakes typically occur in the south/central and north/central regions of the delta, respectively (Bigras, 1990). The lake classifications of high-, low-, and no-closure, originally proposed by Mackay (1963), were quantified by Marsh and Hey (1989) for a study site in the east-central delta. Ranges in sill elevation (metres above sea level) were determined for each lake class (Fig. 3.4), and on this basis the study lakes were apportioned among the categories. Water colour during summer indicates whether a lake is connected to the channel network (brown and turbid) or disconnected (dark).

Delta lake ice cover typically forms in late October, and remains until late May or early June (Mackay, 1963). Channel ice generally forms 1–2 weeks after lake ice, and disappears approximately two weeks earlier in spring (Burn 1995). In permafrost environments, lakes and channels produce the greatest local departure from climate-induced ground temperature (Lachenbruch et al., 1962). Mean annual lake-bottom temperatures at maximum depth have been found to be 3°C, 5.7°C, and 6.0°C at sites on northern Richards Island, in taiga uplands near Inuvik, and in the eastern portion of the central delta (NRC Lake), respectively (Burn and Kokelj, 2009). The width of delta lakes and channels, in conjunction with above-zero mean annual bottom temperatures, often results in a talik which penetrates permafrost (Mackay, 1963; Smith, 1976; Burn, 2002).

3.1.5 Vegetation

The Mackenzie Delta is a site of ecological transition, where subarctic boreal (taiga) forest and low-shrub tundra ecological regions meet. Open spruce woodlands with thick

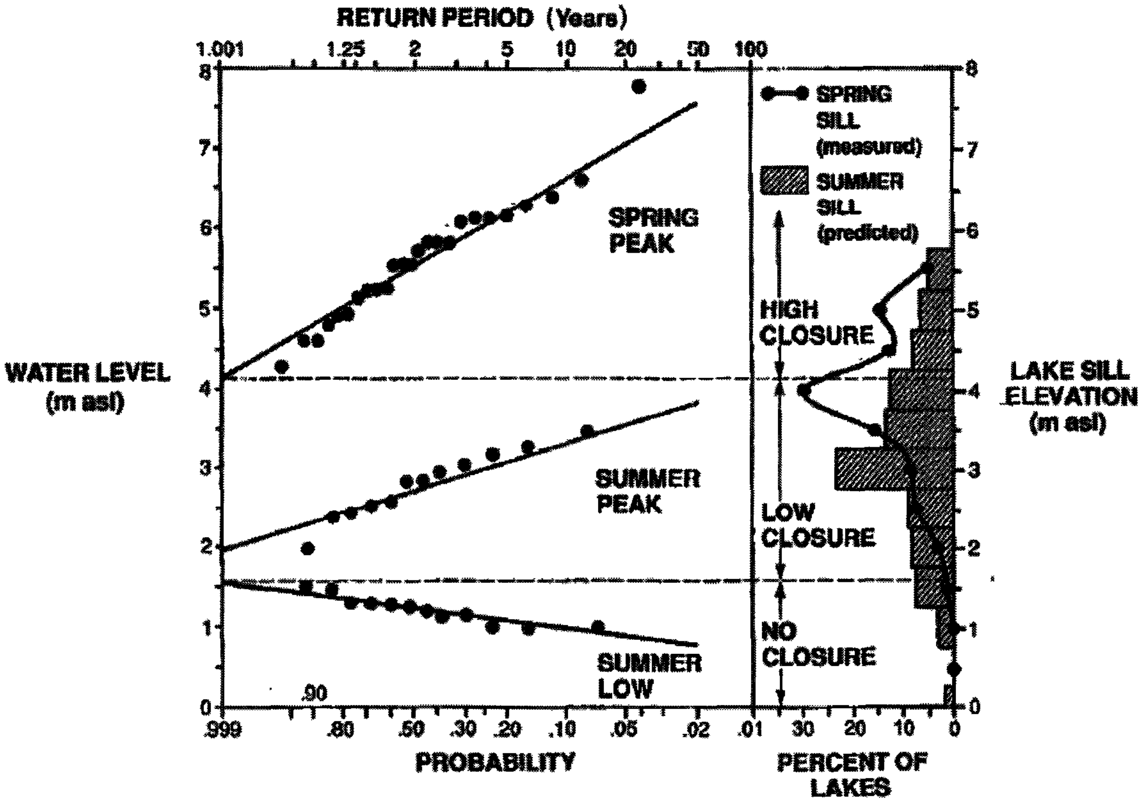

Figure 3.4. Return periods of extreme spring and summer peaks, and summer lows for East Channel at Inuvik. The right side shows the measured spring and estimated summer sill levels for the NRC Lake area. Data are from Marsh and Hey (1989). Source: Marsh and Lesack (1996, Fig. 2).

surface peat layers characterize the southern portion of the delta region (Mackay, 1963). Through the forest-tundra transition zone (approximately 68°30' to 69°30' N), tree cover declines in favour of tall shrubs. Further north, vegetation communities are composed of sedges and dwarf shrubs less than 75 cm in height (Mackay, 1963), including willow (*Salix* spp.), alder (*Alnus crispa*) and ground birch (*Betula nana*).

Within the delta, flooding and sedimentation are the primary influences on vegetation succession (Gill, 1972). Willows grow on aggrading point-bars in mineral soils, and alders in poorly-drained areas (Burn and Kokelj, 2009). Above the elevation of annual flooding in the southern delta, white spruce (*Picea glauca*) forest represents the final successional stage. Prior to this, as surfaces aggrade and flood frequency decreases, spruce/alder bearberry (*Arctostaphylos rubra*) and then spruce/feathermoss communities thrive. Section 2.3 and Fig. 2.7 describe and illustrate vegetative succession in a point-bar environment. Boreal forest extends further north in the delta than on adjacent uplands. Variations in vegetation community structure influence snow accumulation within the delta. Snow blown from channels and lakes may be trapped by tall willows adjacent to water bodies, causing talik formation (Gill, 1972). Closed canopy spruce forest intercepts snowfall, resulting in greater winter heat loss from the ground and relatively low ground temperatures (Burn and Kokelj 2009; Kanigan et al., 2009).

3.1.6 Permafrost

Continuous permafrost underlies the uplands surrounding the Mackenzie Delta. Within the delta permafrost is continuous, as over 90% of the land surface is underlain by perennially frozen ground (Nguyen et al., 2009). This is despite the relatively warm ground caused by the abundance of water bodies and shifting of channels (Smith, 1976). Delta permafrost thickness, generally <100 m, is variable and may exceed 100 m in some areas, especially in the outer delta where sediments are being deposited over formerly submerged permafrost (Smith and Burgess, 2002). In the new emerging sedimentary environments of the outer delta, permafrost is thin, though aggrading (Dyke, 2000). Uplands east and west of the delta, glaciated until the end of the Wisconsinian, are underlain by permafrost approximately 100 m thick (Allen et al., 1988). Regions unglaciated for much of the Pleistocene, including northern Richards Island and portions of the outer delta submerged during the Holocene, have permafrost approximately 500 m thick (Burn and Kokelj, 2009).

Ground thermal regime is distinctive between the four main ecological units of the delta region, as shown in Fig. 2.8. The spatial variation of ground temperature in the delta region was discussed in section 2.3. Figure 3.5 illustrates near-surface ground temperature measured between 2003 and 2007 in the delta area. Comparisons between these MAGT values and those observed by Brown (1966a) and estimated by Mackay (1967) reveal an increase of 1 to 3°C over the past four decades.

Ground ice is present in Mackenzie Delta sediments predominantly as pore ice, due to sediment deposition in channels and subsequent freezing due to channel migration (Williams, 1968; Smith, 1976). Syngenetic ice wedges account for much of the high ice content in the uppermost 5 m of permafrost. Ice wedges crack periodically in the outer delta under present climatic conditions (Burn and Kokelj, 2009). The melting of ground ice is responsible for the thermokarst expansion of lakes in the delta and adjacent uplands.

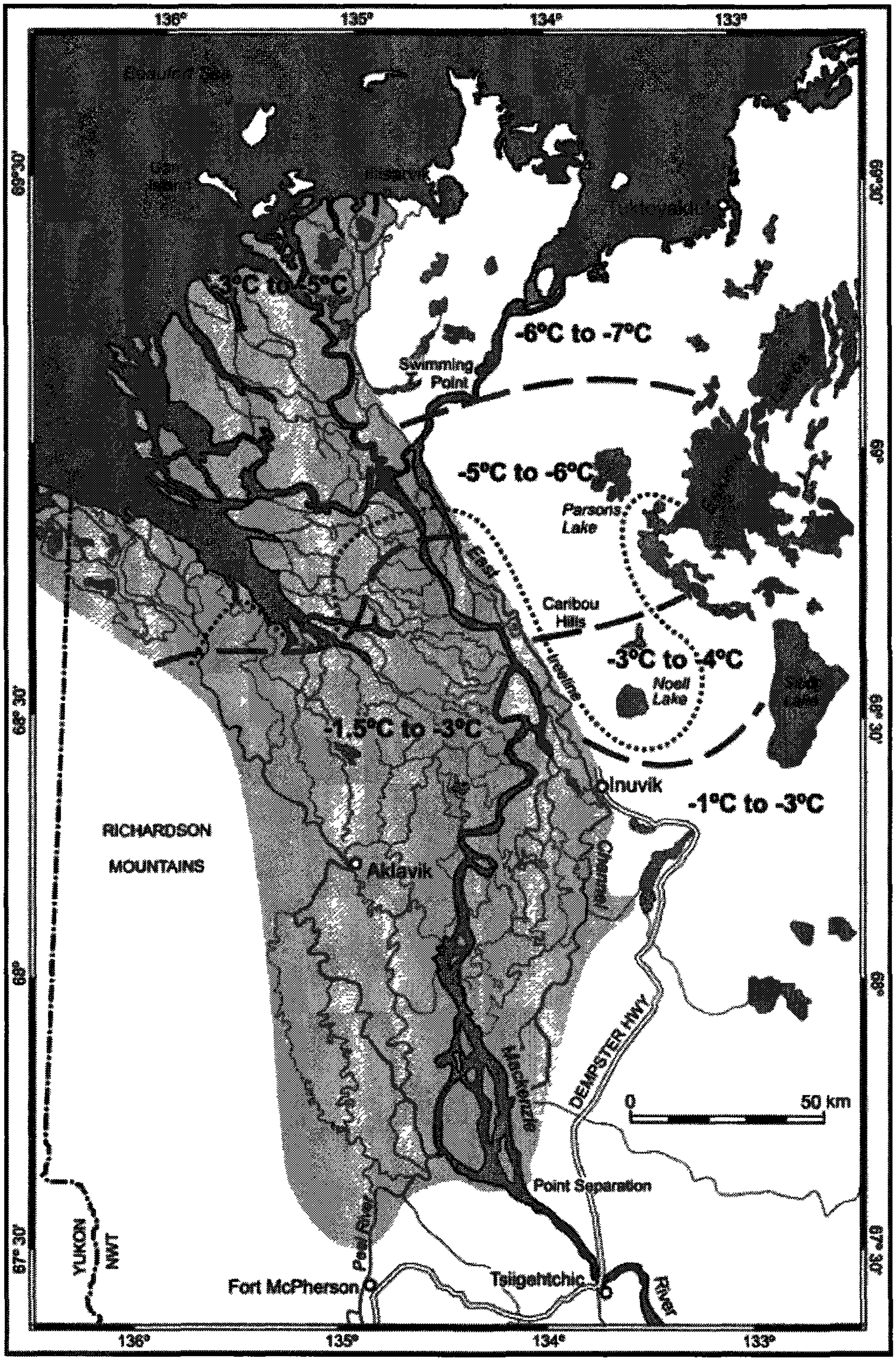

Figure 3.5. Near-surface ground temperatures measured between 2003 and 2007, Mackenzie Delta area. Source: Burn and Kokelj (2009, Fig. 11).

The presence of adjacent and subjacent ground ice is thus an important control on lake stability, and the thawing of solute-rich permafrost influences lake chemistry (Kokelj et al. 2005).

3.1.7 Infrastructure and Development

The varied climatic, geomorphic, and ecological conditions and histories within the Mackenzie Delta region create diverse permafrost conditions. These conditions present opportunities for scientific study, and pose unique challenges to the development of civilian and resource infrastructure. Since the 1960s the delta has seen considerable hydrocarbon exploration. Quite recently, the Mackenzie Gas Project – a proposal to develop three gas fields and construct a pipeline from the outer delta to northern Alberta – has received the conditional support of the National Energy Board. Management decision making must consider the intricacies of ground thermal regime, ground ice distribution, hydrologic regime, and the impacts of observed and anticipated climate warming in the western Arctic on these and other factors (Burn and Kokelj, 2009). Environmental data sets must be expanded and developed in many of these areas to enable informed decisions.

3.2 Research Methods

3.2.1 Site Selection

Initial selections of lake and channel sites were made using 1:30,000 aerial photographs taken over the Mackenzie Delta in August 2004. Criteria for site selection were good north-south and east-west coverage of the delta; geographically proximate groupings of channel, connected lake, and perched lake sites; and reasonable boat accessibility for all channel and connected lake sites.

Lake connectivity was characterized by the presence or absence of distributary channels connecting with the channel network. Late-summer lake colour was also indicative of connectivity. Dark water indicates high water clarity and little or no connectivity, whereas lighter, turbid water indicates high connectivity with the channel network (Burn and Kokelj, 2009). Thirteen channel sites and 17 lake sites were selected, ranging from the Inuvik area in the east to near Aklavik in the west, and from the divergence of the Husky and Peel channels in the south to a site along Harry Channel at Taglu in the outer delta (Fig. 3.6). Sites were examined from a helicopter in June 2009 to confirm lake connectivity. Sample lake imagery, from August 2004 and June 2009, is presented for Lakes 1 and 2 in Fig. 3.7.

3.2.2 Instrumentation

3.2.2.1 Thermistor Cable

For periodic temperature measurements, a graduated 21-metre cable with a thermistor and weighted tip was connected to a multimeter. Thermistor resistance values were adjusted by +5 Ω, as prescribed by calibration in a 0°C ice bath, and then converted to °C using the method presented in Appendix A.

3.2.2.2 Temperature Loggers

Thirty Hobo Watertemp Pro v.2 (Onset Data Corporation) submersible temperature data loggers (Fig. 3.8) were programmed to take temperature readings at 0:00, 04:00, 08:00, 12:00, 16:00, and 20:00 each day.

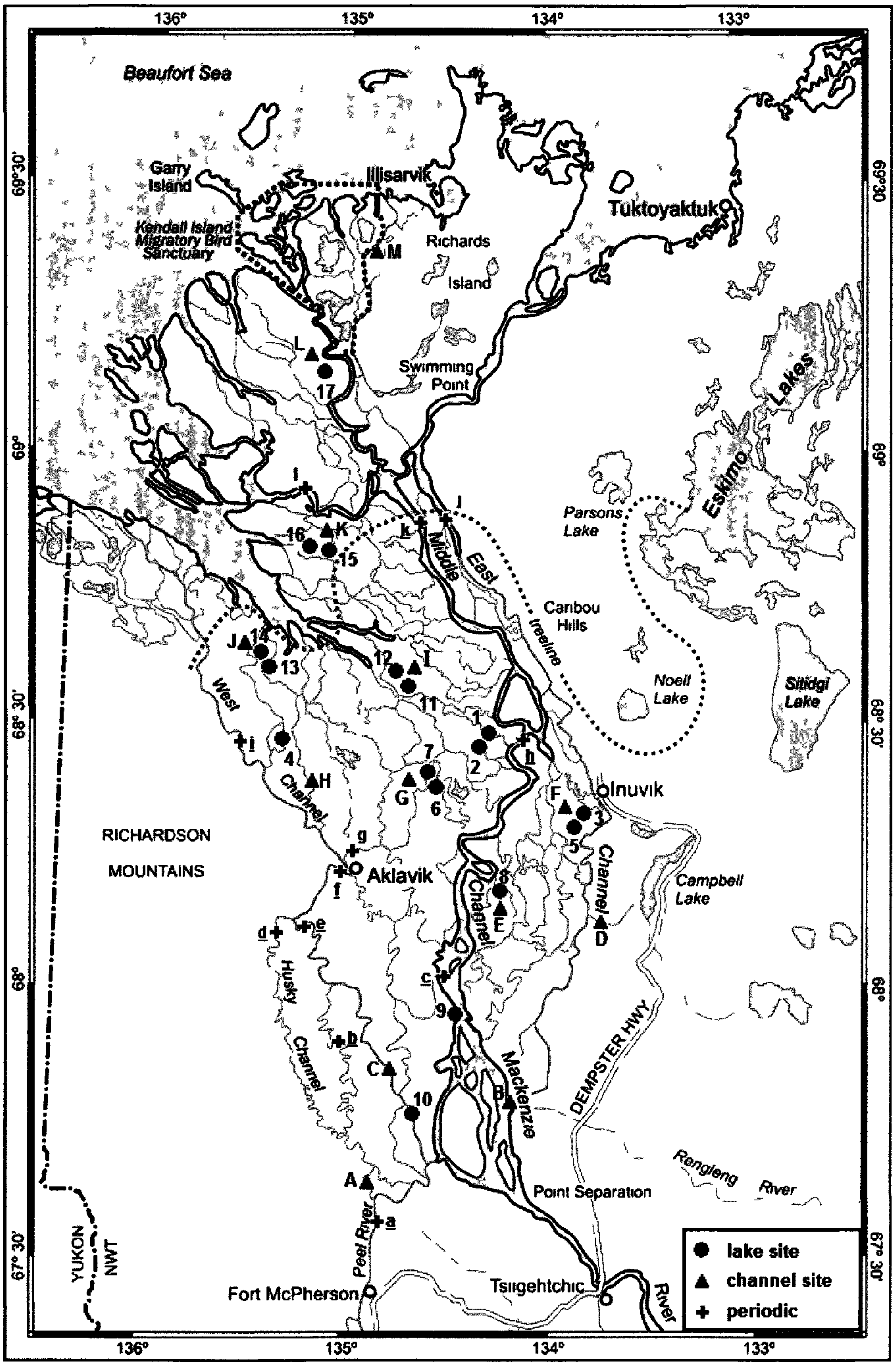

Figure 3.6. Lake and channel sites in Mackenzie Delta instrumented for continuous temperature record, June 2009–2010. Also shown are locations of periodic channel temperature measurement during summer 2009. Lakes, channels, and sites of periodic measurement are labelled with numbers, capital letters, and underlined lower-case letters, respectively.

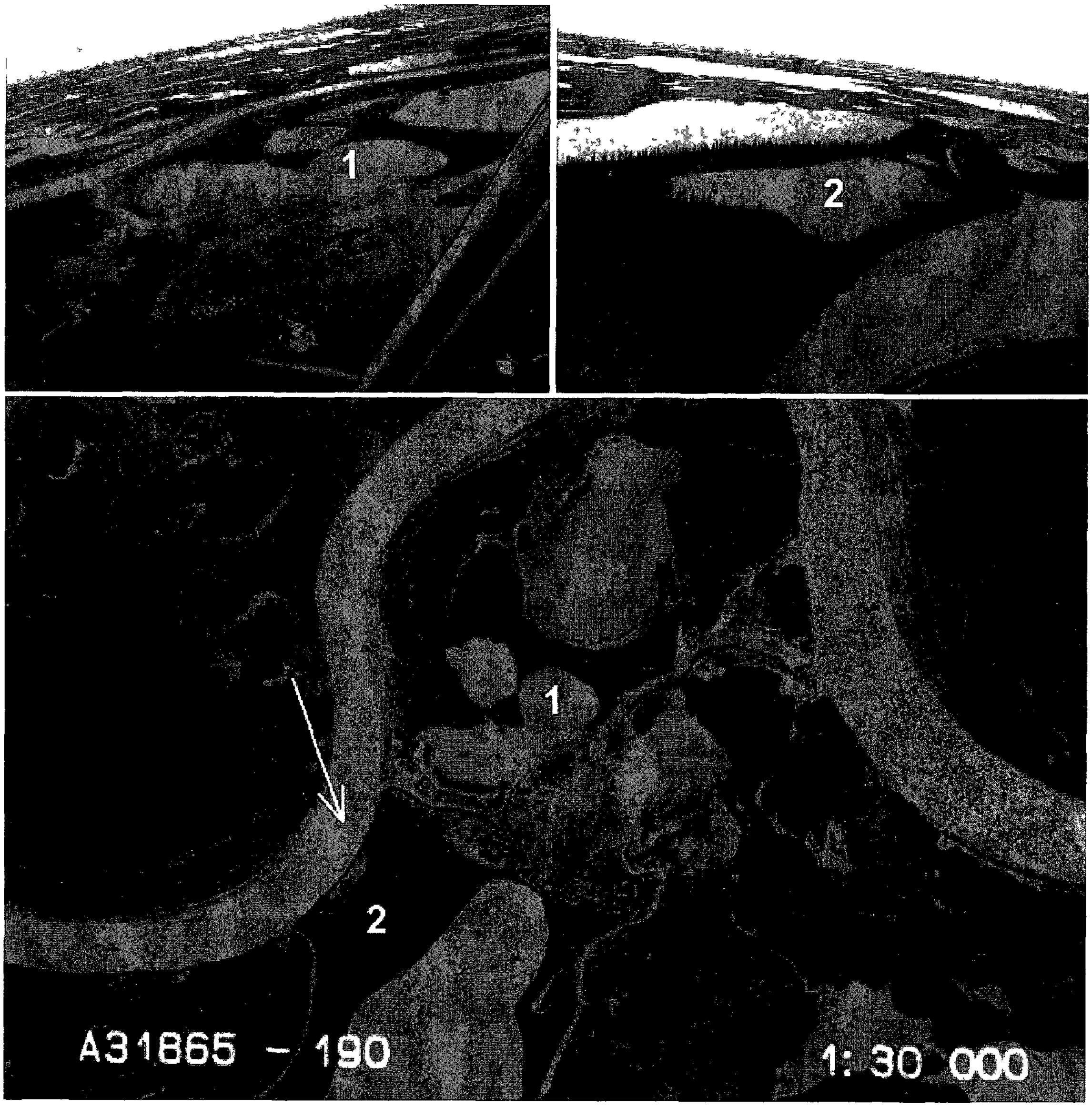

Figure 3.7. Lake 1 (connected) and 2 (perched) in August 2004, and as observed by helicopter in June 2009 (top frames). Arrow indicates Lake 2 view angle from helicopter.

Figure 3.8. Submersible temperature data logger ready for deployment.

Logger manufacturer specifications indicate an instrument accuracy of ±0.2°C and a resolution of 0.02°C for the range 0–50°C. To confirm proper calibration, fifteen of the loggers were placed in a container and stirred regularly as water temperature was brought from 22°C to 0°C over three hours in a large freezer maintained at -10°C. Three data loggers in the container (Campbell Creek, Hope Lake, and Channel I) were known to provide temperature measurements with mean and maximum deviations of 0.133°C and 0.137°C, respectively, from concurrent measurements using the calibrated thermistor cable. The mean of these three loggers for each measurement over the range of temperatures, adjusted by -0.133°C, was taken as the temperature standard. The relation between these standard temperatures and readings from the Channel K data logger during the calibration check is shown in Fig. 3.9. Appendix B presents relations with temperature standard for the remaining 14 loggers. All readings from each logger were within 0.2°C of standard temperatures through the 0–22°C range tested. Given this rate of adherence to specifications, it was assumed that the 15 loggers not checked also performed within specifications.

3.2.3 Bathymetry and Field Installation

To guide logger deployment and characterize bed morphology, a coarse bathymetric survey was conducted at each lake and channel site in June 2009 using a GPSMap 168 Sounder (Garmin Corporation; Fig. 3.10). Bathymetric profiles were created across-channel, and through the centre of study lakes where possible.

One temperature logger was installed at each channel or lake site between 9 and 25 June, 2009. Figure 3.11 illustrates deployment schemes used for lakes and channels. For

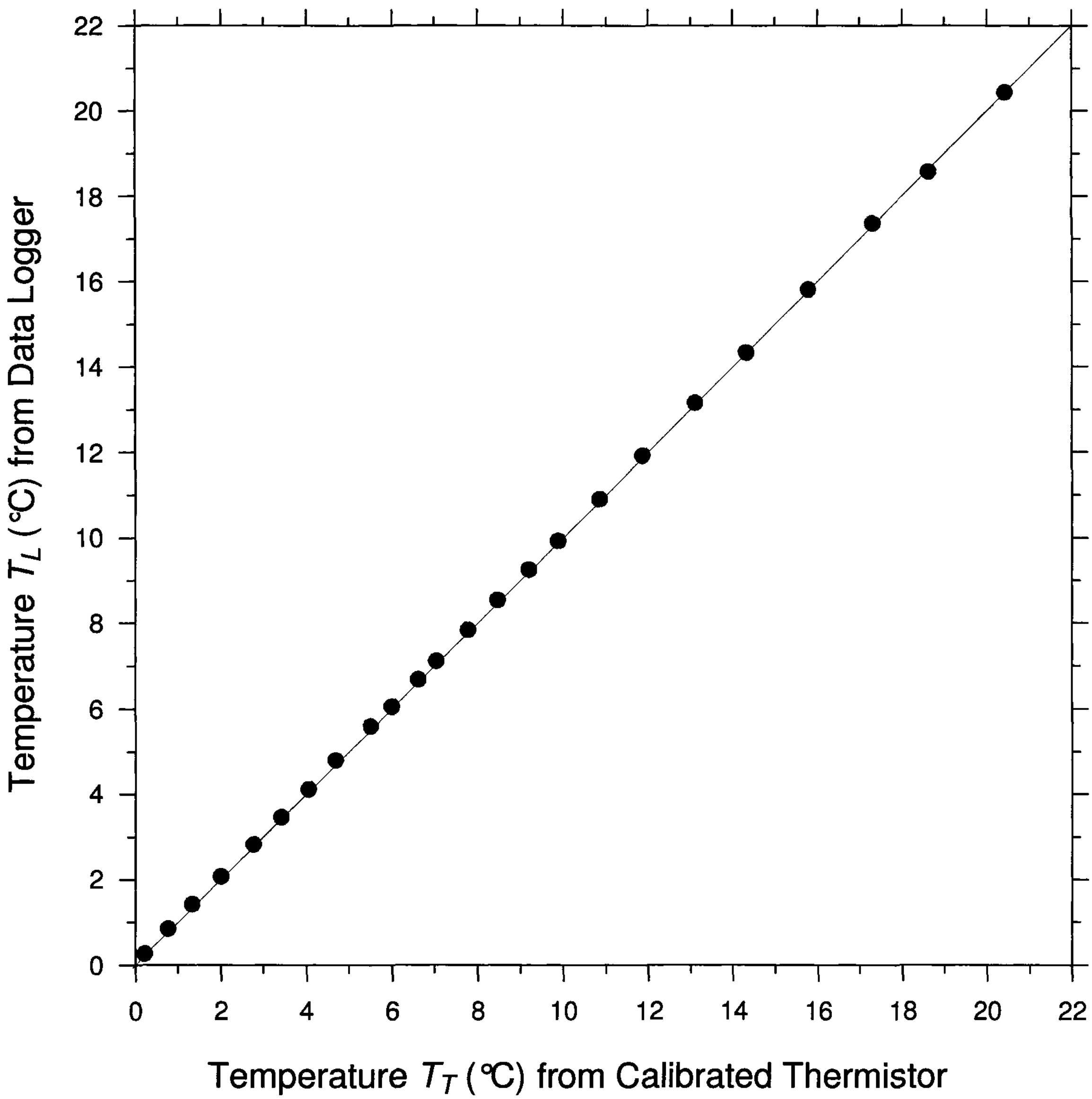

Figure 3.9. Relation between standard temperature T_T and measurements T_L by Channel K data logger (black dots) in laboratory ice bath. Solid line has 1:1 slope, for reference.

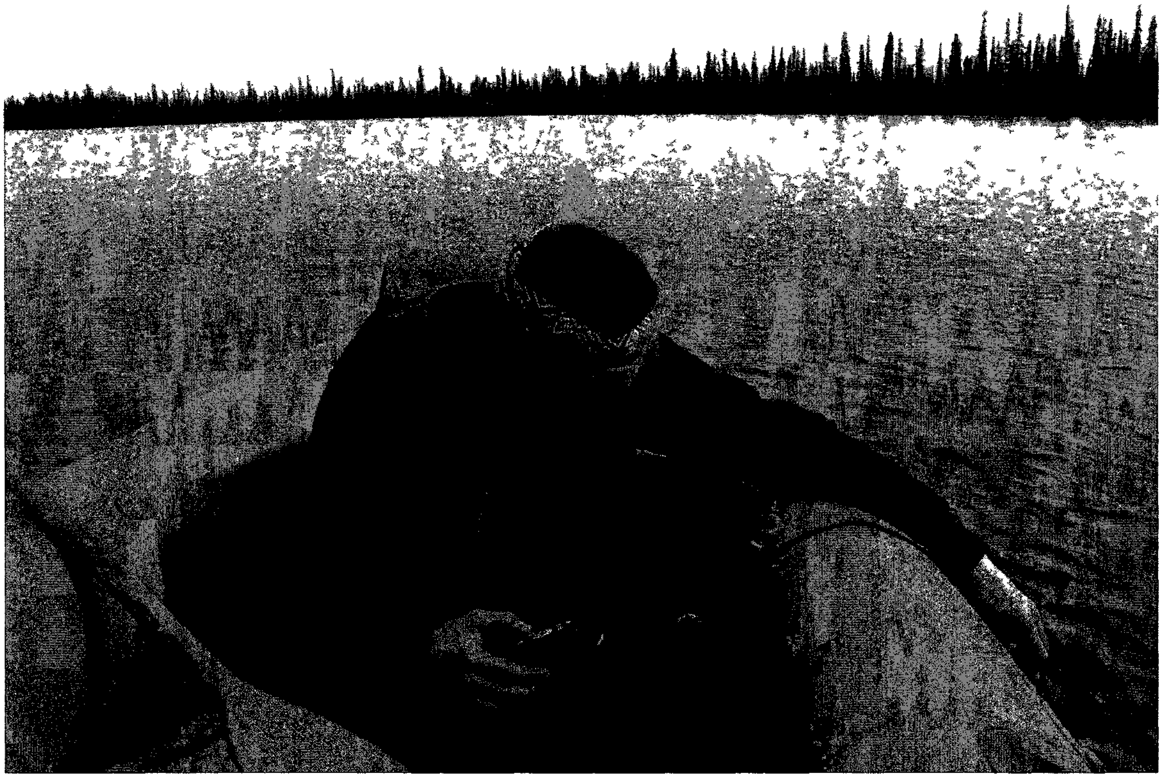

Figure 3.10. Bathymetric survey of Lake 7. The handheld sounder and GPS unit enable the simultaneous collection of depth measurements and geographic coordinates.

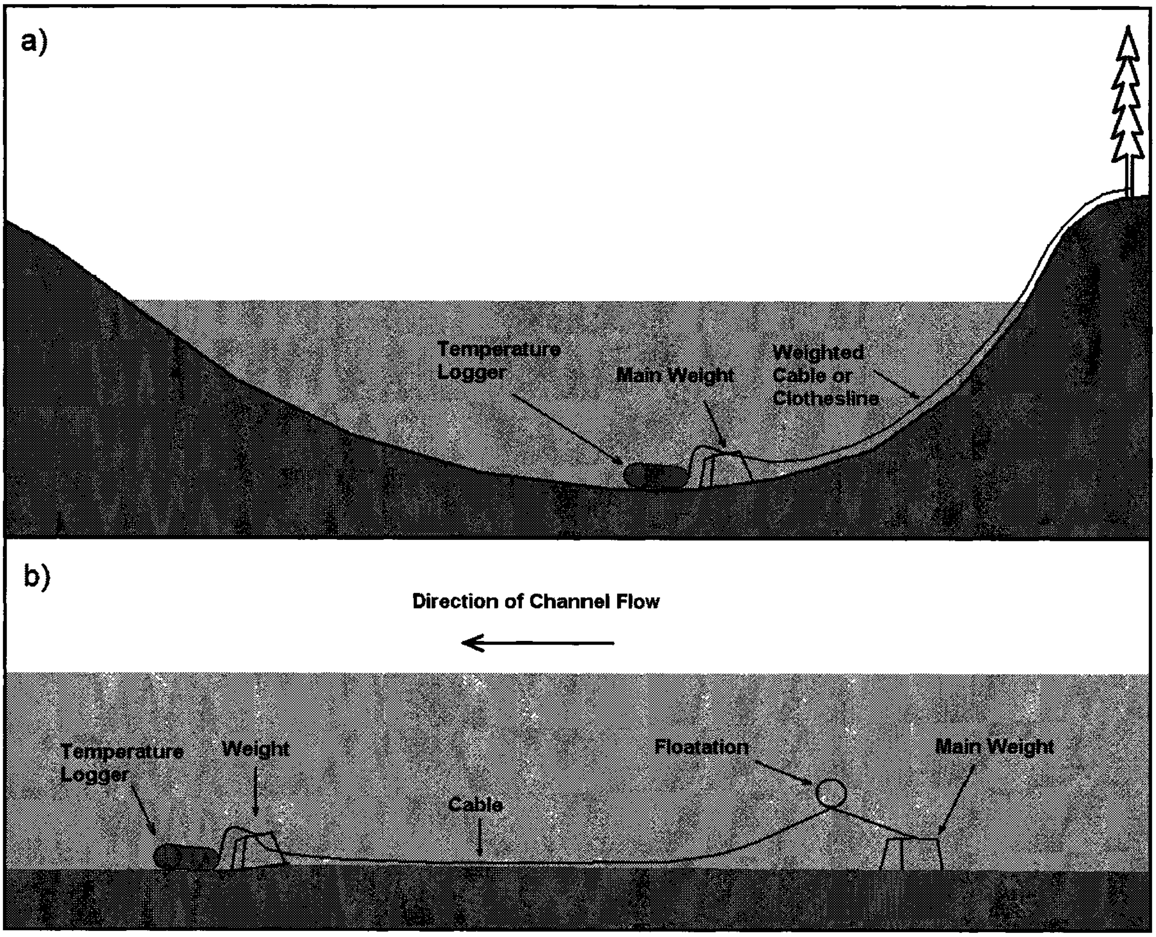

Figure 3.11. Data logger deployment schemes for Mackenzie Delta water bodies. Lakes and channels (in summer) are instrumented as in (a), while channels are re-instrumented as in (b) prior to the formation of ice cover in autumn.

summer data collection (Fig. 3.11a), data loggers were weighted to the deepest possible location in a lake or channel and fastened by a light cable to a tree on shore. For curved channels, the data logger was deployed as close as possible to the thalweg, usually found closer to the outside bank. Cables were weighted to the bottom to reduce the risk of fouling boat propellers or snagging submerged or floating debris. To reduce the risk of instrument loss arising from the down-channel movement of ice during spring breakup, data loggers were re-deployed at all channel sites in August 2009 with no cable extruding from the water surface (Fig. 3.11b). Under this winter deployment scheme, each channel data logger was fixed to a cable running along the thalweg parallel to channel flow between two large weights. A small buoyant canister was used to keep the cable from resting on bottom immediately downstream of the initial weight, to enable retrieval with a submerged extendable hook. The locations of the upstream and downstream limits of the cable at each channel site were recorded using a GPS, and retrieval attempts at the time of deployment were successful. In June 2010, six of the 13 channel loggers were successfully retrieved. Figures 3.12 and 3.13 show logger installation locations within bathymetric cross-sections obtained for most lake and channel locations. Previous examinations of Mackenzie Delta lake bathymetry have revealed that lake-bottoms commonly drop off quickly near shore and have relatively flat bottom topography (Fee et al. 1988, Marsh and Bigras 1988). Some channel bathymetries included abrupt depth changes (Fig. 3.13), however such distinctive features are also apparent in the bathymetric profiles presented by Mackay (1963, pp. 114-117) for Mackenzie Delta channels.

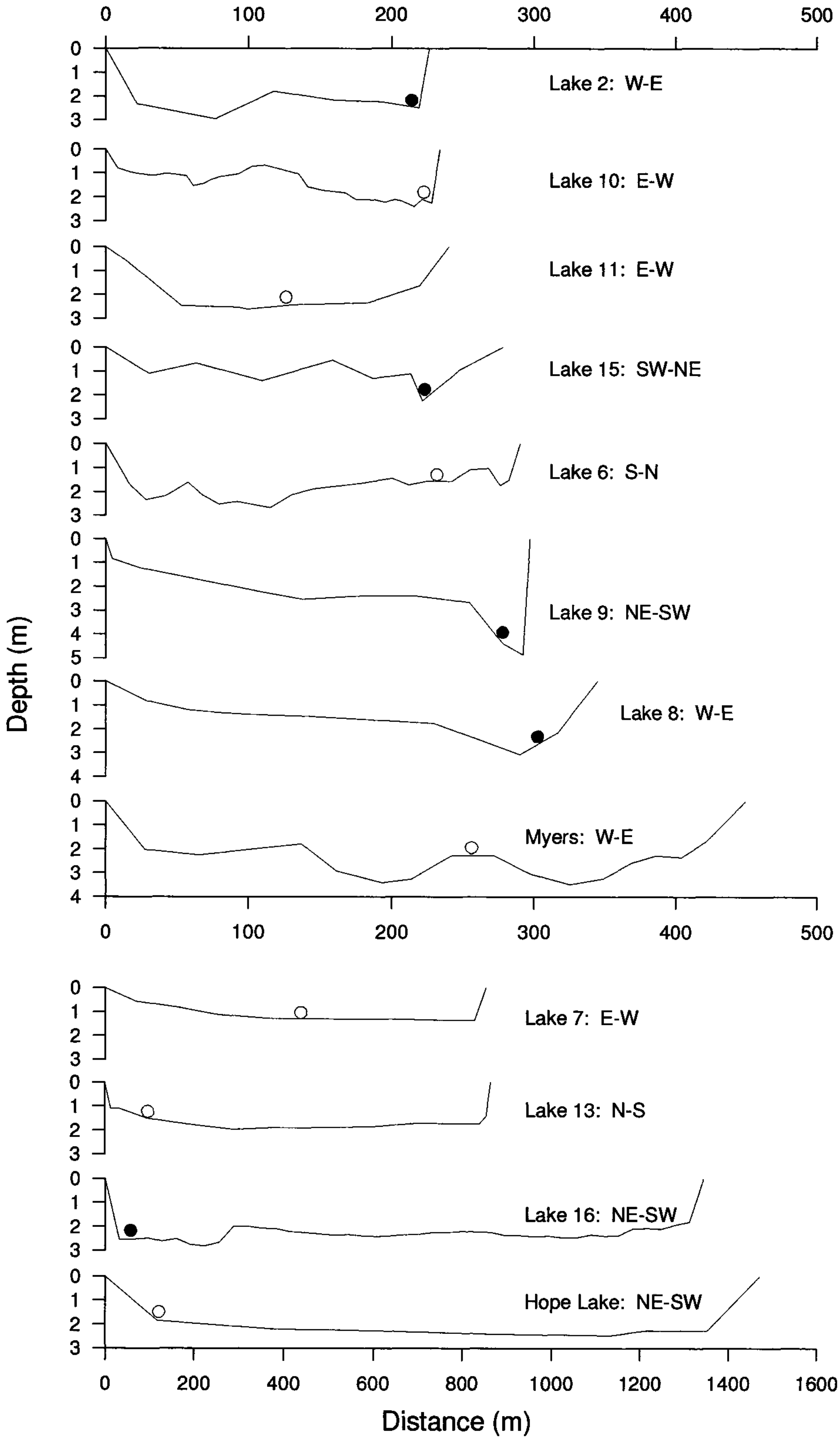

Figure 3.12. Bathymetric cross-sections for study lakes. Cross-section orientations are indicated in labels. Black circles indicate temperature logger locations within cross-section. Open circles indicate data loggers not aligned with cross-section.

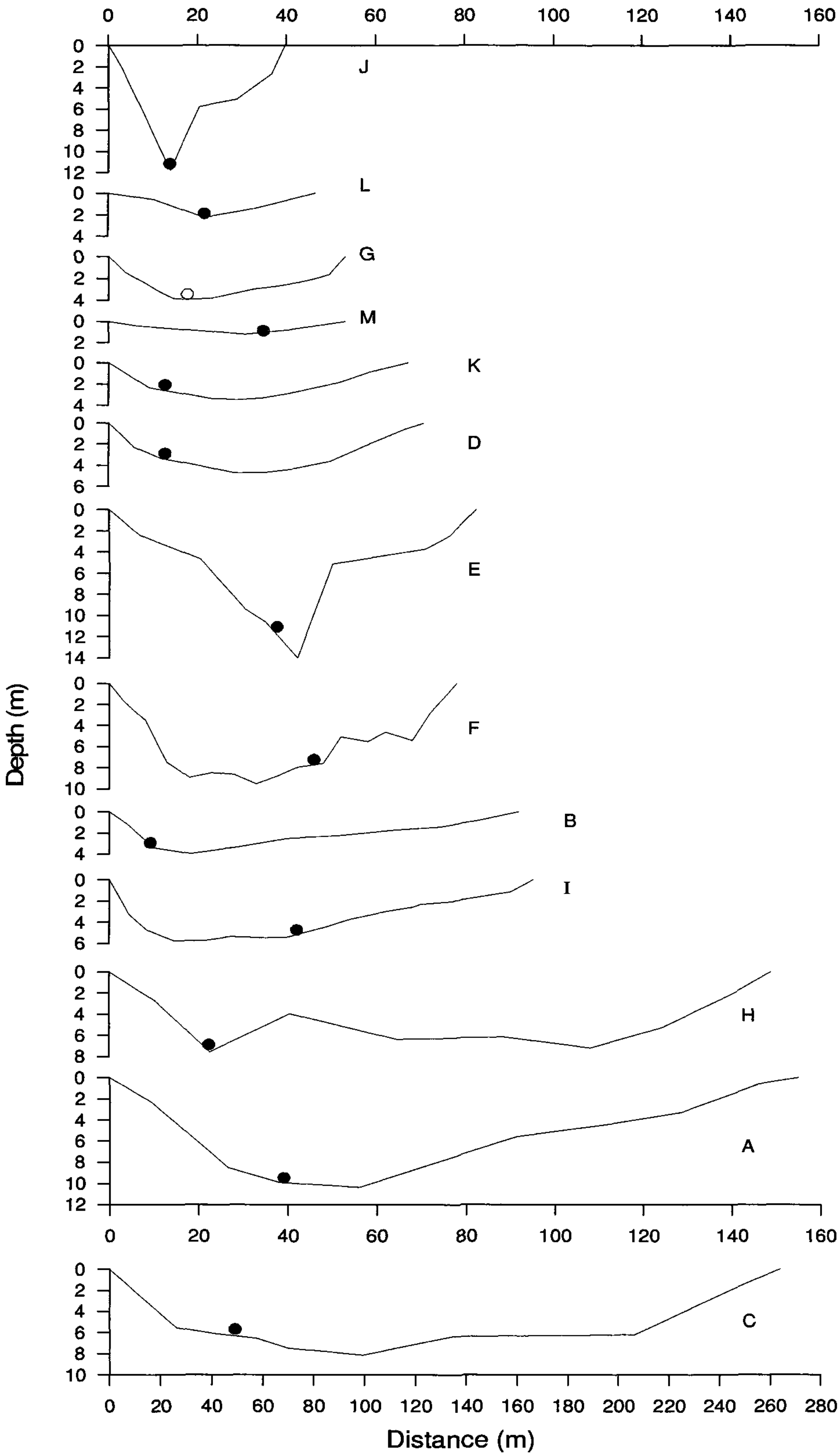

Figure 3.13. Channel bathymetric profiles, from left upstream bank to right upstream bank. Data loggers are indicated as in Fig. 3.12.

3.2.4 Data Analysis and Modelling

After the recovery of temperature loggers, data were transferred from each to a portable field data shuttle by an optical Universal Serial Bus interface. Once transferred to a computer, data were converted to Microsoft Excel format to enable a variety of analyses including the calculation of a MAWT for each series.

3.2.4.1 Critical Dimensions for Through Talik Occurrence

Mackay (1962, pg. 39) presents the following two equations which together relate lake MAWT T_w (°C), surrounding MAGT T_g (°C), and the critical lake radius R (m) beyond which a through talik will occur beneath a circular lake under steady-state conditions:

$$R = [(IBz)^2/(IB+IT_g+z)^2 - z^2]^{0.5} \tag{8}$$

$$z = I[(B^2T_w)^{1/3} - T_w] \tag{9}$$

The variable B is defined as $(T_w - T_g)$, z is the maximum talik depth beneath the lake centre (m) before the occurrence of a through talik, and I is geothermal gradient (m°C^{-1}) as previously described. When the range of mean annual near-surface ground temperature (MAGT) values presented for the delta region by Burn and Kokelj (2009, p. 98) is used for T_g, and an I value of 40 m°C^{-1} is adopted (as in Smith 1976, p. 21; Burn 2002, p. 1293), the relation between R, T_w, and T_g may be illustrated as in Fig. 3.14.

In the case of elongate lakes and channels, critical half-width for through talik development may be determined by iteratively solving Eq. 6 (Section 2.5). Figure 3.15 presents the relation between critical half-width, T_w, and T_g, over a range of T_w, and T_g, values. Available lake and channel geometries, specific T_w, and the range of T_g values

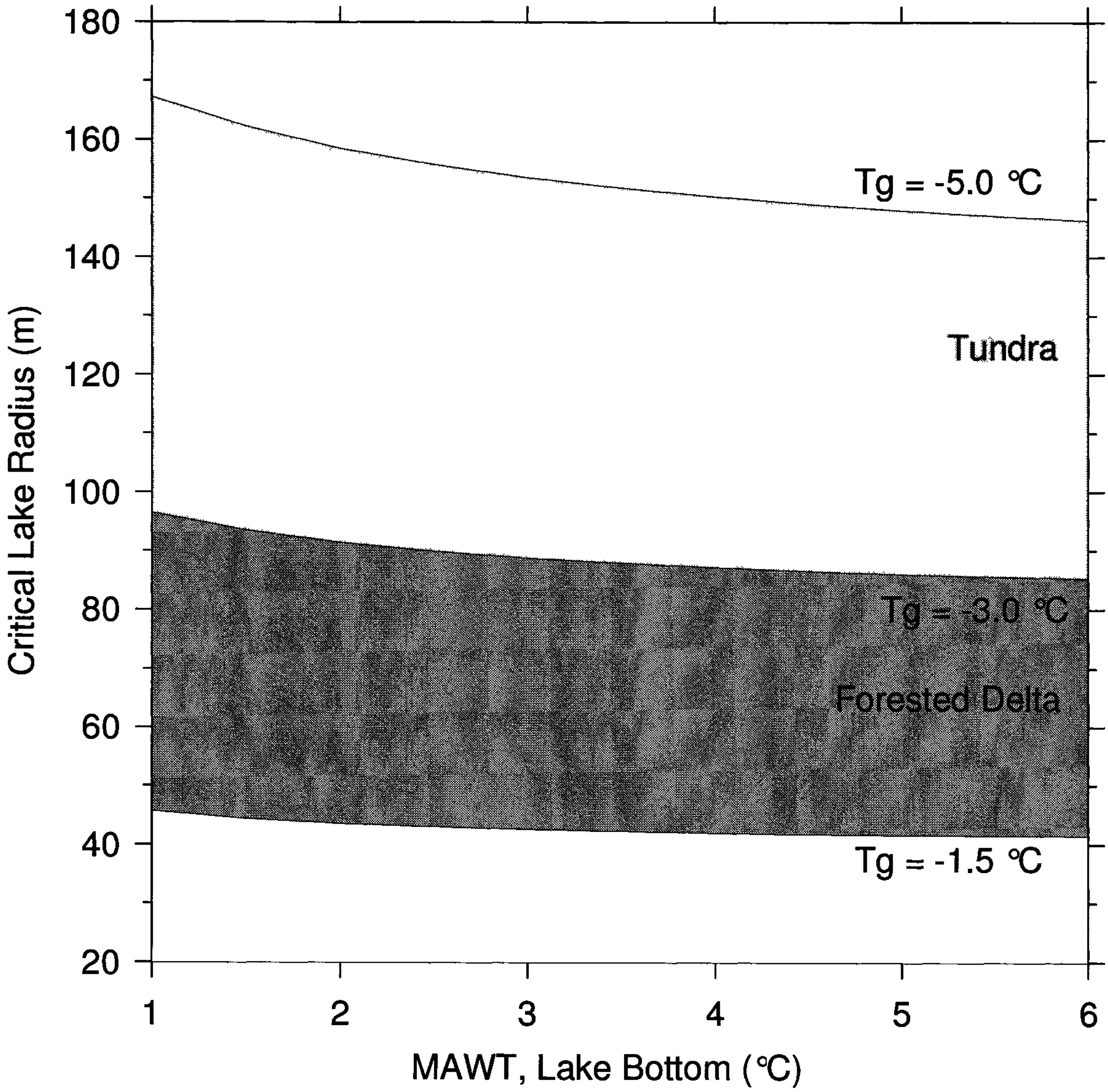

Figure 3.14. Critical radii for the occurrence of through taliks beneath circular Mackenzie Delta lakes, obtained using equations 8 and 9. The ranges provided for mean annual near-surface ground temperature Tg correspond with those determined for forested and tundra regions of the Mackenzie Delta (Burn and Kokelj, 2009).

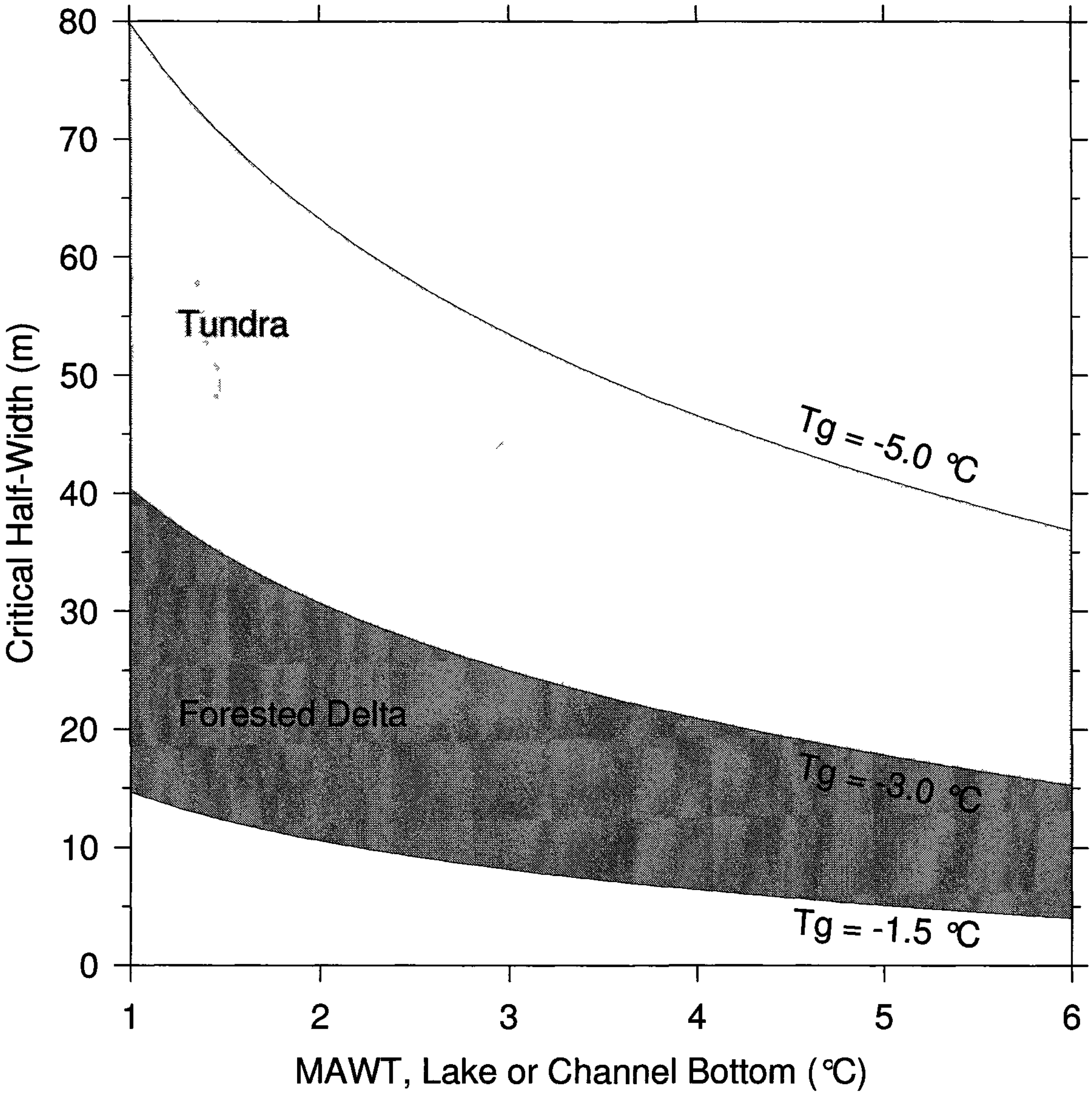

Figure 3.15. Critical half-widths for the occurrence of through taliks beneath elongate lakes and channels in the Mackenzie Delta, obtained iteratively using equation 6. The ranges provided for mean annual near-surface ground temperature Tg correspond with those determined for forested and tundra regions of the Mackenzie Delta (Burn and Kokelj, 2009).

identified for the delta enable the prediction of through talik occurrence beneath elongate water bodies. While 40 m°C^{-1} is adopted as I in all modelling in this thesis, the geothermal gradient is known to vary around this value (between 20 and 30°C/km, or 33 to 50 m°C^{-1}) within the Mackenzie Delta (Pelletier, 1987).

3.2.4.2 Lake and Channel Dimensions

Channel and lake widths, required for the prediction of through talik occurrence, are obtained from vector shapefiles representing all water polygons in the Mackenzie Delta. These shapefiles, produced from the 1:50,000 National Topographic Series, were obtained online from the CanVec database available through GeoGratis (Natural Resources Canada, 2009). Using ArcView Geographic Information System v. 9.2, the polygons representing perched and connected lakes in the forested and tundra regions of the delta were edited to achieve as close as practical to a 1:1 relationship between polygons and lakes. Lake polygons were classified as connected if a linkage to the channel network was present in the form of a polygon. No line features were used. Once edited, area calculations were made for each lake polygon.

As in Burn (2002), each lake polygon was fitted with a minimum bounding rectangle (MBR). This was achieved through the download of the open-source MBR script from Environmental Systems Research Institute (2009), and its execution in a GIS to append MBR geometric properties (length, width, area) to attribute tables for all lake polygons in the Mackenzie Delta. Those lakes with MBR lengths equal to or greater than twice their MBR width value were classified as elongate. Where MBR area was greater than twice that of the associated lake polygon, the lake width was taken as lake polygon area divided by MBR length, to prevent the overestimate of talik area. Lake and MBR geometries in GIS attribute tables were imported to a spreadsheet, where a series of IF statements enabled the enumeration of lakes producing through taliks under specified MAWT and MAGT conditions, through the comparison of half-width or radius with calculated critical values.

Channel network width distribution was determined in a GIS by reducing channel network width in steps of 50 m until no channel network area remained. At each step, the total length of the resulting diminished channel network was calculated, as was the total area (using actual widths) of the portion of the channel network not truncated.

3.2.4.3 Mean Annual Water Temperature

In estimating through talik abundance in the Mackenzie Delta, two sets of MAWT values were used for each water body. In the 'Observed' series of MAWT values, each perched lake, connected lake, and channel in the delta is assumed to have a MAWT equal to the average among MAWT values measured respectively at perched lake, connected lake, and channel sites in the same region (forest or tundra) of the delta for the period June 2009–June 2010. The 'Adjusted' MAWT series for water body x (Adj. MAWT_x) provides estimates exactly as above, however it relies on an existing four-year temperature record for NRC Lake, and is calculated as follows for each delta water body:

$$\begin{aligned}
&\text{Adj. MAWT}_x \\
&= \quad \text{Obs. MAWT}_x \; + \\
&\qquad [(\text{NRC Lake MAWT, June 2006–May 2010}) \\
&\qquad - (\text{NRC Lake MAWT, June 2009–May 2010})] \qquad (10)
\end{aligned}$$

where

[(NRC Lake MAWT, June 2006–May 2010)

– (NRC Lake MAWT, June 2009–May 2010)]

= 5.8°C - 6.2°C

= -0.4°C

and Obs. $MAWT_x$ = Observed MAWT for water body *x*

Adjusted MAWT is intended to offer a more representative estimate of through talik area, if inter-annual variation in MAWT for NRC Lake is representative of delta water bodies in general.

CHAPTER 4: MACKENZIE DELTA SUMMER THERMAL REGIME

4.1 Introduction

This chapter examines the summer thermal regime of Mackenzie Delta lakes and channels. Spatial variability within and between water bodies is discussed, as is the temporal variability of the thermal regime at diurnal and daily scales. Potential controls on spatial and temporal thermal regime are examined. The chapter concludes with a discussion of the significance of the summer thermal regime of delta water bodies within the annual regime.

Continuous measurements of basal water temperature (logged every four hours) were obtained for 17 lakes and 13 channel sites in the Mackenzie Delta during summer 2009. The period of 26 June–10 August 2009 provides concurrent temperature logs from all but two water bodies (Peel Channel and Campbell Creek), and is adopted as the summer period as it provides a basis for the comparison of summer thermal regime among sites. Table 4.1 indicates lake connectivity (perched or connected), perimeter and area, depth, location within the delta, and mean summer water temperature (MSWT; 26 June–10 August 2009) for each site. These lakes are on average larger than the 6.8 ha (0.068 km^2) mean area reported by Emmerton et al. (2007) for Mackenzie Delta lakes. At the time of depth measurement (whose dates in June 2010 coincide with the beginning of the period of temperature record), average study lake depth was 2.9 m. This exceeds the value of 1.5 m, obtained by Emmerton et al. (2007) as the approximate average of mean summer lake depths for 30 lakes in the Inuvik region of the delta (Squires et al. 2002) and 50 mean summer lake depths in the midwestern delta (Mackay, 1963).

Table 4.1. Summary statistics for instrumented Mackenzie Delta lakes and channels, summer (26 June–10 August) 2009. 'C' and 'P' refer to 'Connected' and 'Perched' lakes, respectively. 'Delta Region' refers to the Eastern, Western, Northern, or Southern delta. MSWT is mean summer water temperature. Values in parentheses are estimates where logged temperature is unavailable for this entire period, and do not contribute to the MSWT value among all channels.

Site	C/P	Perim. (km)	Area (ha)	Depth (m)	Delta Region	Geographic Coordinates (NAD '83)		MSWT (°C)
Lakes								
3 (NRC)	P	1.0	7.2	2.0	E	68°18'43.4"N	133°50'9.7"W	17.0
5 (South)	C	4.3	34.2	3.2	E	68°18'19.4"N	133°51'0.7"W	10.0
1	C	1.7	13.0	2.5	E	68°26'9.5"N	134°20'45.5"W	13.7
2	P	1.3	8.01	2.5	E	68°25'45.8"N	134°21'40.6"W	14.7
4 (Myers)	C	10.6	88.7	2.3	W	68°26'13.3"N	135°16'16.2"W	15.0
6	C	9.5	87.2	1.6	E	68°22'9.3"N	134°33'20.4"W	15.3
7	P	2.1	25.0	1.3	E	68°23'0.5"N	134°35'23.1"W	16.3
8	P	3.6	35.9	2.8	E	68°11'25.6"N	134°14'4.7"W	15.6
9	P	1.6	9.6	4.5	S	67°54'41.4"N	134°25'10.7"W	14.6
10	P	1.6	5.5	5.3	S	67°46'20.4"N	134°39'28.0"W	12.5
11	P	0.8	4.6	2.4	E	68°35'24.4"N	134°43'16.2"W	14.9
12	C	6.4	115.0	3.7	E	68°35'36.4"N	134°43'51.3"W	14.9
13	C	3.2	49.6	1.1	W	68°36'6.8"N	135°26'19.3"W	15.4
14	P	3.9	24.9	2.3	W	68°36'23.0"N	135°27'24.9"W	15.3
15	P	3.0	32.4	1.3	N	68°45'44.4"N	135°4'36.6"W	14.7
16	C	4.4	114.0	2.1	N	68°46'17.9"N	135°6'32.4"W	14.2
17 (Hope)	C	6.8	276.0	9.2	N	69°9'37.2"N	135°10'41.0"W	13.4
Mean	--	*3.9*	*55.0*	*2.9*	--			*14.6*
Channels								
A (Husky)				10.1	S	67°38'7.5"N	134°52'11.9"W	14.7
B (East)				4.0	S	67°47'41.4"N	134°10'12.0"W	15.5
C (Peel)				5.6	S	67°50'33.6"N	134°46'29.8"W	(14.6)*
D (Campbell Creek)				4.9	E	68°7'59.3"N	133°44'41.7"W	(14.9)
E				10.8	E	68°10'27.8"N	134°14'28.0"W	15.3
F				3.6	E	68°18'41.2"N	133°50'39.2"W	15.4
G (Schooner)				8.4	E	68°22'38.8"N	134°38'40.9"W	15.3
H (Nikoluk)				7.7	W	68°19'56.0"N	135°9'22.9"W	15.1
I (Pederson)				5.2	E	68°35'26.7"N	134°43'2.7"W	15.2
J (Leland at Jamieson)				12.0	W	68°36'46.0"N	135°28'14.1"W	15.1
K				3.7	N	68°45'53.4"N	135°4'41.9"W	14.9
L				2.3	N	69°9'45.3"N	135°12'29.9"W	14.5
M (Harry)				1.2	N	69°22'12.8"N	134°54'16.9"W	14.2
Mean				*6.1*	--			*14.9*

*On 25 July, the Peel Channel logger was removed from the channel and placed on shore by an unknown party.

4.2 Spatial Variability of Summer Thermal Regime

4.2.1 Within-Site

Temperature measurements made across channel beds indicated variability ≤0.1°C at each study site, and therefore isothermal conditions. Temperature profiles taken in mid-June following spring turnover indicated that most study lakes were vertically isothermal at that time. The two exceptions were Lake 1 (11.8°C, 13.8°C, and 13.8°C, respectively at bottom, mid-depth, and surface, respectively), and Lake 15 (3.9°C and 7.4°C at bottom and surface, respectively).

4.2.2 Regional

For individual lake and channel sites, MSWT ranged from 10.0°C (South Lake) to 17.0°C at NRC Lake (Table 4.1). Figure 4.1 maps MSWT measurements for water bodies instrumented with temperature loggers and MSWT estimates at 15 additional channel sites. These estimates are based on channel-bottom thermistor readings from two to four periodic visits to these locations during the summer, and are obtained using their proportionality to the concurrent measurements by the nearest channel temperature logger providing record for the full summer period. Figure 4.1 also delineates the four delta regions (North, South, West, and East) identified in Table 4.1. MSWT is presented in Table 4.2 by region and by water body type. Averages in Table 4.2 exclude the 15 channel temperature estimates from periodic measurements, and also those two instrumented sites (Campbell Creek, Peel Channel) whose summer temperature records are unavailable for the entire 26 June–10 August 2009 period.

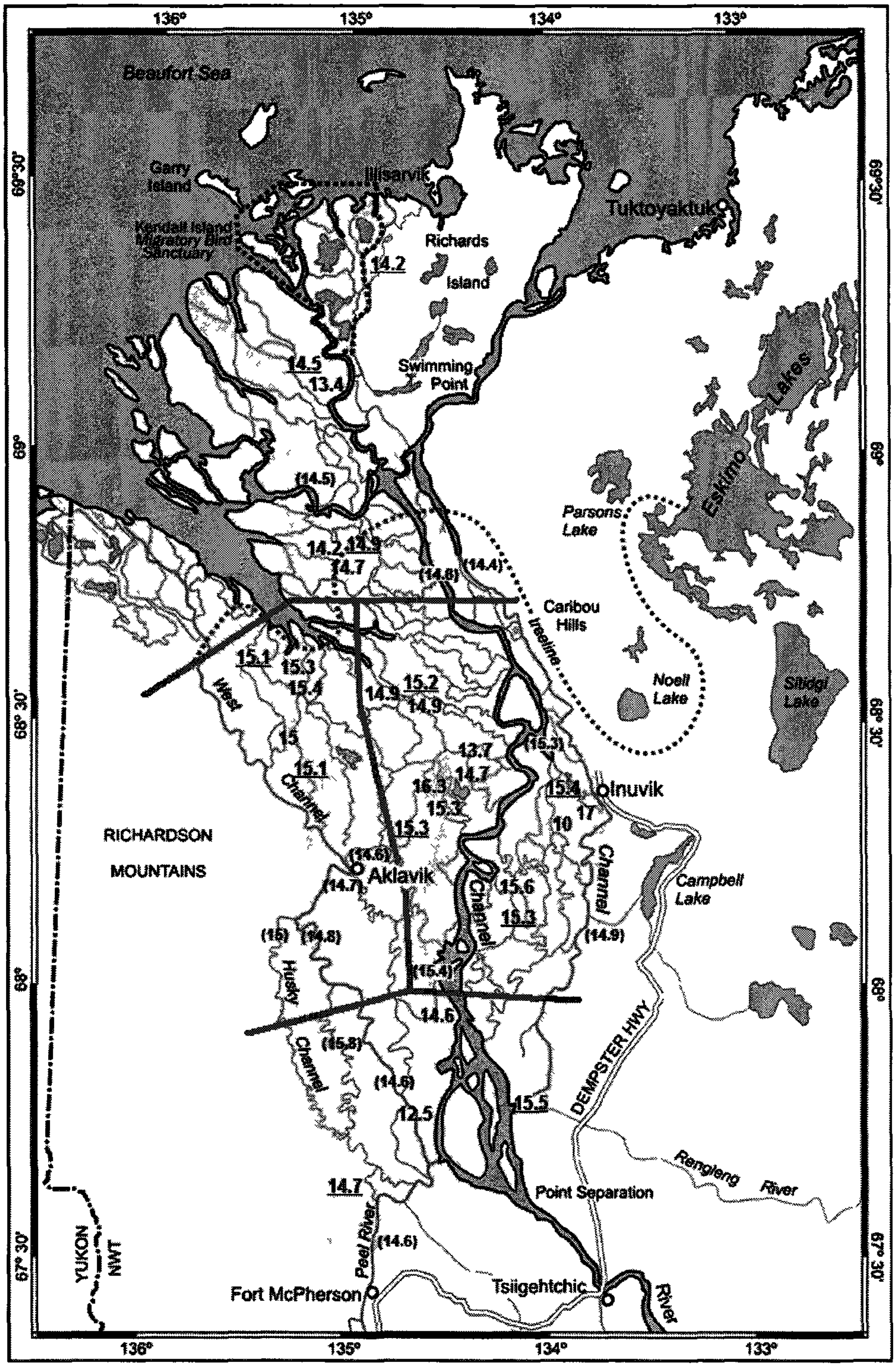

Figure 4.1. Mean summer (26 June–10 August) 2009 water temperatures (°C) in the Mackenzie Delta. Lake and channel temperatures are given in regular type and underlined type, respectively. Values in parentheses are estimates for additional channel sites based on periodic temperature measurements, or incomplete logged temperature series in the cases of Peel Channel (C) and Campbell Creek (D). Heavy gray lines delineate northern, western, southern, and eastern delta regions.

Table 4.2. Mean summer (26 June–10 Aug.) 2009 temperature (°C) for Mackenzie Delta study lakes and channels, by region. The number of study sites is given in parentheses. 'SE' is standard error among mean summer temperatures for all water bodies in the region or of the type specified.

	Channels	Perched Lakes	Connected Lakes	Mean ± SE
Northern Delta	14.5 (3)	14.7 (1)	13.8 (2)	14.3 ± 0.2 (6)
Southern Delta	15.1 (2)	13.5 (2)	No Data	14.3 ± 0.7 (4)
Eastern Delta	15.3 (4)	15.7 (5)	13.5 (4)	14.9 ± 0.5 (13)
Western Delta	15.1 (2)	15.3 (1)	15.2 (2)	15.2 ± 0.1 (5)
Mean ± SE	15.0 ± 0.2 (11)	15.1 ± 0.4 (9)	14.0 ± 0.6 (8)	14.7 ± 0.4 (28)

Mean lake and channel basal temperatures for the summer period were 14.5°C and 15.0°C, respectively (Table 4.2). Connectivity to the Mackenzie River likely explains the low spatial variability in channel temperature. The apparent spatial consistency of lake water temperature amongst delta regions may result from spatially consistent forcings from air temperature and solar insolation, particularly across delta. If the convectional and radiative heating of surface waters is similar throughout the delta, wind-induced mixing of lakes and inherent turbulence in channel waters may transmit these effects throughout the water body. Mixing is likely stronger in shallow or well-exposed lakes. The mean summer basal temperature for southern delta water bodies is equal to that for northern delta water bodies (14.3°C; Table 4.2). One might expect southern delta water temperatures to exceed those of the north, as mean monthly air temperature in Fort McPherson (southern delta region) exceeds that of Tuktoyaktuk (northern delta region.) by approximately 7°C, 4°C, and 3°C during June, July, and August, respectively, for 2000–2006 (Environment Canada, 2009). The similarity in mean basal temperature may be a result of small sample size in the northern and southern delta region (n = 3 and 2 lakes, respectively), and the significantly greater average depth of the southern delta study lakes than the overall mean (4.9 m and 2.9 m, respectively). Both southern study lakes are perched. Relations between MSWT and connectivity and depth are discussed further in sections 4.4.3 and 4.4.5.

4.3 Temporal Variability of Summer Thermal Regime

4.3.1 Daily Variability

Daily variability in channel temperatures, and in mean temperature among all channels, was relatively low and consistent through the summer period (Fig. 4.2a). In contrast,

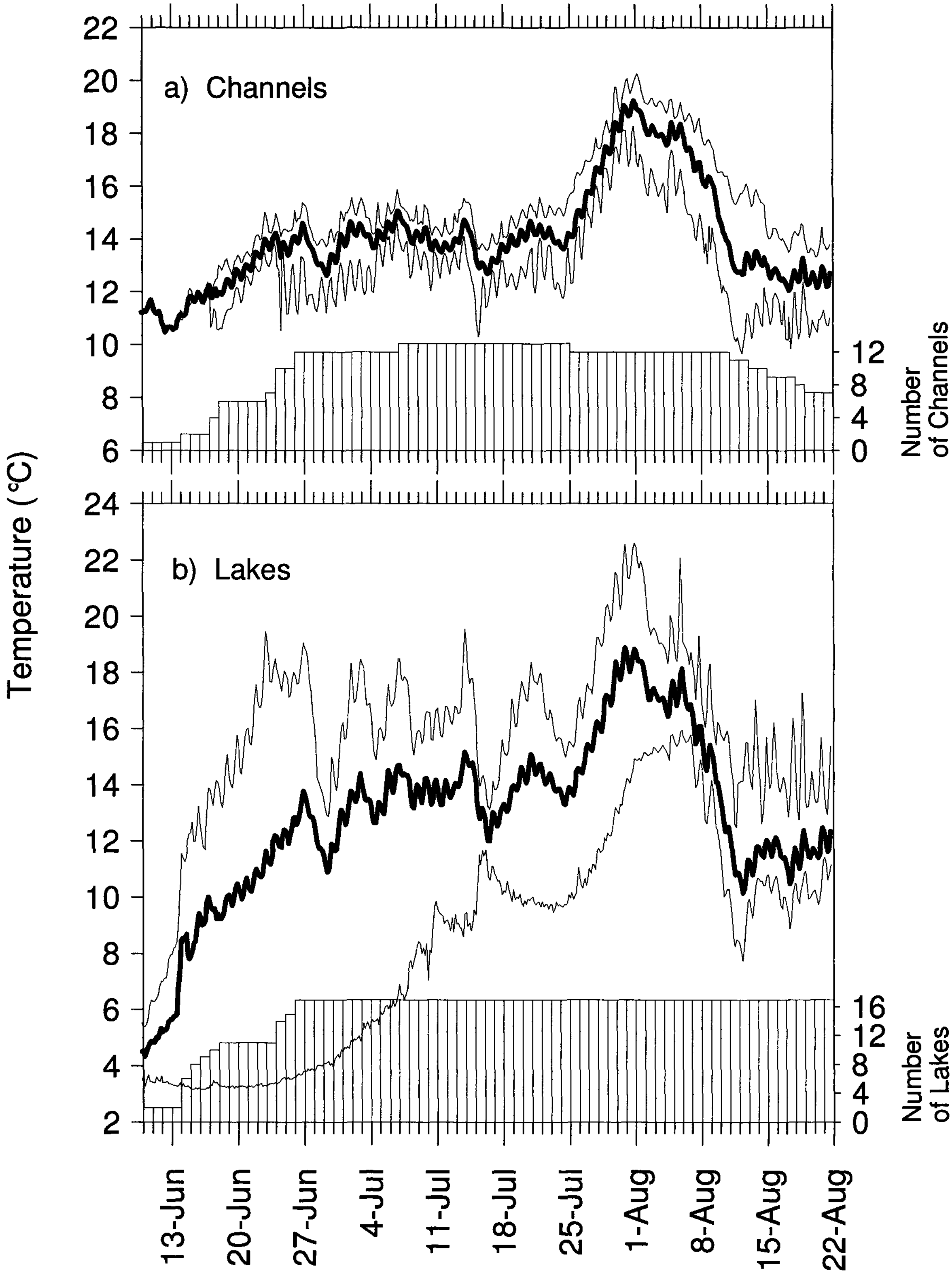

Figure 4.2. Summer (10 June–21 Aug.) 2009 maximum, mean, and minimum water temperatures among (a) Mackenzie Delta channel sites and (b) lakes. Columns show the number of water bodies providing temperature data.

lakebed temperatures converged during the summer period (Fig. 4.2b). NRC Lake and South Lake represented the extremes of lake temperature until the beginning of August. These converged from 17.6°C (NRC) and 3.7°C (South) on 26 June to 18.6°C and 18.1°C, respectively, on 6 August. As shown in Fig. 4.2, lake and channel temperatures exhibited a synchronous trend through the summer. Mean temperature among connected lakes peaked (19.1°C) on 30 July, while peak mean temperature for perched lakes (17.7°C) and channels (20.1°C) occurred on 31 July.

The reduction in temperature variability among study lakes over the summer period (Fig. 4.2b) may occur as a result of the concurrent water level reductions typical for delta lakes during summer (Bigras, 1990; Emmerton et al., 2007). Due to wind mixing, this increase in the ratio of lake surface area to volume may strengthen the dependence of lake-bottom temperature on air and lake surface temperature, increasing spatial consistency of basal temperatures in the late-summer.

4.3.2 Diurnal Variability

In addition to daily variability over the summer, water temperatures at all instrumented study sites followed a diurnal cycle. Figure 4.3 shows temperature values for a selected channel, connected lake, and perched lake over a two-day period in mid-summer. Harry Channel and South Lake show the maximum and minimum average diurnal temperature range (1.99°C and 0.25°C, respectively) of all water bodies through the summer. The peak in mean diurnal temperature for the summer period occurred at 20:00 for all water bodies other than Myers Lake, Hope Lake, and channel sites E, I, J, K and H. Average water temperatures were slightly higher at 0:00 for the first six of those sites, and at

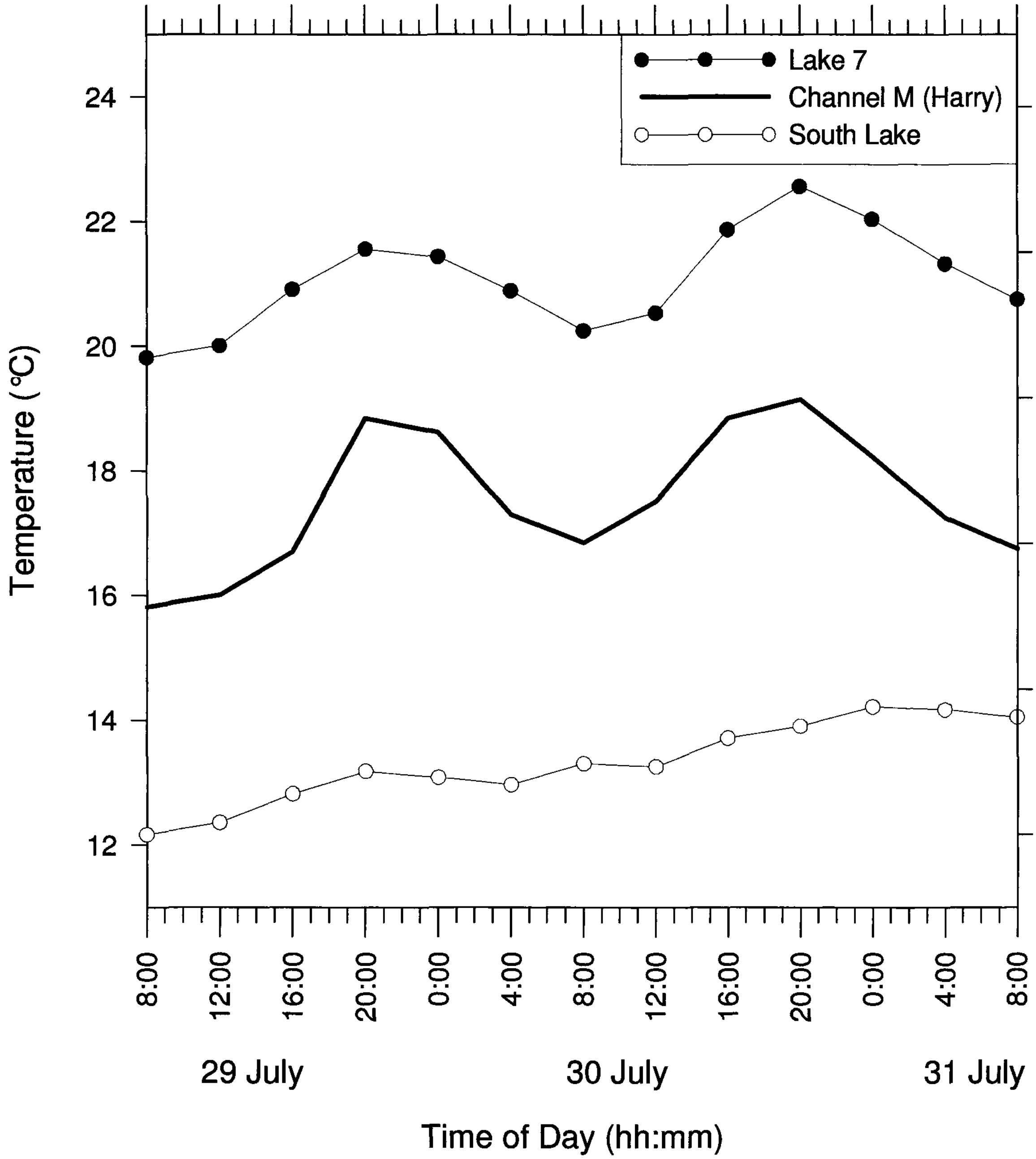

Figure 4.3. Forty-eight hour temperature series for Lake 7, Harry Channel, and South Lake, illustrating diurnal temperature variation.

12:00 for Channel H. Given the strong isothermal nature determined for channel water columns, likely due to the mixing of turbulent water, it is not surprising that the greatest diurnal variability is exhibited by a shallow channel (Harry) where basal water may be heated and cooled by air and sun most rapidly. Diurnal temperature variability at any point location on a channel might be somewhat reduced through interference from the same diurnal cycle propagating from various distances upstream.

Figure 4.4 shows the relation between water body depth and diurnal temperature range for the summer period. Water at depths <2 m tends to exhibit a diurnal temperature range greater than average among all water bodies investigated. This inverse relation between depth and diurnal temperature range, although not strong, remains evident among both channels and lakes when considered separately.

4.4 Controls on Summer Channel and Lake Temperature

4.4.1 Air Temperature and Insolation

The consistency in the date and time of peak summer temperature among study lakes may result from a strong dependence on air temperature, or factors associated with conditions when air temperature is high. Figure 4.5 compares records of summer 2009 air temperature from two locations in the delta with those of the nearest channel and lake. The steep rise in air temperature observed between 24 and 26 July, prior to the 30 July air temperature peak, may induce the steady increase in mean channel and lake temperature observed between 24 and 31 July (Fig. 4.2), which is similar to the rise and peak of Lake 17, Channel L, NRC Lake, and Channel F temperatures (Fig. 4.5). The second peak in mean water temperature, observed 5 August for lakes and channels (Fig. 4.2, 4.5), may occur due to the simultaneous peak in air temperature.

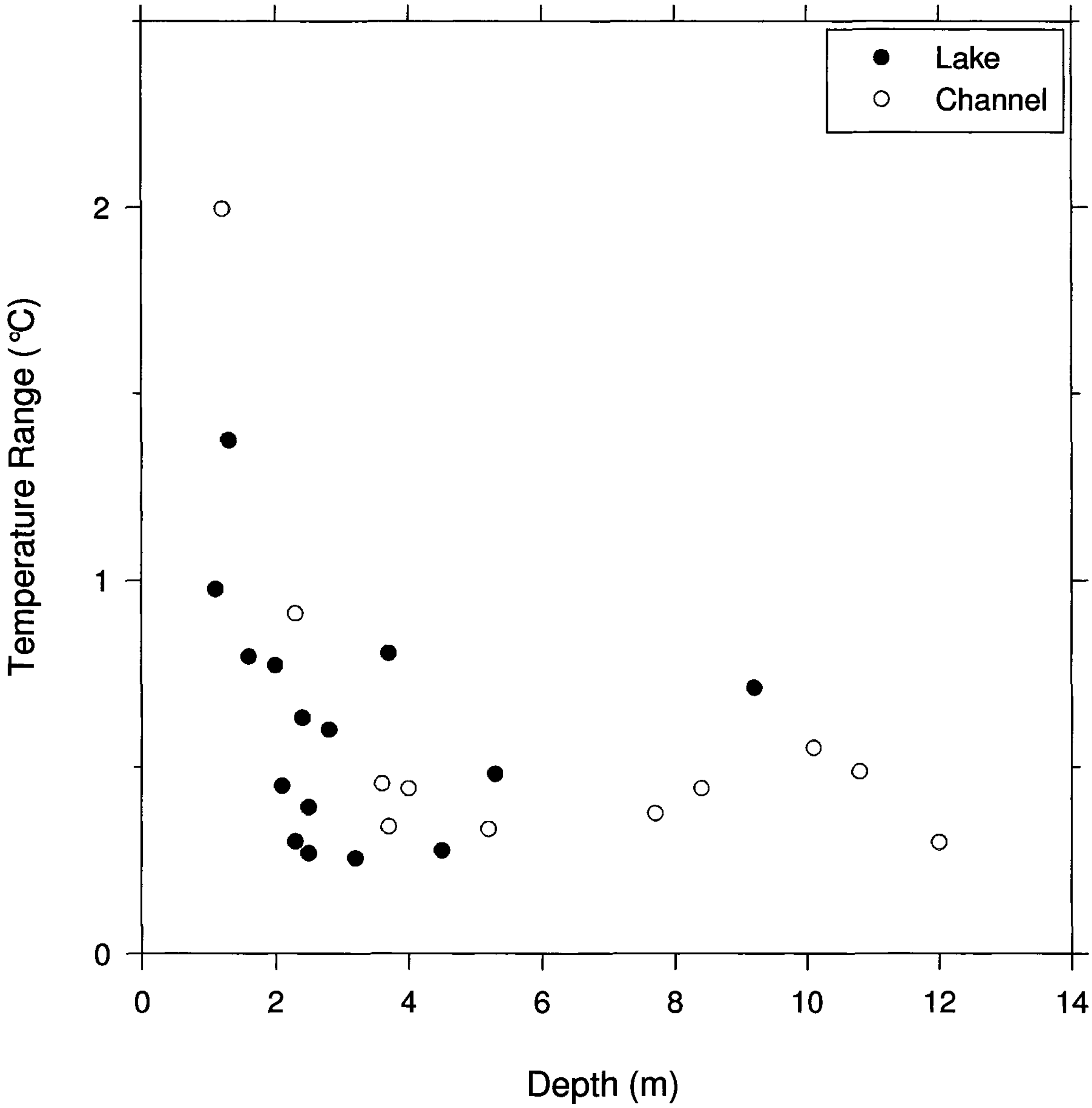

Figure 4.4. Logger depth vs. average summer (26 June–10 Aug.) 2009 diurnal temperature range for Mackenzie Delta channels and lakes.

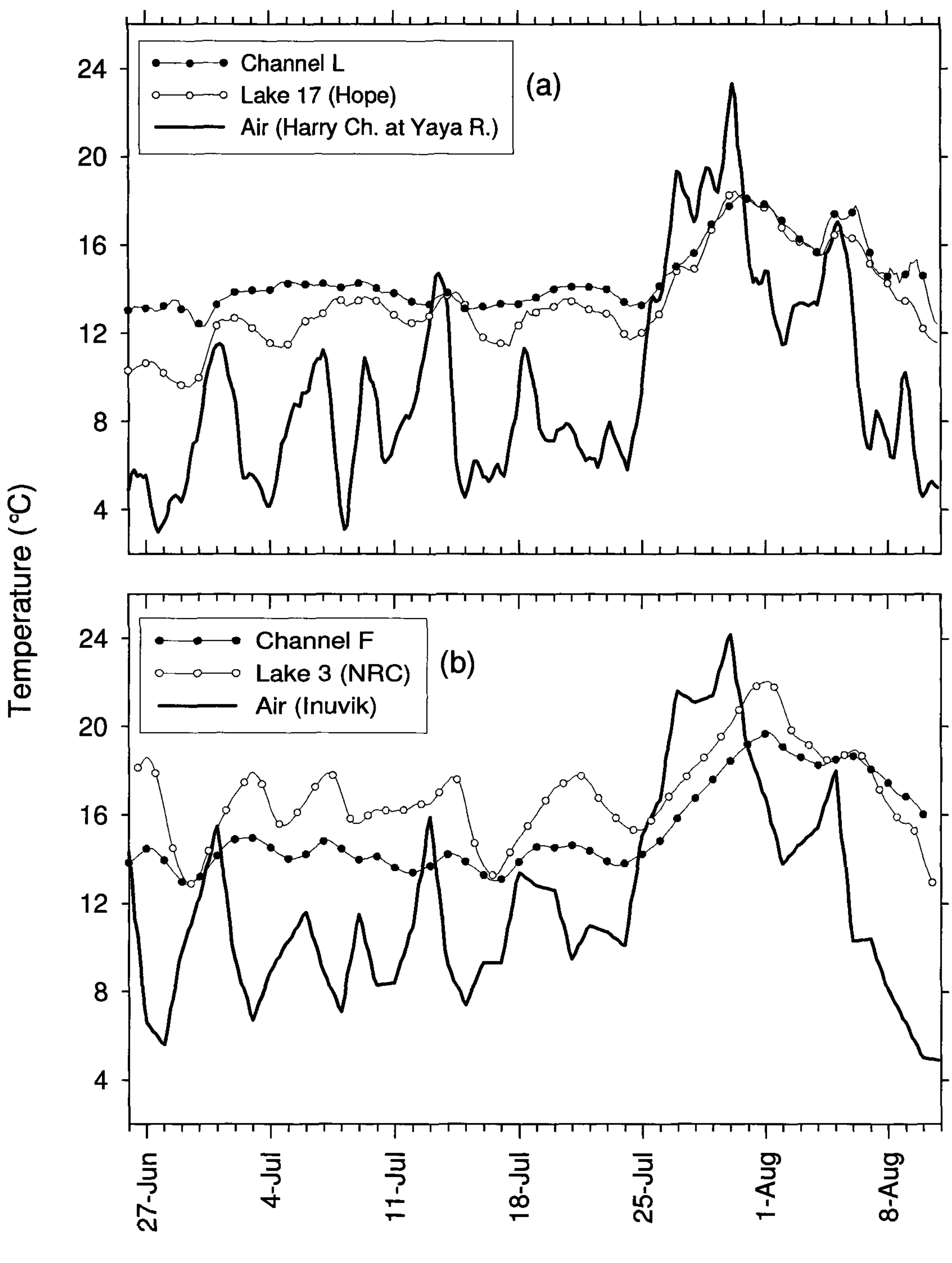

Figure 4.5. Summer (26 June–10 Aug.) 2009 basal water temperature for proximal lake and channel sites, and nearby daily air temperature. Diurnal variability has been smoothed using a 6-sample (1 day) running mean. Figure (a) compares Hope Lake and Channel L temperature with air temperatures measured at the INAC meteorological station on Harry Channel by Yaya River. Figure (b) compares water temperature at NRC Lake and adjacent Channel F with air temperature from Inuvik airport. Water temperature was measured every four hours, and symbols are plotted daily for clarity.

Figure 4.2b reveals 16–17 July as a period of reduced spatial variability in lake temperature. At this time temperatures are similar at most sites. On 15 July the strongest winds of the study period were observed at Inuvik (41 km/h sustained 11:00-12:00, max. gust 65 km/h; Environment Canada, 2009) and in the northern delta near the confluence of Harry Channel and Yaya River (25 km/h average of 24 hours). These winds may have provided sufficient mixing to remove some existing stratification, bringing lake-bottom temperatures closer to those of surface waters already more spatially uniform. The azimuth of wind direction on 15 July at the Harry Channel meteorological station in the northern delta was between 301° and 337°. This northerly wind may produce some degree of storm surge, forcing relatively cool ocean water upstream in the outer delta as is common in the late summer (Marsh and Schmidt, 1993). While a local decrease is evident in the temperature series for Lake 17 in the northern delta (Fig. 4.5a) at the approximate time of this wind event, this change is of no greater magnitude than other concurrent water temperature variations elsewhere in the delta (Fig. 4.5b).

In addition to wind and air temperature, a solar insolation record is available from Indian and Northern Affairs Canada's meteorological station (134°59'10.5"W, 69°12'54.4"N) near the confluence of Harry Channel and Yaya River. Using this record and that of Channel L water temperature, the relation between daily mean channel water temperature and daily mean downwelling solar radiation (K↓) may be compared with that between channel water temperature and air temperature (Fig. 4.6a, b). While neither comparison reveals a strong correlation, these relations appear negative and positive, respectively. As air and water temperature are generally ascending at this location until late July (Fig. 4.5a) and daily average K↓ is in decline following the summer solstice, all three time series are

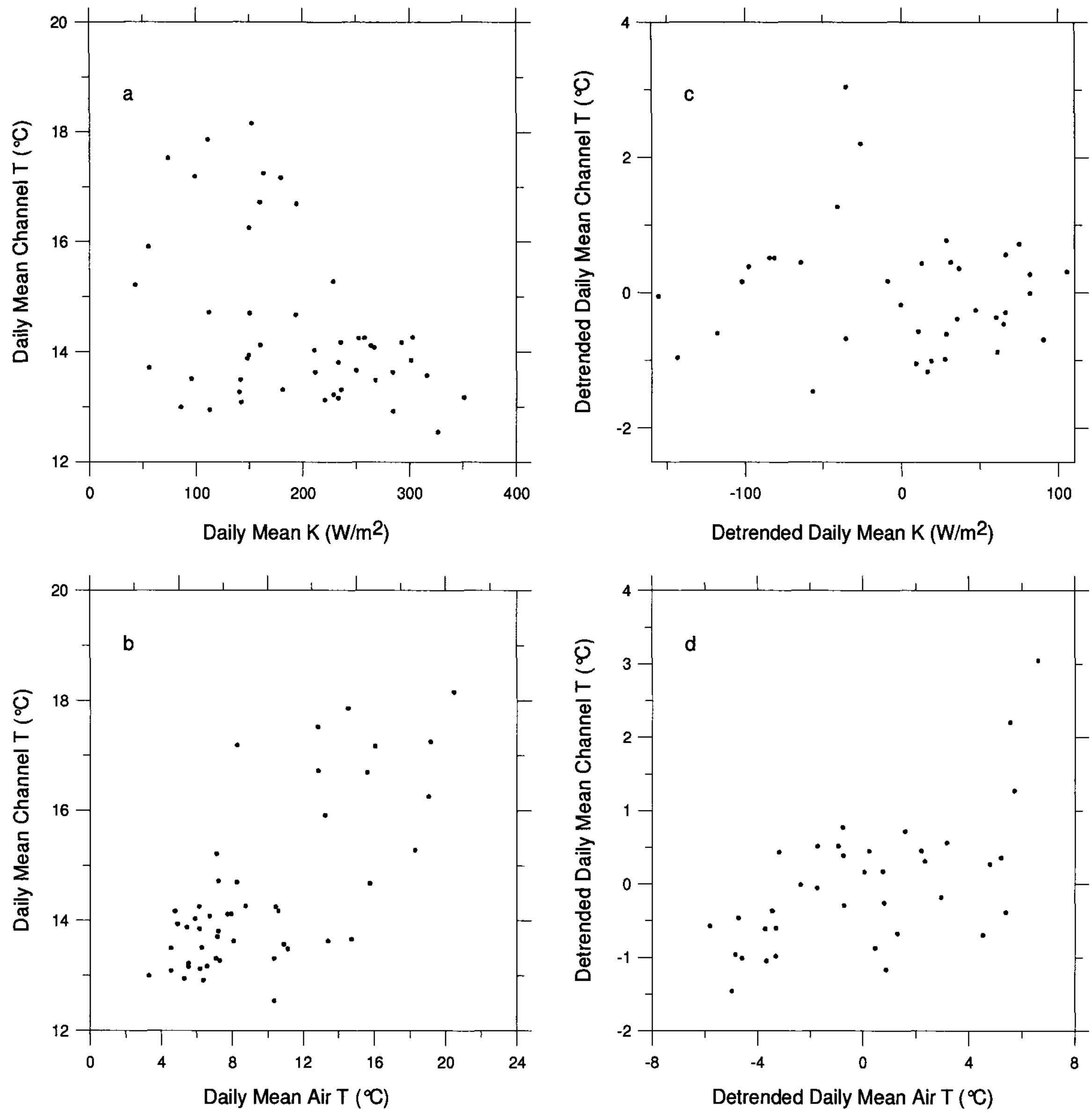

Figure 4.6. Relation between (a) daily mean K↓ and daily mean Channel L temperature, (b) daily mean air temperature and daily mean Channel L temperature, (c) detrended daily mean K↓ and detrended daily mean Channel L temperature, and (d) detrended daily mean air temperature and detrended daily mean Channel L temperature for the period 26 June–10 August 2009. Air temperature and insolation records were obtained from the INAC meteorological station approximately 10.6 km east-northeast of the Channel L site.

detrended to permit examination of the relations between residual values. Figure 4.6c presents the relation between detrended values of daily mean insolation and detrended daily mean Channel L water temperature. Figure 4.6d presents the relation between detrended values of daily mean air temperature and detrended daily mean Channel L water temperature. In both comparisons, only the 26 June–30 July 2009 record is used, as air and water temperature trends reverse after 30 July 2009 (Fig. 4.5). Relations between detrended daily mean Channel L temperatures and detrended daily mean air temperature and insolation are not strong and do not have a definite sign. No influence by air temperature or insolation on channel water temperature is suggested in this analysis. Although main peaks in summer air and water temperature do appear to generally correspond in both the northern delta and near Inuvik (Figs. 4.5a and b, respectively), it is suggested that the summer temperature cycle of water in Mackenzie Delta channels is developed primarily by forcings on broad geographic scales upstream, and to a lesser extend by local forcings within the delta.

4.4.2 Precipitation

June and July 2009 were drier than normal for Inuvik (Fig. 3.1). Due to a storm event on 1 August, that month approached its normal – 39.9 mm – by 10 August with 32 mm rain. Figure 4.7 shows Inuvik precipitation events, all rain, during the summer study period. Rainfall events may contribute in small part to observed daily variability in proximal, and possibly regional mean, channel and lake temperatures. Channel and lake mean temperatures (Fig. 4.2a and b, respectively) and Channel F (Fig. 4.7) each show a primary summer peak on 31 July and a secondary peak on 6 August. The interlude

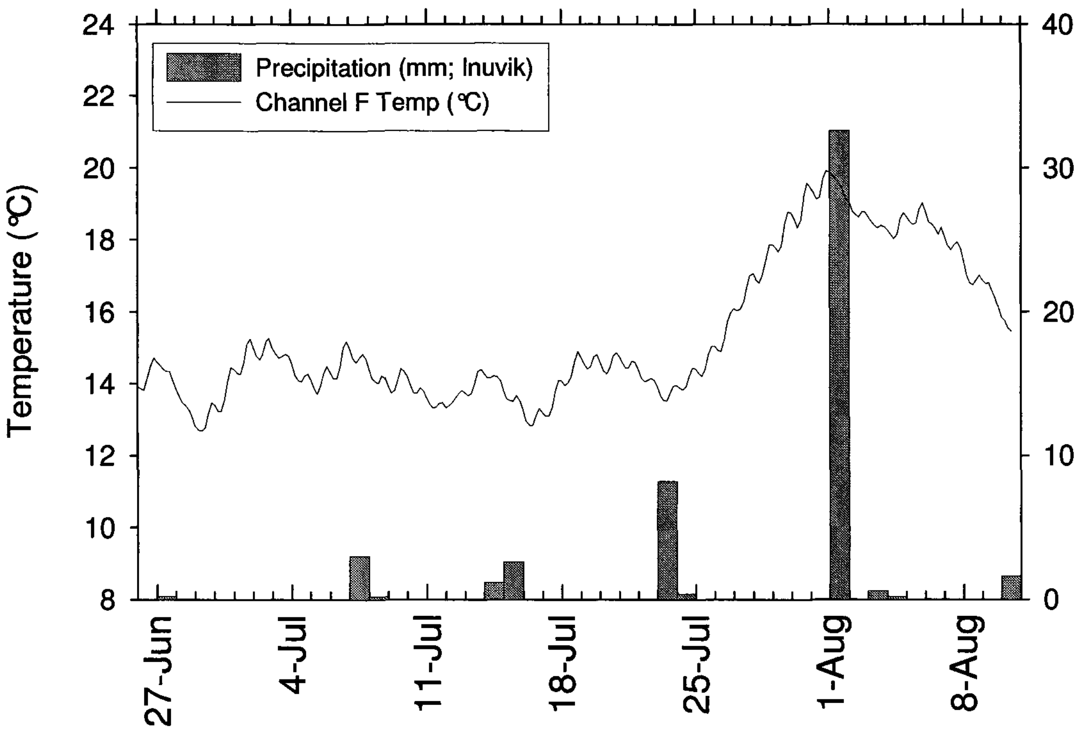

Figure 4.7. Summer (26 June–10 Aug.) 2009 Channel F water temperature and precipitation at Inuvik.

between these peaks corresponds with a week of relatively low air temperatures (Fig. 4.5) which follows a 33 mm rainstorm on 1 August. This rainfall event may contribute to the temperature reduction in delta water bodies following their 31 July peak. Smaller rainfall events on 14 and 15 July may contribute to a small reduction in water temperature on 15–17 July (Fig. 4.7). While an 8 mm rainfall event occurred in Inuvik on 23 July, it does not precede the corresponding dip in Channel F temperature enough to strongly suggest causality. Given the relative volumes of rainfall inputs and most recipient water bodies, however, it should be emphasized that thermal changes in water bodies are driven primarily by cool air temperatures associated with weather systems producing precipitation.

4.4.3 Depth

As indicated, depth likely influences lake basal water temperature during the summer period, and hence modifies the spatial variability of lake temperatures from what might be expected based only on summer climate. At the time of instrumentation, water bodies ranged in depth from 1.1 m (Lake 13) to 10.8 m (Channel E; Table 4.1). Figure 4.8 compares early summer (26 June) and late summer (10 August) basal temperature with depth for each study lake. An inverse relation is apparent in the early summer between depth and basal temperature, however this does not persist through the summer. The same pattern holds true for both perched and connected lakes when considered separately. This results from gradual warming of basal waters of deeper lakes through the summer by wind mixing. Depth may be an important control on the MSWT of delta lakes. It likely explains, in part, unexpected spatial relations in MSWT such as the identical northern and southern delta lake averages (Table 4.2).

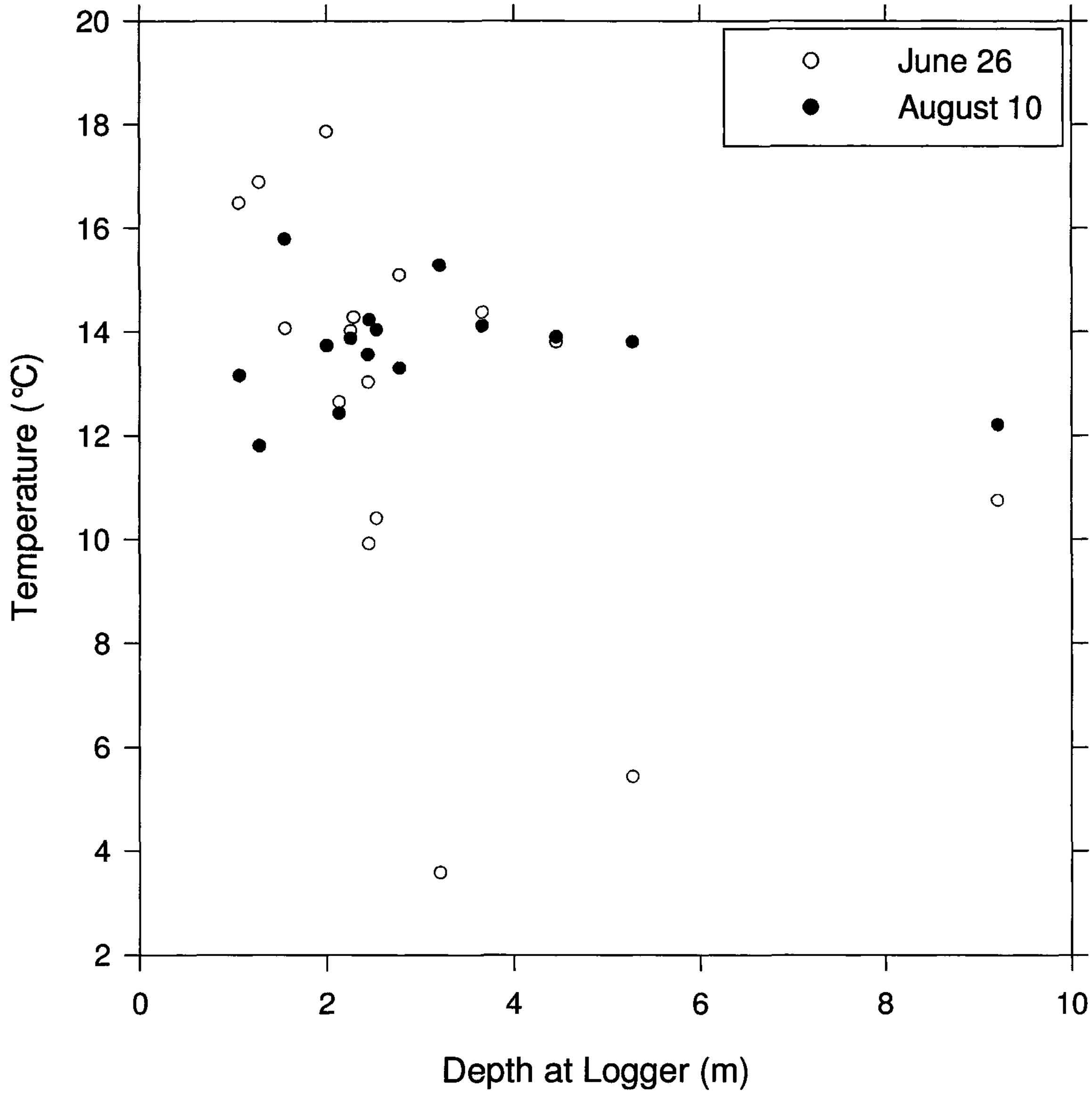

Figure 4.8. Depth of temperature logger (m) vs. 26 June and 10 August temperature (°C) for 15 Mackenzie Delta lakes.

4.4.4 Temperature Wave Propagation along Channels

The connectivity of the Mackenzie Delta channel network suggests that water temperatures at channel study sites may result from regional forcings (air temperature, precipitation, and insolation) and the discharge of the Mackenzie River upstream. To examine the possible downriver propagation of major peaks and troughs in water temperature, summer temperature series for several channel sites have been smoothed using a one-day (six measurement) moving average to remove the diurnal signal, and are presented in Figs. 4.9, 4.10, and 4.11. In Fig. 4.9, which illustrates the western delta, Channel J temperatures appear to slightly lag those taken at Channel H, approximately 40 km upstream, until late July when major trends become nearly concurrent. The Channel A (Husky) record is also shown, which is likely identical to that of the Peel River given its location. Corresponding peaks and troughs between the Channel A record and those of Channel H and Channel J are not obvious. This may be due to the great distance between the channel sites. Mackay (1963, p. 100) estimates that discharge entering the southwest side of Shallow Bay (i.e. discharge in Channel sites H and J) is likely approximately 15% Mackenzie River water (via Aklavik Channel) and is otherwise accounted for by Peel River discharge and mountain rivers entering the Husky Channel. Mountain stream contributions may therefore play a significant role in the summer temperature series of western delta channels, as one might otherwise expect greater similarity between the Channel H, J, and Channel A temperature signals in Fig. 4.9 than is apparent. The Channel J temperature signal can be seen to lag that of Channel H by an average of 24 hours prior to summer peak temperature. This suggests a channel flow of approximately 1.6 km/h along the 40 km Nicoluk Channel route between the sites, or a

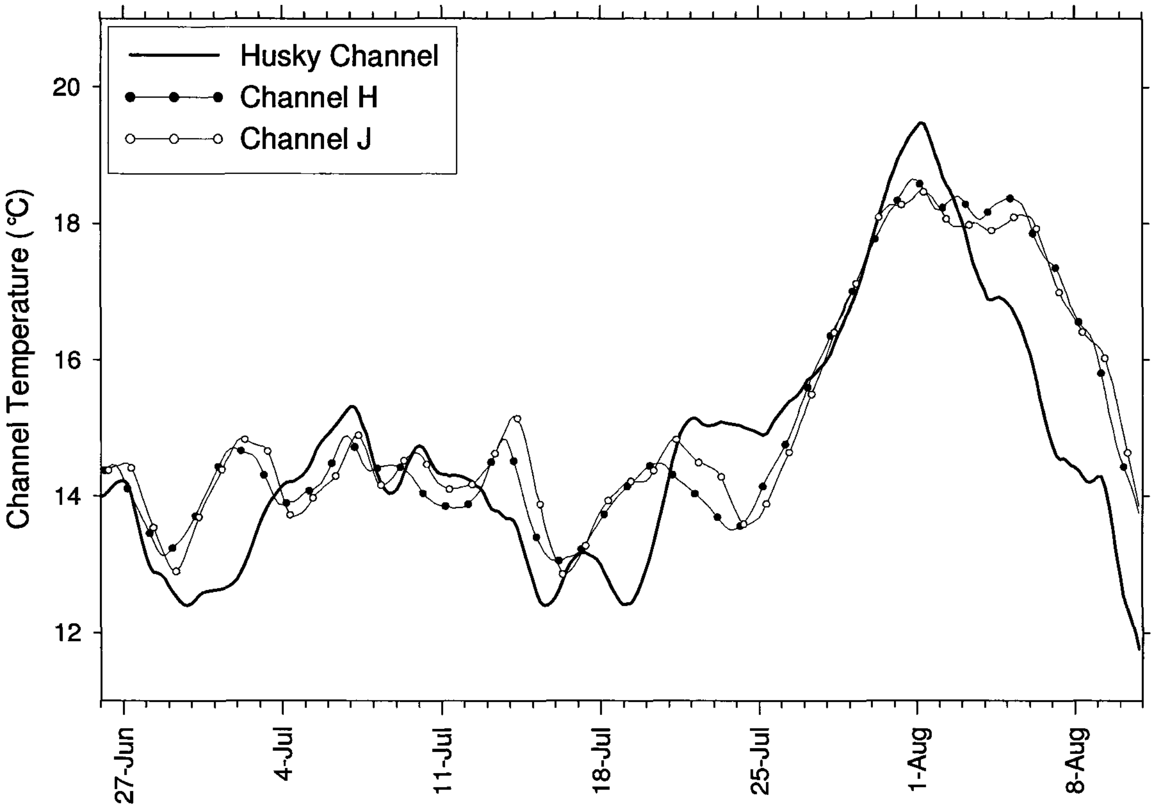

Figure 4.9. Summer (26 June–10 Aug.) 2009 channel temperature series for western Mackenzie Delta. Channel sites A (Husky), H (Nicoluk) and J (Jamieson) represent the southern, middle, and northern regions, respectively. Temperature was measured every four hours, and symbols are plotted daily for clarity.

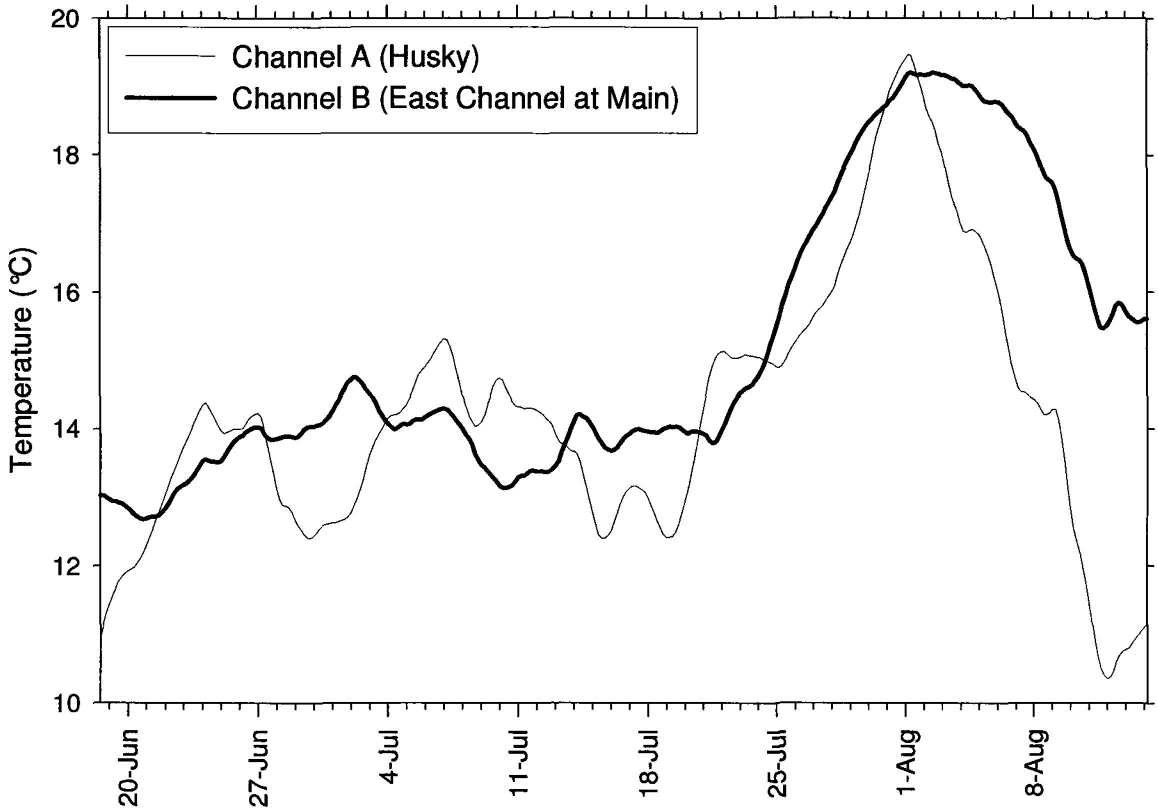

Figure 4.10. Channel A (Husky) and B (at separation of East Channel from Main Channel) temperatures (°C) for common period of record, 2009. Channels A and B are likely representative of Peel River and Mackenzie River temperatures, respectively, at the locations where these rivers enter the Mackenzie Delta.

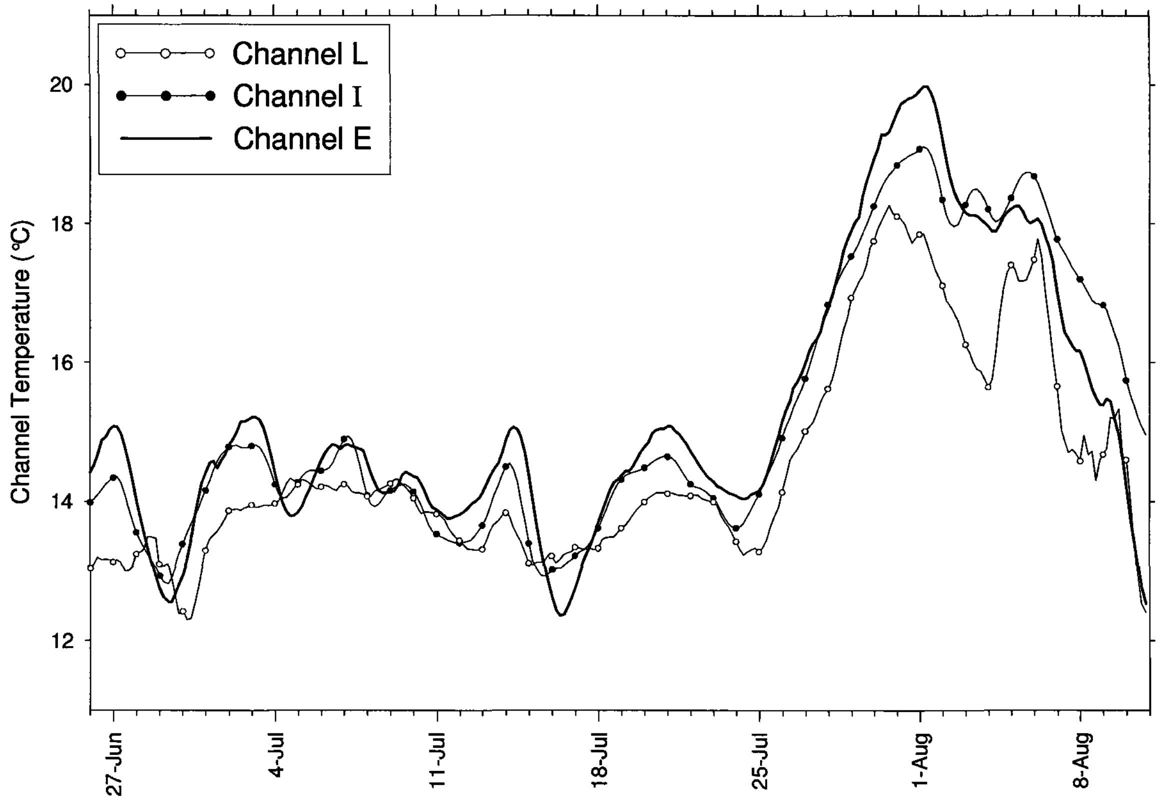

Figure 4.11. Summer (26 June–10 Aug.) 2009 channel temperature series for eastern Mackenzie Delta. Channel sites E, I, and L are located at low, middle, and high relative latitudes in the Mackenzie Delta, respectively.

2.25 km/h flow velocity along the West Channel and Jamieson Channel linkage between sites if this latter route is the primary flow route between sites.

The summer temperature series of the Main Channel is likely best illustrated by the Channel B temperature series. This comes from the inlet to a distributary of the East Channel immediately downstream from the divergence of the East Channel from the Main. As shown in Fig. 4.10, this series exhibits a relatively gradual summer temperature peak and has a different general form from Channel A (the Husky Channel site likely indicative of the Peel River) temperature series. The same general form of the Channel B temperature series is exhibited in temperature series from channel sites over a range of latitudes in the eastern delta (Fig. 4.11). In this case, peaks and troughs belonging to southerly sites do not clearly precede those from sites further north, as might be expected if temperature changes are being propagated downriver, from the south. The pronounced linear temperature increase towards the summer peak commences on 24 July for most channels, and on 22 July for Channel B. The decline of channel temperatures following the summer peak does not appear, however, to be driven from upriver, as the channel temperature for the most northerly site considered (Channel L) begins decreasing first. An inverse relation between channel temperature and latitude is apparent, particularly in late summer, while temperature wave propagation downriver is not.

4.4.5 Lake Connectivity

Perched and connected lakes showed mean temperatures of 15.1°C and 14.0°C, respectively, for the 26 June–10 August 2009 period. Perched lakes in the eastern, western, and northern delta averaged 2.2°C, 0.1°C, and 0.9°C warmer than connected lakes in those regions, respectively (Table 4.2). Unfortunately, region-controlled comparisons of mean temperature between lake types were not possible in the southern delta. Lake depth may contribute to this difference, as perched and connected lake depths averaged 2.7 m and 3.2 m in June 2009 in the delta as a whole, and 2.2 m and 2.8 m, respectively, in the east delta.

As shown in Fig. 4.12, a difference in mean temperature of nearly 2°C persists between perched and connected lakes until late July when lake temperatures are ascending towards their summer peak. Perched and connected lake mean temperatures are then similar through the primary and secondary peaks, and during subsequent descent. If the timing and magnitude of depth reduction in connected and perched study lakes during summer were known, differences between the two groups might provide some insight into the behaviour of the temperature series (Fig. 4.12) described above.

4.4.6 Channel Stage

Variations in channel stage are relatively small after the spring flood peak, which typically occurs in the delta in late May or early June (Bigras 1990). Figure 4.13 shows the portion of the summer 2009 stage record, concurrent with channel temperature records, for Inuvik, Aklavik, and locations on the Mackenzie and Peel rivers near their entry to the delta. Two proximal channel temperature series are included for comparison. Temperatures in both the Peel and Mackenzie rivers show a general increase corresponding to a reduction in stage, however it is unknown if there is a cause-effect relation between channel stage and temperature. Stage variability present in the

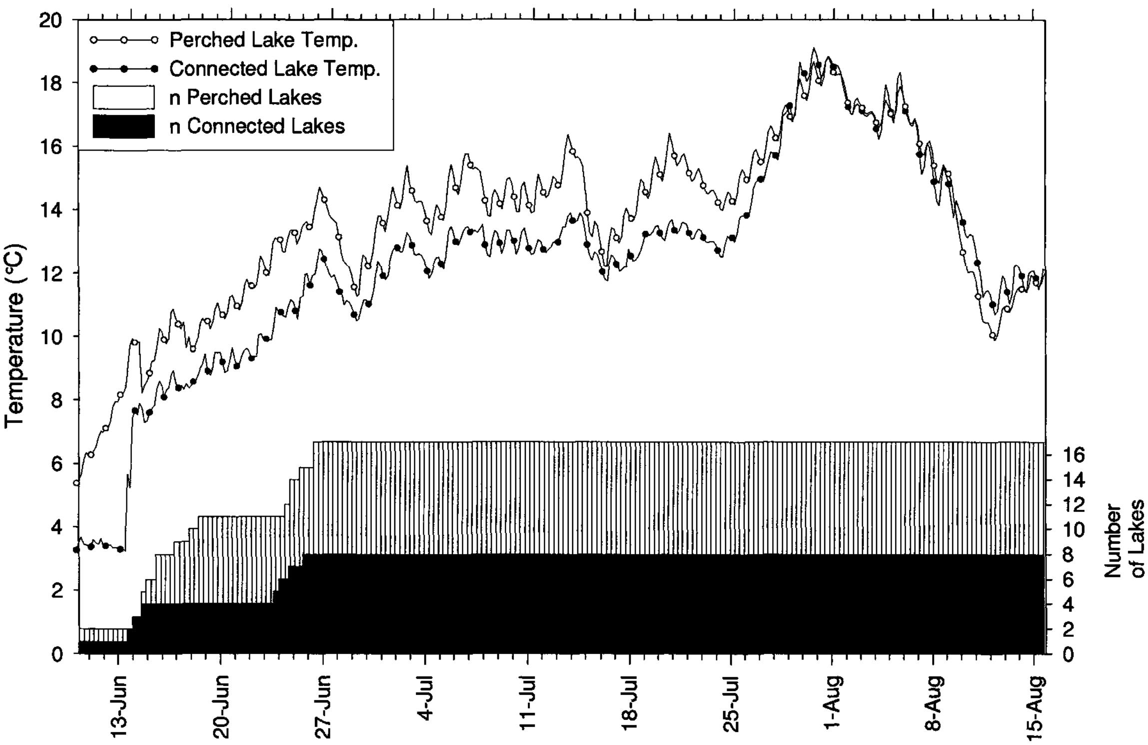

Figure 4.12. Summer (9 June–15 Aug.) 2009 average basal temperature among perched and connected Mackenzie Delta lakes. Columns indicate the number of lakes contributing to each average, with no overlap (hence the number of connected and perched lakes is 8 and 9, respectively, after 25 June). Measurements were made every four hours and symbols are plotted daily for clarity.

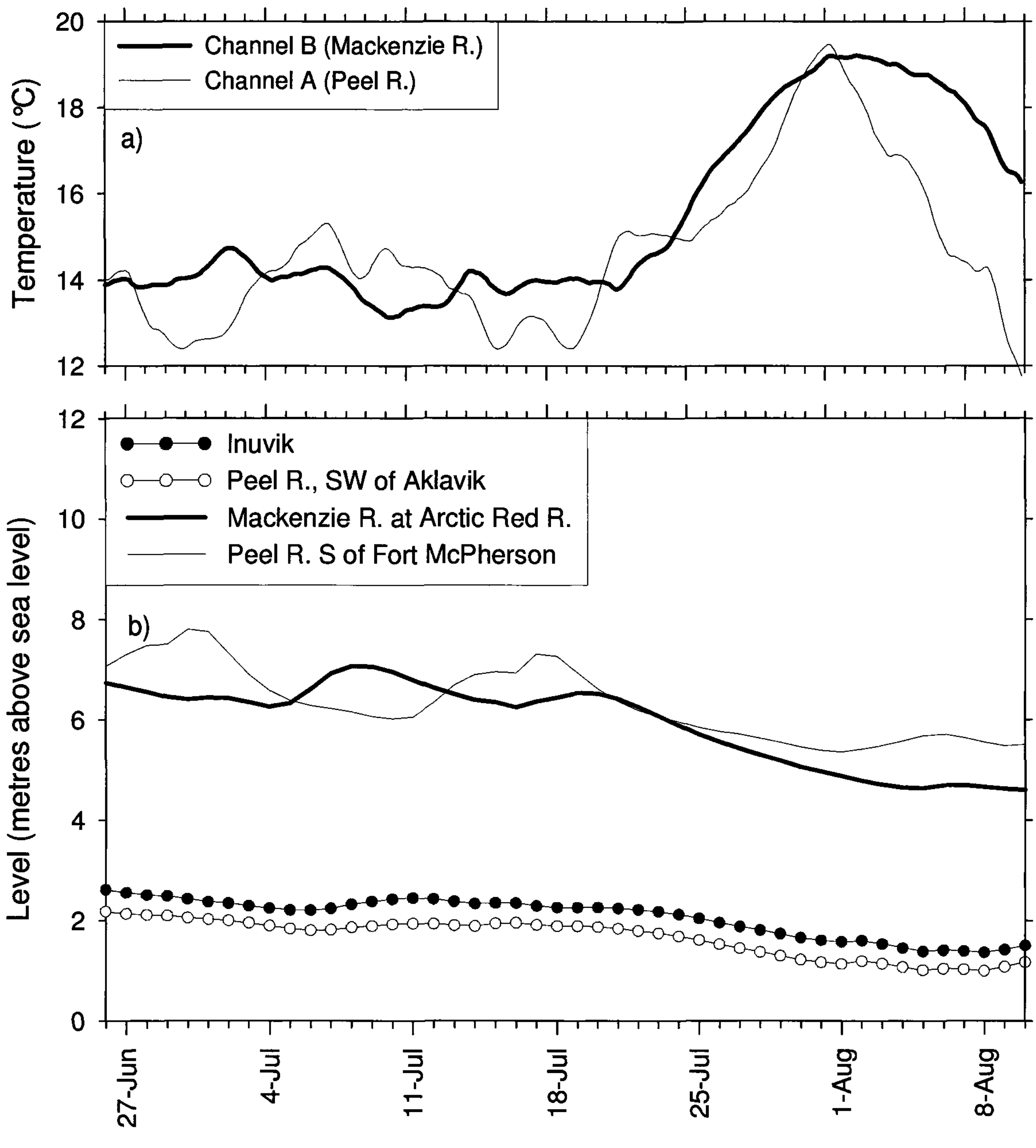

Figure 4.13. Channel level, relative to mean sea level at Tuktoyaktuk, at four locations in the Mackenzie Delta region, summer 2009. Source: Water Survey of Canada, 2009.

Mackenzie and Peel rivers is less pronounced at Inuvik and near Aklavik, and it is the stage variability of the Mackenzie River, rather than the Peel, whose general form is evident (at a reduced amplitude) in the two mid-delta channels.

The reduction of water level in connected lakes between early June and mid-August is likely greater than that in perched lakes due to drawdown from connected channels, whose levels decline following the spring flood. A representative 2009 summer channel level series, including spring flood, is given in Fig. 3.2. Channel water level during the open water period is variable, however, responding to precipitation events in the Mackenzie basin and tides and storm surges in the northern delta (Marsh 1998). It is estimated that a connected lake in the middle delta may experience an average of five inflow and outflow events during the open water period, and one in the northern delta is likely to experience 10 such events (Bigras 1990). Perched lakes typically experience steady water loss during the open water period. Bigras (1990) estimates water level reductions of 193 to 330 mm in perched lakes during summer, of which 60 to 85% is through evaporation.

Lake levels were not monitored concurrently with basal temperature in this research, however this has the potential to yield new insight into factors controlling summer lake temperature. The input of water from adjacent channels to connected lakes, during periods of summer flood, may induce basal temperature fluctuations in those lakes. Peaks in the summer 2009 hydrograph for East Channel at Inuvik (Fig. 3.2) do not appear to correspond to basal temperature fluctuations among connected lakes (Fig. 4.5) to an extent suggesting causality. Individual lake basal temperature series, basal temperature records from proximal channels, air temperature records, and (if available) water level series for the lake(s) of interest would permit an examination of the influence, relative to air temperature, of channel temperature through flood occurrence on the thermal regimes of specific connected lakes.

4.5 MAWT Estimates from MSWT

Lake ice is generally present between 15 Oct. and 1 June, and channel ice breakup and formation usually occur approximately 2 weeks earlier in spring and approximately 1.5 weeks later in autumn (Burn 1995). A recent examination of records by Goulding et al. (2009) revealed that between 1974 and 2006, Mackenzie River breakup initiation at the Arctic Red River (Tsiigehtchic, NWT) occurred 1.54 days earlier each decade. Trends in the onset of the open water period for delta lakes are unknown. If lake and channel water temperatures are assumed to be 0°C while ice cover exists (25 Oct. to 16 May for channels), and the temperature transition between initial and final measured values and the ice-on period is assumed linear, mean annual temperature estimates are possible. Using 2009 summer data, MAWT at delta lake and channel beds was estimated at 3.4°C and 4.1°C, respectively. For a study area approximately 50 km north of Inuvik, Smith (1976) reported mean annual temperatures of 3.5°C and 3.0°C (1968, 1969) for lakes, and 3.7°C, 4.0°C, 3.8°C, and 4.2°C (1967-1970) for channels. The assumption of lakewater at 0°C for the entire ice-on period likely underestimates MAWT, given the observed increase in basal temperature each autumn after ice formation at NRC Lake (Fig. 4.14). This results from heat emission from lake sediments, and heating by solar insolation through clear ice prior to snow accumulation (Brewer 1958). This reinforces the importance of year-round temperature measurements to verify MAWT.

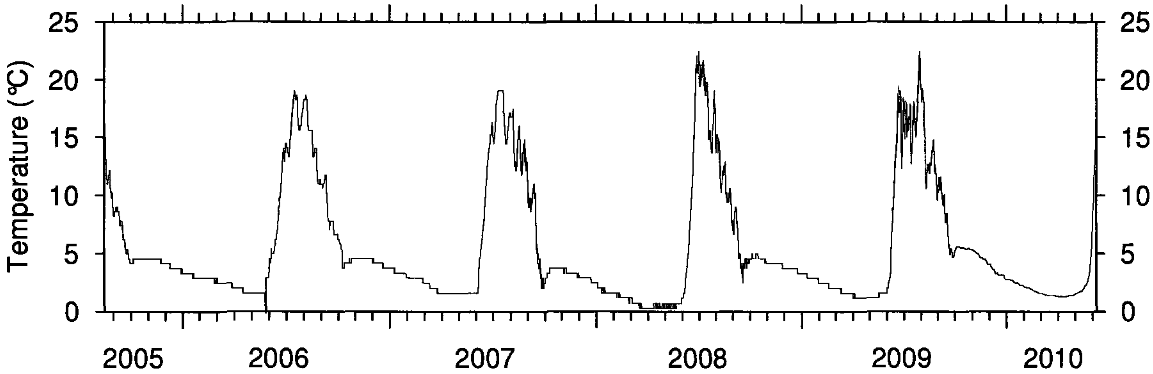

Figure 4.14. NRC Lake basal water temperature, Aug. 2005–Jun. 2010.

4.6 Conclusion

Spatial variability in the summer thermal regime of Mackenzie Delta water bodies is low. While channels are isothermal at all study sites, depth may be an important source of variation in thermal regime between lakes. While spatial consistency of lake and channel basal temperature during winter will be discussed in the next chapter, sources of variation – namely air temperature – present during summer are not expected to influence water thermal regime appreciably beneath the ice and snow cover. It is therefore likely that the limited spatial variability in thermal regime during summer represents the greatest annual spatial variability in Mackenzie Delta channels and lakes.

CHAPTER 5: MACKENZIE DELTA ANNUAL THERMAL REGIME

5.1 Introduction

This chapter examines both spatial and temporal variability in the annual thermal regime of Mackenzie Delta surface waters. Potential controls on this variability are discussed, and results are placed in context with existing knowledge of northern lake and river thermal regimes. Predictions of through talik occurrence in the Mackenzie Delta are then made based on the annual thermal regime of its lakes and channels. Records of basal water temperature were obtained every four hours from June 2009 to June 2010 for all 17 study lakes and six of the 13 channel sites. Table 5.1 indicates the lake connectivity, geometry, record period, and mean annual basal water temperature (MAWT) of study sites providing one year of data.

5.2 Spatial Variability

Average mean annual water temperatures were 4.5°C and 4.6°C for study lakes and channels, respectively. As shown in Table 5.1, MAWT among study lakes ranged from 2.8°C (Lake 12) to 6.8°C (Lake 8). For channels, it ranged from 4.2°C (Campbell Creek site) to 4.8°C (Husky Channel site).

Values for lake and channel MAWT are mapped in Figs. 5.1 and 5.2, respectively. MAWT is relatively low amongst study lakes north of or near treeline. It is variable in the central delta, and relatively high among lakes in the southern delta. For the channel network, a gradual decrease in MAWT with distance north is observed. MAWTs for delta lakes north of treeline compare favourably with estimates of >2°C made for the

Table 5.1. Mean annual basal water temperature (MAWT) for instrumented Mackenzie Delta lakes and channels. Other summary statistics are the same as presented in Table 5.1. Italicised values indicate less than one year of temperature data. In these cases, the gap (26 days for Campbell Creek, ≤ 7 days for all others) is filled using linear interpolation between the first and final temperature measurements.

Site	C/P	Perim. (km)	Area (ha)	Depth (m)	Delta Region	Period of Record (dd/mm/yyyy)	MAWT (°C)
Lakes							
3 (NRC)	P	1.0	7.2	2.0	E	6/6/2006 – 6/6/2010	5.8[1]
5 (South)	C	4.3	34.2	3.2	E	6/6/2009 – 6/6/2010	3.3
1	C	1.7	13.0	2.5	E	13/6/2009 – 13/6/2010	3.1
2	P	1.3	8.01	2.5	E	15/6/2009 – 15/6/2010	6.4
4 (Myers)	C	10.6	88.7	2.3	W	25/6/2009 – 16/6/2010	*3.1*
6	C	9.5	87.2	1.6	E	15/6/2009 – 15/6/2010	3.4
7	P	2.1	25.0	1.3	E	15/6/2009 – 15/6/2010	3.9
8	P	3.6	35.9	2.8	E	16/6/2009 – 14/6/2010	*6.8*
9	P	1.6	9.6	4.5	S	17/6/2009 – 14/6/2010	*6.5*
10	P	1.6	5.5	5.3	S	17/6/2009 – 11/6/2010	*5.2*
11	P	0.8	4.6	2.4	E	14/6/2009 – 14/6/2010	6.3
12	C	6.4	115.0	3.7	E	13/6/2009 – 13/6/2010	2.8
13	C	3.2	49.6	1.1	W	25/6/2009 – 16/6/2010	*3.9*
14	P	3.9	24.9	2.3	W	25/6/2009 – 16/6/2010	*5.4*
15	P	3.0	32.4	1.3	N	24/6/2009 – 18/6/2010	3.5
16	C	4.4	114.0	2.1	N	24/6/2009 – 17/6/2010	*3.9*
17 (Hope)	C	6.8	276.0	9.2	N	24/6/2009 – 18/6/2010	*3.6*
Mean	--	*3.9*	*55.0*	2.9	--	--	4.5[2]
Channels							
M (Harry)				1.2	N	24/6/2009 – 18/6/2010	*4.3*
A (Husky)				10.1	S	17/6/2009 – 11/6/2010	*4.8*
D (Campbell Creek)				4.9	E	6/7/2009 – 10/6/2010	*4.2*
I (Pederson)				5.2	E	23/6/2009 – 18/6/2010	*4.6*
E				10.8	E	16/6/2009 – 14/6/2010	*4.6*
K				3.7	N	23/6/2009 – 18/6/2010	*4.5*
Mean				*6.1*	--	--	4.6[2]

[1]NRC Lake MAWT based on additional data collected 2006–2009 by C.R. Burn. MAWT for NRC Lake for 6 June 2009–6 June 2010 is 6.2°C, as shown in Fig. 5.1.
[2]Standard error of MAWT for lakes and channels is 0.3°C and 0.1°C, respectively.

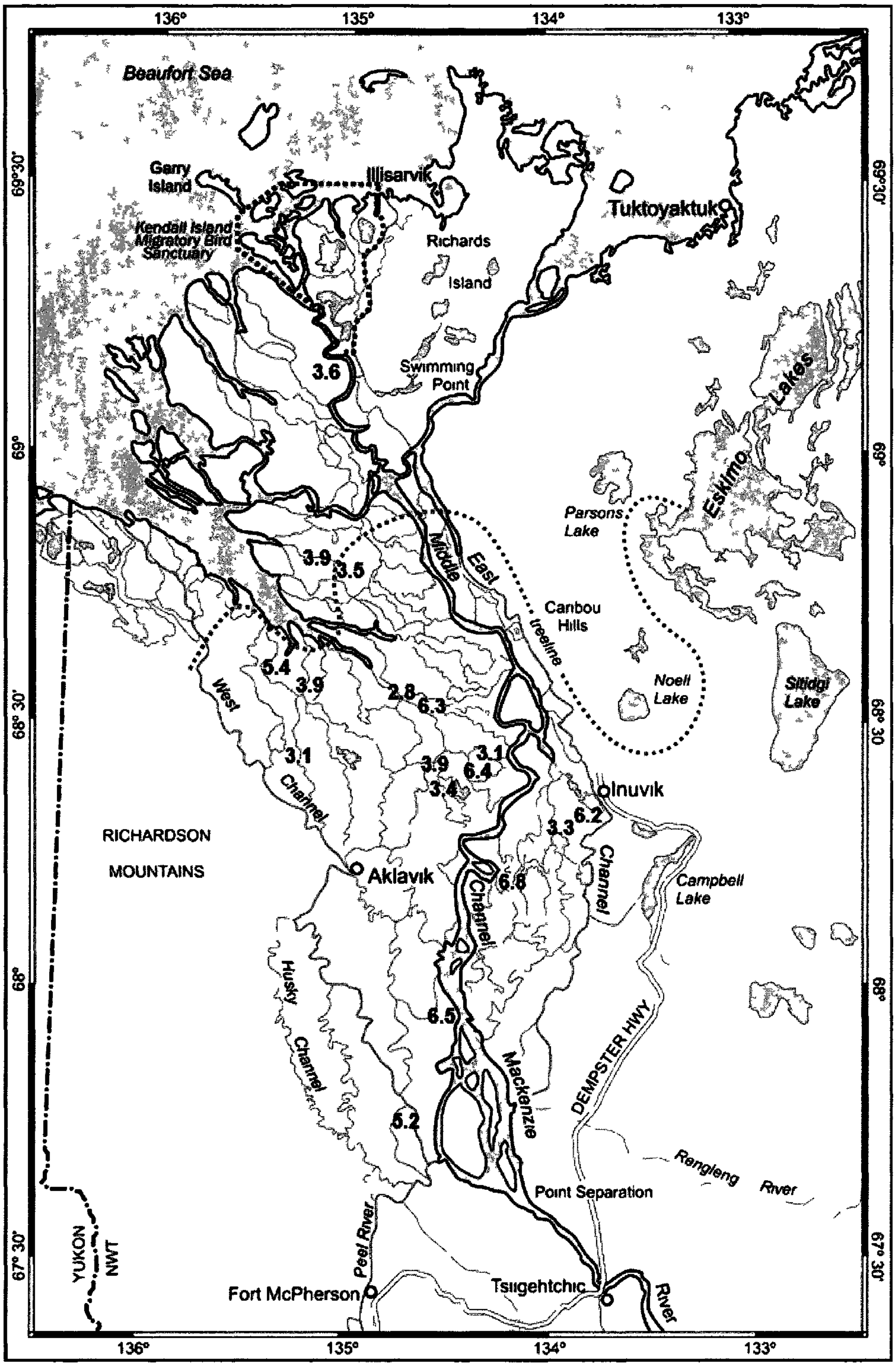

Figure 5.1. Mean basal water temperature for 17 Mackenzie Delta lakes, June 2009–2010.

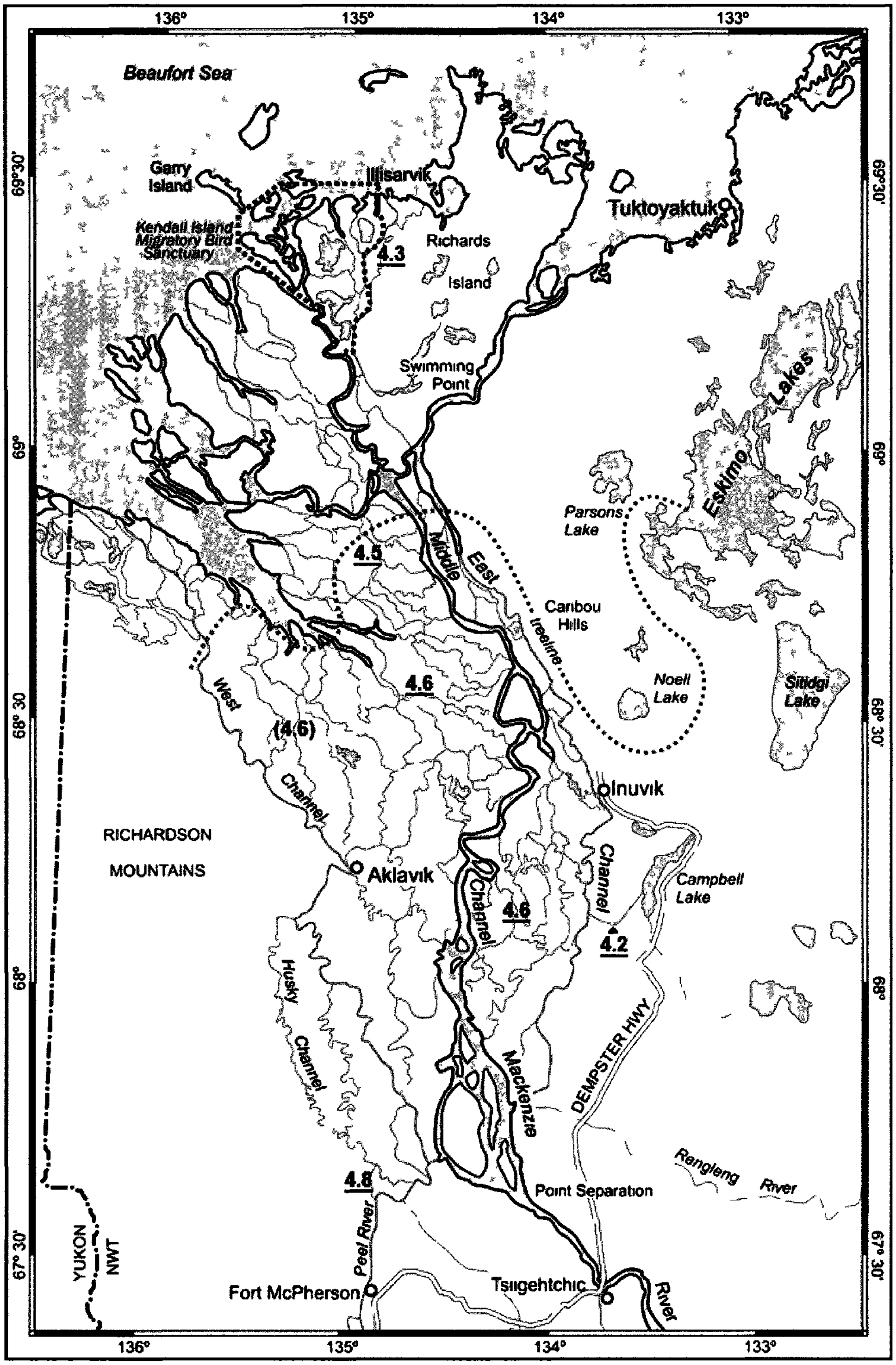

Figure 5.2. Mean basal water temperature for five Mackenzie Delta channel sites and Campbell Creek, June 2009–2010. The value in parentheses is estimated using the relation between mean summer channel temperature in the western delta and the summer and annual means of all other available channels.

central pools of Richards Island lakes by Mackay (1962, 1963), and with measurement-based estimates of 3.7 to 4.8°C by Burn (2002).

The relatively low MAWT observed for lakes near and beyond treeline (Fig. 5.1) may result from reduced surface insulation during winter compared with lakes in the forested portion of the delta. Burn (2005) observed MAWT values of 5.6°C, 3.3°C, and 3.5°C for a taiga and two tundra lakes, and noted that a thicker snowpack is likely to develop on the ice of a sheltered lake than one in the tundra. This insulating layer aids the retention of heat released from lake sediments during the period of ice cover, and reduces ice thickness. The earlier breakup of ice cover in forested regions initiates the process of warming by forced convection earlier.

Within the forested portion of the delta, MAWT appears to be controlled to a greater extent by a lake's connectivity than latitude. Lake MAWT values appear bimodal, with an average among perched lakes 2.1°C greater than among connected (Table 5.2). A likely cause of the difference is the drawdown of water in connected lakes in response to decreasing channel water level in the late summer and autumn. This would leave connected lakes relatively shallow during winter, with ice cover forming closer to the lake-bottom. As shown in Fig. 5.3, depth does not appear to have a strong influence on lake basal temperature on an annual basis.

The apparent decrease in channel MAWT with greater latitude (Fig. 5.2) may be in response to the gradient in mean annual air temperature between the southern and northern regions of the Mackenzie Delta, described by Burn and Kokelj (2009) and outlined in Section 3.1.3. The relatively low MAWT value of 4.2°C for Campbell Creek

Table 5.2. Mean annual water temperature (°C) for Mackenzie Delta study lakes and channels, by region. The number of study sites is given in ( ). 'SE' is standard error among mean annual temperatures for all water bodies in the region or of the type specified.

Delta Region	Channels	Perched Lakes	Connected Lakes	All Lakes	Mean ± SE
Tundra	4.4 (2)	3.5 (1)	3.7 (2)	3.6 (3)	4.0 ± 0.2 (5)
Forest	4.7 (3)[1]	5.8 (8)	3.3 (6)	4.7 (14)	4.7 ± 0.3 (17)
Southern	4.8 (1)	5.9 (2)	No Data	5.9 (3)	5.5 ± 0.5 (3)
Eastern	4.6 (2)	5.8 (5)	3.2 (4)	4.7 (9)	4.6 ± 0.4 (11)
Western	[4.6][2]	5.4 (1)	3.5 (2)	4.1 (3)	4.1 ± 0.7 (3)
Mean ± SE	4.6 ± 0.1 (5)	5.5 ± 0.4 (9)	3.4 ± 0.1 (8)	4.5 ± 0.3 (17)	4.5 ± 0.3 (22)

[1] The MAWT of Campbell Creek, due to period of record, is not included in the calculation of average MAWT among channels.

[2] Value is estimated using the relation between mean summer channel temperature in the western delta and the summer and annual means of all other available channels.

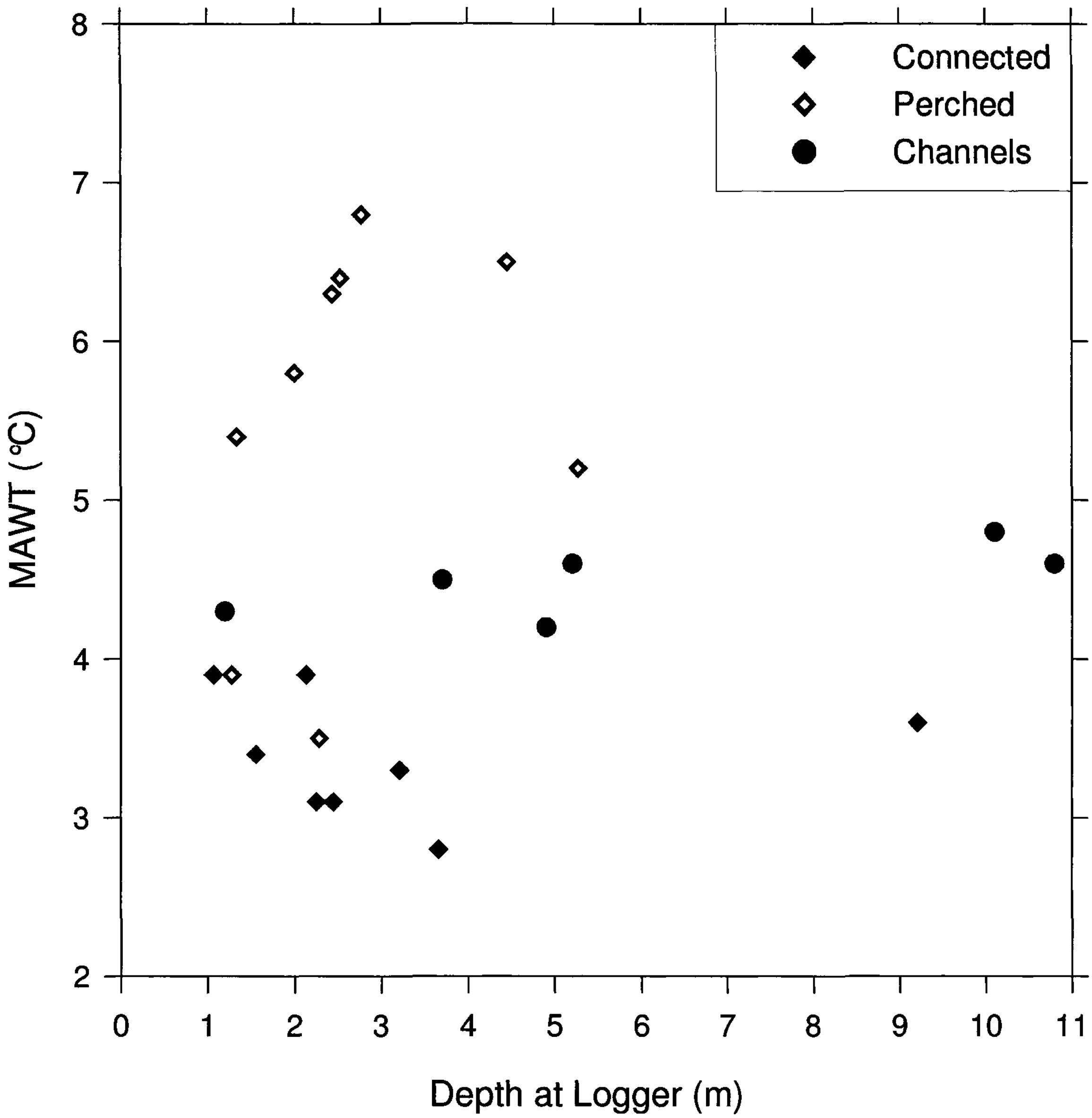

Figure 5.3. Relation between mean annual basal water temperature and depth for perched and connected study lakes and channel sites in the Mackenzie Delta.

(Fig. 5.2) may result from the large volume of Campbell Lake, which feeds Campbell Creek following the annual spring flood of the Mackenzie River. Campbell Lake is a large connected lake (area ~ 31 km^2) whose basal temperature averaged 1.3°C over the period of 10 August 2009 to 10 June 2010 for which it was logged. Due to this limited period, the Campbell Lake temperature record is not reported or included in analyses elsewhere.

5.3 Hypothesis Testing

Section 1.5 set out three specific hypotheses about the spatial variability of MAWT in the Mackenzie Delta. Each is reviewed here and tested statistically using MAWT values determined for the water bodies studied. Appendix C presents the distributions of sample data used in selecting appropriate hypothesis tests. Nonparametric statistics are required in each case, and consequently tests cannot lead to statistical claims about the relation between the means of the two sample groups being considered. It remains possible to assess and state whether a significant difference exists between the groups, based on the values comprising each sample group, without reference to group mean. The results of each hypothesis test have been stated accordingly.

5.3.1 MAWT Across Treeline

The MAWTs of water bodies in the tundra region of the delta were expected to be lower than those of water bodies in the forested delta. As forest region MAWT values are not normally distributed, the hypothesis above will be tested using the nonparametric Mann-Whitney U test (Ebdon, 1985). The sample symbols x and y will represent measured values of MAWT from water bodies in the tundra and forest delta regions, respectively.

The symbols X and Y will represent MAWT values from the entire population of water bodies in tundra and forested delta, respectively. The following null hypothesis H_0 and alternate hypothesis H_1 are therefore adopted for testing purposes:

H_0: $X = Y$ H_1: $X < Y$

Note that in this and in subsequent cases, the alternate hypothesis is the same as the original hypothesis. When MAWTs from all measured water bodies (i.e. all x and y values) are ranked together (where rank 1 is the lowest MAWT value), the sum of ranks for forest water bodies $\sum r_y$ and tundra water bodies $\sum r_x$ are 208 and 45, respectively. Tundra and forest sample sizes are 5 and 17, respectively, and a one-tailed test at significance level $\alpha = 0.05$ is selected (Ebdon, 1985). These conditions specify 20 as the critical value of U (U_{crit}). The Mann-Whitney test statistics U_x and U_y are calculated as 55 and 30, respectively, as shown in Appendix C. The alternate hypothesis of $X < Y$ requires the comparison of U_{crit} with U_{y}.. Since $U_{crit} < U_y$, the null hypothesis cannot be rejected. While water bodies in the Mackenzie Delta may appear to have lower MAWTs north of treeline than south of it, there is no statistically significant difference between MAWTs from tundra water bodies and those in the forest.

5.3.2 MAWT Between Channels and Lakes

The MAWTs of channels were expected to be lower than those of lakes in the delta. The null (H_0) and alternate hypotheses (H_1) which correspond are given as:

H_0: $X = Y$ H_1: $X < Y$

where X and Y now refer to values of MAWT within the population of delta channels and lakes, respectively. The sum of ranks for lakes $\sum r_y$ and channels $\sum r_x$ are 188 and 65, respectively, and with the same α and sample sizes as in the previous test, the U_{crit} value of 20 falls beneath the U_y value of 50 (Ebdon, 1985). There is again insufficient evidence to reject H_0, and hence no statistically significant difference between the MAWTs of delta lakes (when both connectivity types are taken together) and those of delta channels.

5.3.3 MAWT Variability Among Channels and Lakes

Variability in MAWT was expected to be lower among channel sites than among lakes in the Mackenzie Delta. An F statistic of 69.9 is calculated as the quotient of the two samples' variances, which were 2.08°C^2 and 0.03°C^2 for lakes and channels, respectively. This is well within the critical region bounded by the F_{crit} value of 8.7, determined using degrees of freedom of 16 and 4 for lakes and channels, respectively, at $\alpha = 0.05$ (two tails) (Triola et al., 1999). This would suggest that the variances of the two groups are statistically unequal. The F test requires that each sample have a normal distribution, however, and this is not the case among the samples of lake MAWT. While the spatial variabilities of channel and lake MAWT are indeed distinct, with standard errors of 0.1°C and 0.3°C, respectively (Table 5.2), the significance of this difference is not assessed.

5.3.4 MAWT Between Perched and Connected Lakes

No hypothesis was made at the outset as to the relation between perched and connected lake MAWTs. The averages of MAWT values for perched and connected lakes are 5.5°C and 3.4°C respectively (Table 5.2). Values for MAWT of perched and connected lakes are shown to differ significantly using the Mann-Whitney U test where $\alpha = 0.05$, rank sums $\sum r_y$ (perched lakes) and $\sum r_x$ (connected lakes) are 39 and 114, respectively, and the value of U_y (3) is less than the U_{crit} value of 18. On this basis, a null hypothesis of no difference between values from the two groups of lakes would be rejected in favour of an alternate hypothesis of greater MAWT values for perched lakes than connected lakes.

5.4 Temporal Variability

Following their summer maxima at the end of July, study lake basal temperatures exhibited a peak in late August, averaging 15°C (Fig. 5.4). Ice cover formed at the end of September, as shown in Fig. 5.5 by the rebound in the time series of average temperature for perched lakes. Among perched lakes, basal water temperature increased quickly over the first few days where ice cover was present. This was observed at Barrow, Alaska, by Brewer (1958), who attributed it to continued solar insolation through clear ice prior to snow accumulation, in the absence of convective cooling by wind. Following snow accumulation, heat emission from lake sediment is the likely cause of the continued gradual warming of basal waters until their mean winter peak of ~5°C in mid-October.

Average basal temperature among connected lakes dropped below 0°C at the end of November, suggesting that ice cover began to reach and aggrade around data loggers. The minimum mean temperature among perched and connected lakes occurred on 27 March. Between this minimum and the rapid temperature increase observed in late May, a zero curtain is apparent in the connected lake mean temperature series (Fig. 5.4). Basal temperature remains near 0°C for approximately one month between late April and late May. Figure 5.4 reveals abrupt changes in the minimum temperature among study lakes during October 2009. These fluctuations, which include temperatures below -10°C, belong exclusively to Lake 6. This is a shallow connected lake, which likely drained into

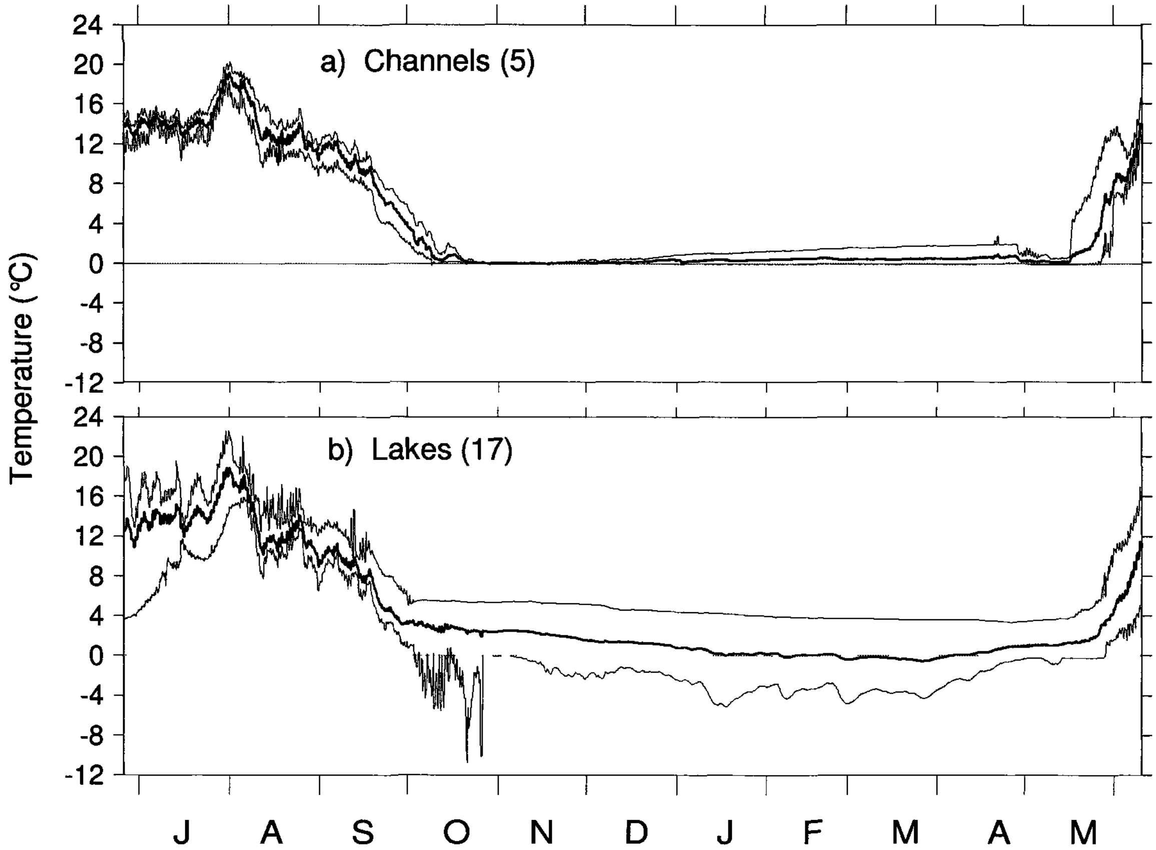

Figure 5.4. Maximum, mean, and minimum basal water temperatures among (a) 17 Mackenzie Delta lakes and (b) 6 Mackenzie Delta region channel sites for the period 25 June 2009–10 June 2010. Measurements at Lake 6 alone account for the low values and abrupt changes in the minimum lake temperature series during October.

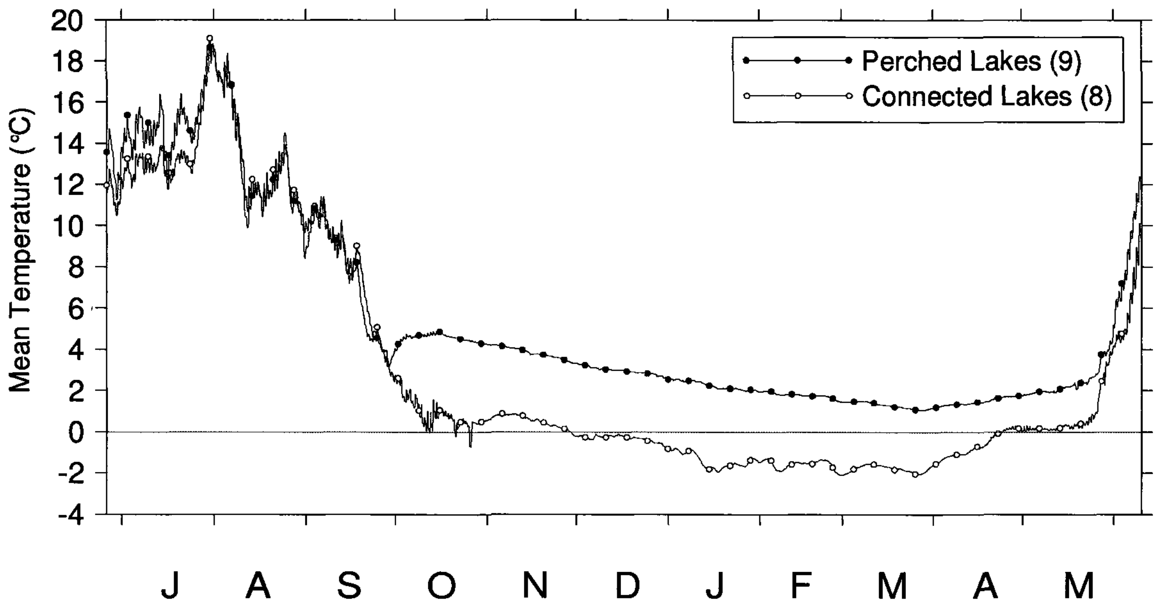

Figure 5.5. Average basal water temperature among nine perched and eight connected lakes, Mackenzie Delta, June 2009–2010.

the connecting channel to the extent that the data logger recorded air temperature for a time interval in early and mid-October 2009. In late October basal temperature returned to 0°C, and the zero-curtain which is evident until early November suggests the subsequent freezing of a shallow layer of water. An accumulation of a thick snow cover may also explain the sudden resumption of a steady 0°C basal temperature at Lake 6 in late October 2009. The equivalence of Lake 6 MAWT (3.4°C) to the average MAWT for all connected lakes (Table 5.2) suggests that winter conditions there may be representative of other connected lakes. Snow cover may permit the retention of heat by lake bed sediments upon which the data logger rests. If snow cover distribution is similar over the entire area of the lakebed, winter basal temperatures may not vary appreciably from one lake bed location to another, regardless of their proximity to or depth beneath ice cover. If moderate winter basal temperatures, despite the likely presence of bottom-fast ice, characterize connected lakes, then their MAWTs are likely to be strongly dependant on their summer thermal regimes. Despite the potential absence of a water layer in some lakes during winter, high-magnitude temperature fluctuations in early winter contribute nonetheless to mean annual basal temperature. No effort is made to correct for these fluctuations when applying MAWT in predictions of talik configuration.

Among channel sites, mean basal temperature showed a peak in late August similar to that observed among study lakes (Fig. 5.4). The subsequent decrease in temperature was almost linear until it approached 0°C in the second week of October. For nearly two months between mid-October and mid-December, spatial and temporal variability around the mean channel basal temperature of 0°C was almost nonexistent. Beginning in early December, the basal temperature of Husky Channel exhibited a gradual increase of less than 0.4°C/month. This departure of Husky Channel basal temperature from 0°C was the primary cause of the small corresponding departure of mean basal temperature among all five channel sites from 0°C. At the end of April, basal temperature at the Husky Channel site abruptly fell again to 0°C. This may have occurred as a result of the cessation of basal water flow in the vicinity of the data logger due to an ice blockage in the early winter. Warming may be the result of heat released to stagnant water as in lakes. The removal of a blockage in the early stages of spring breakup may account for the late-winter temperature drop.

5.5 Ground Thermal Regime

Investigations of ground thermal regime in the Mackenzie Delta region have been made at several scales. These include NRC Lake (Brown et al. 1964), a site in the northeastern delta containing several lakes and a distributary channel (Smith 1976), and Richards Island (Burn 2002). All studies included predictions of talik configuration surrounding water bodies and confirmed these through field investigations. The purpose of the remainder of this chapter is to use previously reported MAGT for the forest and tundra regions of the delta, estimated MAWT of delta surface water bodies reported earlier in this chapter, and surface geometry for the delta lake and channel network to produce an estimate of the pervasiveness of through taliks in the entire Mackenzie Delta. The steady-state thermal models employed are presented in sections 2.5 and 3.2.4.

5.6 Analysis of Mackenzie Delta Surface Water Coverage

The number and total area of connected lakes, perched lakes, and channels in both tundra and forest regions of the delta, obtained through GIS analysis, are presented in Table 5.3.

Table 5.3. Mackenzie Delta lake and channel summary statistics from GIS analysis.

	Connected Lakes	Perched Lakes	All Lakes	Channels	All Water Bodies
Forested Delta (8,959 km^2)					
n Lakes	574	39,606	40,180		
n Elongate Lakes	270	15,272	15,542		
n Circular Lakes	304	24,334	24,638		
Mean Area (km^2)	0.71	0.06	0.77		
Total Area (km^2)	406	2,394	2,800	859	3,659
% Forested Delta	4.5	26.7	31.3	9.6	40.8
Tundra Delta (4,176 km^2)					
n Lakes	74	7,997	8,071		
n Elongate Lakes	27	3,422	3,449		
n Circular Lakes	47	4,575	4,622		
Mean Area (km^2)	2.21	0.07	2.27		
Total Area (km^2)	163	555	718	501	1,219
% Tundra Delta	3.9	13.3	17.2	12.0	29.2
Entire Delta (13,135 km^2)					
n Lakes	648	47,603	48,251		
n Elongate Lakes	297	18,694	18,991		
n Circular Lakes	351	28,909	29,260		
Mean Area (km^2)	0.88	0.06	0.07		
Total Area (km^2)	570	52,949	3,518	1,360	4,878
% Entire Delta	4.3	22.4	26.8	10.4	37.1

The total number and area of lakes in the Mackenzie Delta were determined to be 48,251 and 3,518 km^2, respectively. These are in reasonable agreement with corresponding determinations of 49,046 and 3,331 km^2 made by Emmerton et al. (2007). As in Burn (2002) and described in section 3.2.4.2, lakes were classified as circular or elongate to determine whether their dimensions needed to be compared with a critical radius or critical half-width to determine through talik occurrence. Critical radius and half-width are prescribed by MAWT and MAGT as described by Equations 6 (section 2.5) and 8 and 9 (section 3.2.4.1).

GIS analyses also determined the width distribution of lakes and channels in the Mackenzie Delta. These are presented in Figs. 5.6 and 5.7, respectively. The figures display the distribution for forest and tundra regions individually, as the two regions were analyzed separately due to different MAGT and average MAWT values.

5.7 Predicted Ground Thermal Regime

Table 5.4 presents the critical radii for circular lakes and critical half-widths for channels and elongate lakes. In these determinations, MAWT values are assumed equal to the average among instrumented water bodies of the corresponding type (perched lakes, connected lakes, or channels) in the same ecological region (tundra, forest). MAGT values are assumed to be -2.25°C and -4°C for forested and tundra regions, respectively, which are the midrange of corresponding thermal envelopes reported by Burn and Kokelj (2009). Two sets of critical dimensions are presented. The dimensions of the 'Observed' MAWT series are based on MAWT estimates from the 2009-2010 study period only (Table 5.2), while the 'Adjusted' MAWT series estimates are obtained as explained in

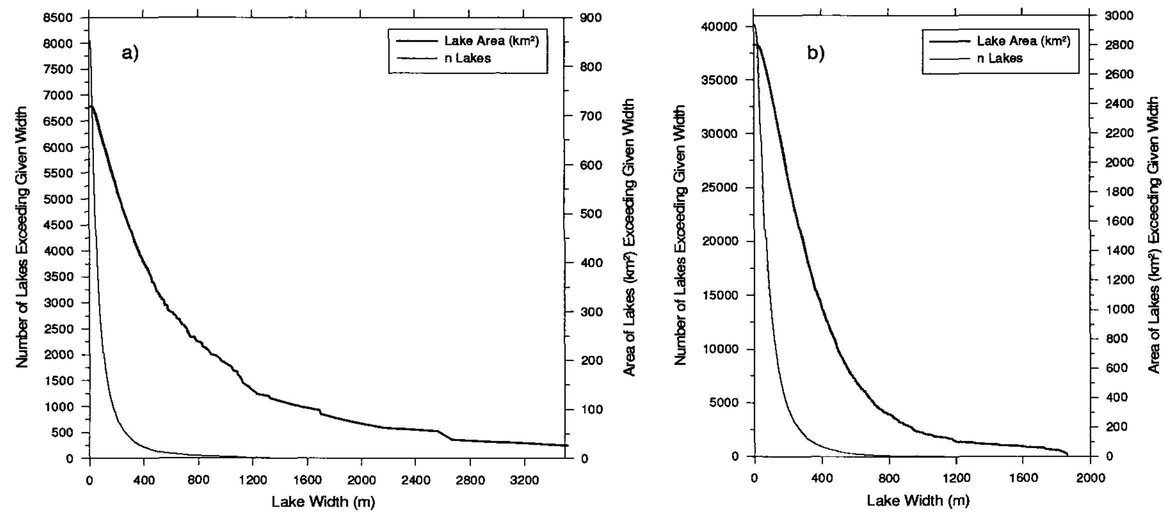

Figure 5.6. Width distribution of lakes in (a) tundra and (b) forested regions of the Mackenzie Delta. Lake widths are represented by Minimum Bounding Rectangle widths, tabulated in a GIS as described in section 3.2.4.2.

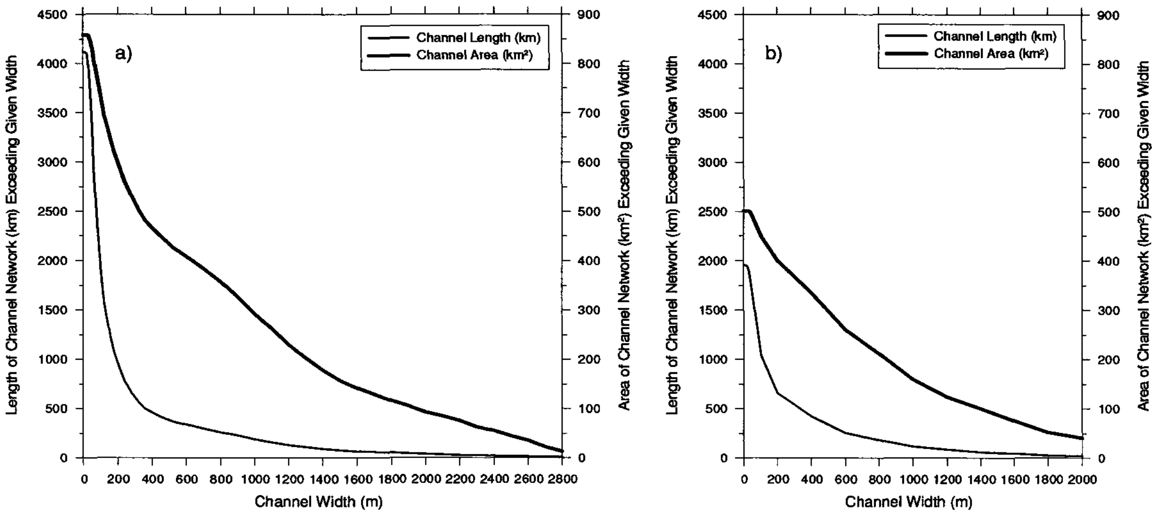

Figure 5.7. Width distribution of channels in (a) forested and (b) tundra regions of Mackenzie Delta as determined by GIS analysis. Distribution is determined as described in section 3.2.4.2.

Table 5.4. Critical radii^{r} and half-widths^{hw} for through talik occurrence, under steady-state conditions, beneath water bodies of specified shape and connectivity in the tundra and forest regions of the Mackenzie Delta. MAWT is based on averaged field measurements for the relevant lake type in the given region, and is specified in parentheses in the final two columns.

MAWT	Shape	Connectivity	Tundra (MAGT = -4°C)		Forest (MAGT = -2.25°C)	
Observed	Circular	Perched Lk.	119.5 m ^{r}	(3.5°C)	63.2 m ^{r}	(5.8°C)
	(eq. 10, 11)	Connected Lk.	119.0 m ^{r}	(3.7°C)	65.0 m ^{r}	(3.3°C)
	Elongate	Perched Lk.	35.8 m ^{hw}	(3.5°C)	9.8 m ^{hw}	(5.8°C)
	(eq. 6)	Connected Lk.	34.8 m ^{hw}	(3.7°C)	14.8 m ^{hw}	(3.3°C)
		Channels	31.3 m ^{hw}	(4.4°C)	11.8 m ^{hw}	(4.7°C)
Adjusted	Circular	Perched Lk.	120.5 m ^{r}	(3.1°C)	63.4 m ^{r}	(5.4°C)
		Connected Lk.	120.0 m ^{r}	(3.3°C)	65.7 m ^{r}	(2.8°C)
	Elongate	Perched Lk.	38.3 m ^{hw}	(3.1°C)	10.3 m ^{hw}	(5.4°C)
		Connected Lk.	36.8 m ^{hw}	(3.3°C)	16.8 m ^{hw}	(2.8°C)
		Channels	33.3 m ^{hw}	(4.0°C)	12.3 m ^{hw}	(4.3°C)

section 3.2.4.3 using the relation between the 2009–2010 and 2006–2010 basal temperature record for NRC Lake.

Using the width distribution of lakes by connectivity type in the forest and tundra regions of the delta, the critical radii and half-widths presented in Table 5.4 specify the proportion of lakes predicted to produce through taliks. These are presented in Table 5.5. While only 60% of all Mackenzie Delta lakes are predicted to produce through taliks, the corresponding area of these lakes is 3,345 km^2, or 95% of the entire lake area of the delta.

As shown in Fig. 5.7, nearly the entire area of the channel network in the tundra and forest regions of the delta is composed of channel reaches whose half-widths exceed the critical half-widths given in Table 5.4. The total area of through talik predicted beneath the delta channel network, as well as that beneath perched lakes and connected lakes, is presented by region in Table 5.6 for a range of MAGT values. Total predicted through-talik area for the entire delta is presented in Fig. 5.8a using both observed and adjusted MAWT values. This figure also provides predictions under consistent departures (up to ±2°C) from MAGT in the tundra (-4°C) and forest (-2.25°C) regions of the delta. Figure 5.8b presents the estimated number of delta lakes to maintain through taliks using observed MAWT values. Figure 5.8b also provides estimates of through talik prevalence when all lake radii or half-widths are adjusted by -2.5, -5, -10, and -20 m from those obtained using National Topographic Series delta maps derived from summer air photos. Such size reductions may be representative of long-term average lake geometries, owing to winter drawdown and ice thickness. Under observed MAGT and MAWT conditions, a 20 m width (or diameter) reduction for all delta lakes is expected to decrease through

Table 5.5. Predicted prevalence of through taliks beneath perched and connected lakes in the forest and tundra regions of the Mackenzie Delta.

Lake Type, Region	Fraction of lakes predicted to have through taliks	Percent of lakes predicted to have through taliks
Perched, Tundra	2,355 / 7,997	29.4
Connected, Tundra	65 / 74	87.8
Perched, Forest	25,881 / 39,606	65.3
Connected, Forest	473 / 574	82.4
Entire Delta	28,774 / 48,251	59.6

Table 5.6. Predicted through talik area (km^2) by Mackenzie Delta region and water body type. Mean annual water temperatures are as reported in Table 5.2.

	Connected Lakes	Perched Lakes	Channels	Total	Percent Area
Forested Delta					
MAGT (°C)					
-0.25	406	2,394	859	3,659	40.9
-1.25	406	2,374	859	3,639	40.6
-2.25	405	2,290	859	3,555	39.7
-3.25	402	2,151	840	3,394	37.9
-4.25	398	1,975	794	3,166	35.3
Tundra Delta					
MAGT (°C)					
-2.0	163	540	501	1,204	28.8
-3.0	163	518	497	1,178	28.2
-4.0	163	487	479	1,129	27.0
-5.0	163	453	458	1,074	25.7
-6.0	162	419	437	1,018	24.4

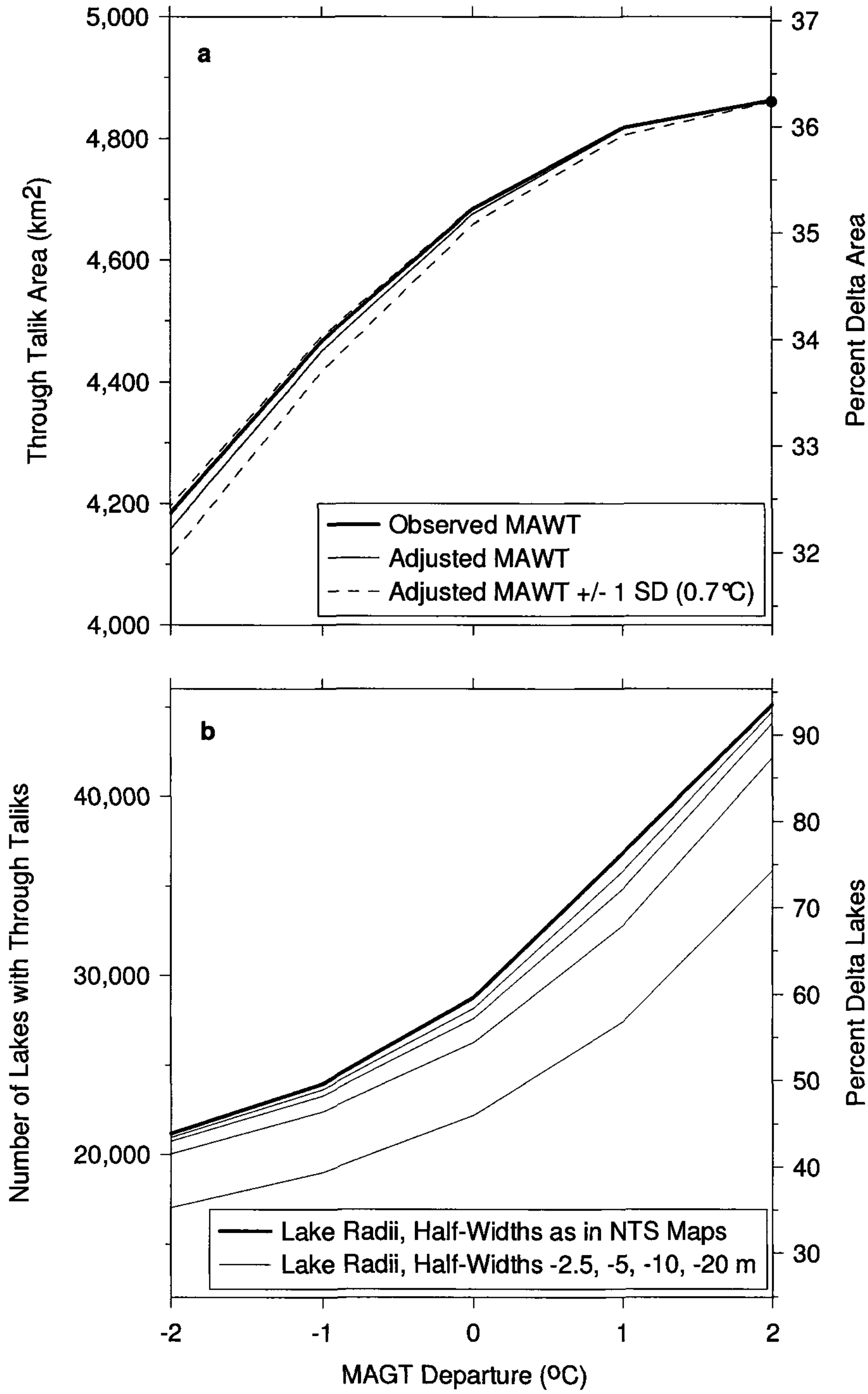

Figure 5.8. Total predicted area (a) and prevalence (b) of through taliks in Mackenzie Delta. Area predictions combine channel and lake through taliks. Adjusted MAWT, shown in (a), is obtained as described in section 3.2.4.3. Four additional estimates of through talik prevalence are made using lake radii or half-widths which differ by -2.5, -5, -10, and -20 m from those in National Topographic Series delta maps. The two heavy plot lines in (a) and (b) are directly comparable.

talik prevalence by 2,519 or 5.2%.

In making these predictions of through talik occurrence, it is assumed that the MAWT of each water body in the delta is similar to the mean measured among water bodies of the same type in the same ecological region of the delta. Secondly, MAWT and MAGT values used in through talik prediction are assumed representative of long-term conditions. These two assumptions cannot be circumvented, and the only means of improving their validity is increasing the sample size of water bodies and years of temperature record. As discussed, observed and adjusted MAWT values are used in determining through talik area in the delta. The adjusted MAWT for each lake and channel is determined as shown in Equation 10 (section 3.2.4.3). Mean NRC Lake basal temperature for June 2009–May 2010 was greater than that for June 2006–May 2010 by 0.4°C. As shown in Table 5.7, Inuvik mean air temperature was also greater for June 2009–May 2010 than for June 2006–May 2010. When summer (June–August) mean temperatures are considered, however, this trend does not persist. In summer 2009, while the average temperature in NRC Lake was relatively high among the past four summers of record, Inuvik air temperature was relatively low. This would imply poor coupling between summer air and lake water temperatures, contrary to what is suggested in Chapter 4. A more likely cause of the relatively high 2009 summer basal temperature at NRC Lake is the movement of the data logger during download on 9 June 2009. The logger was replaced and positioned approximately 50 m from its previous position, where it was affixed by cable to a more stable tree. The re-positioning of the logger within lake sediments, and small depth change, may account for the sharp increase of approximately 2°C on 9 June 2009, illustrated in Fig. 5.9. This change may cause the relatively high

Table 5.7. Comparison of annual and summer mean air temperatures at Inuvik (°C) and annual and summer mean basal water temperatures (°C) for NRC Lake.

	Air, Inuvik		Water, NRC Lake	
	2009-2010	2006-2010	2009-2010	2006-2010
Annual (June to May)	-6.4	-7.2	6.2	5.8
Summer (June, July, Aug.)	11.0	12.4	14.1	13.4

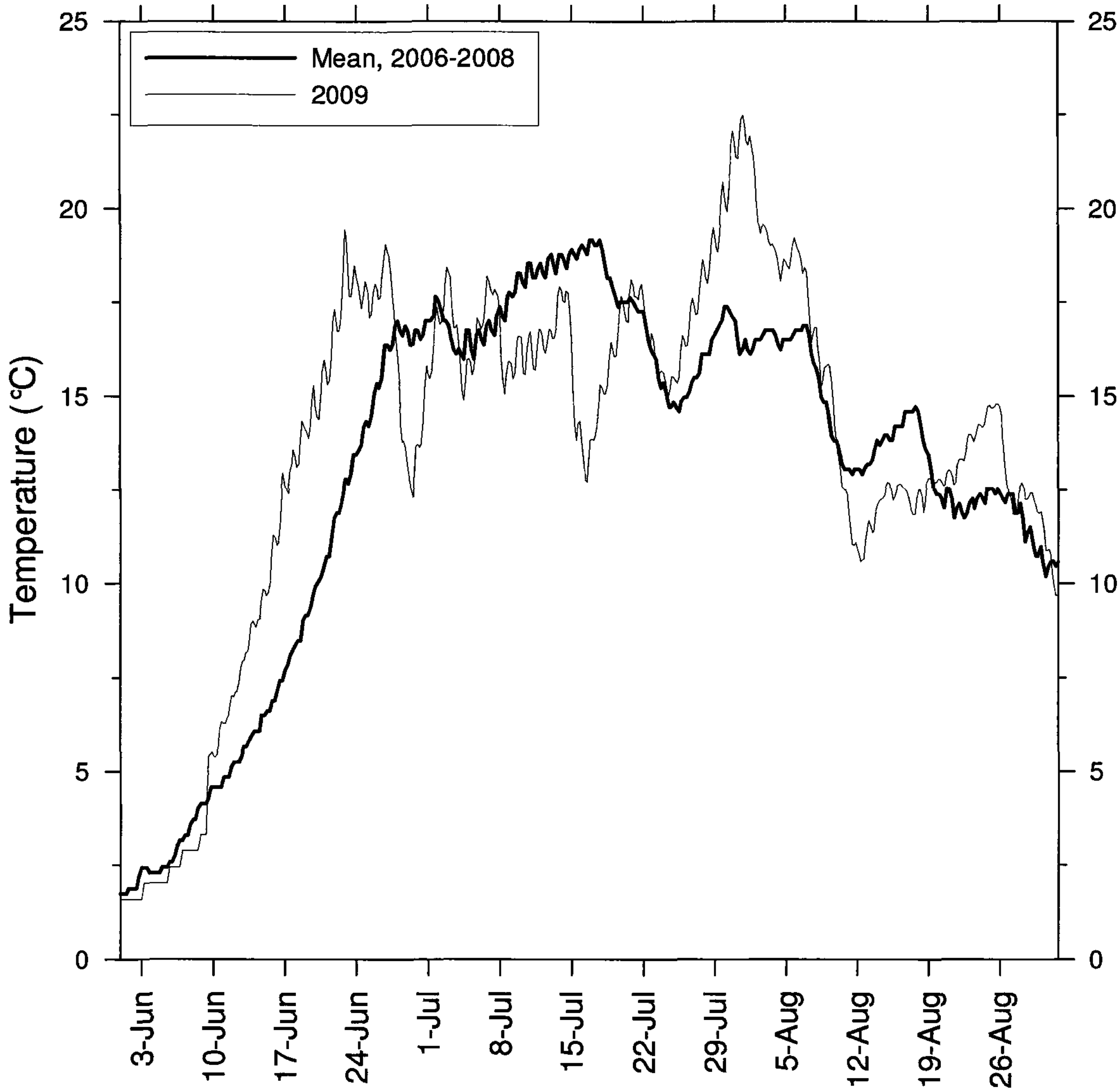

Figure 5.9. NRC Lake summer basal water temperature series for 2009, and average summer basal water temperature series for 2006–2008.

basal temperature which persists until 28 June, 2009 (Fig. 5.9), driving up 2009 MSWT at NRC Lake. If these effects of instrument monitoring are in fact the cause of the relatively high 2009 MSWT at NRC Lake, NRC Lake MAWT for June 2009–May 2010 will also carry a slight positive bias relative to MAWT for the period June 2006–May 2010. Adjusted MAWT values for all water bodies may therefore be negatively biased by up to 0.4°C. Consequently, in Fig. 5.8a, the least biased predictions of through talik pervasiveness may lie between the 'Observed MAWT' and 'Adjusted MAWT' plots.

Through talik surface area is assumed approximately equal to that of the overlying water body. This assumption has been made based on field observations of through taliks typically having steep walls (Burn 2002 p.1291, Smith 1976 p.13, Johnston and Brown 1964 p.174), and on a series of predictions of the steady-state ground temperature field beneath a transect representing NRC Lake and the adjacent channel. Figure 5.10 illustrates the first of seven scenarios run using Temp/W (© Geoslope International). Temp/W uses a finite-element (numerical) approach based on a grid of points at which temperature is approximated. With steady-state (analytical) applications, the temperature isolines shown in Figs 5.10, Fig. 5.11, and all figures in Appendix D are interpolated among points on a 10 m x 10 m grid, at which exact solutions for temperature are possible. MAGT, indicated in Fig. 5.10, corresponds to a closed spruce feathermoss (CSF) community (Kanigan et al., 2009) and is thus set at -4.4°C. Output from Scenarios 2–7 (Appendix D) use MAGT values for various vegetation communities and delta regions, and MAWT for various water body types. All model output suggests that through talik width remains similar to that of the water body when critical size is exceeded. Temp/W uses a 2-dimensional model, however, which likely explains in part

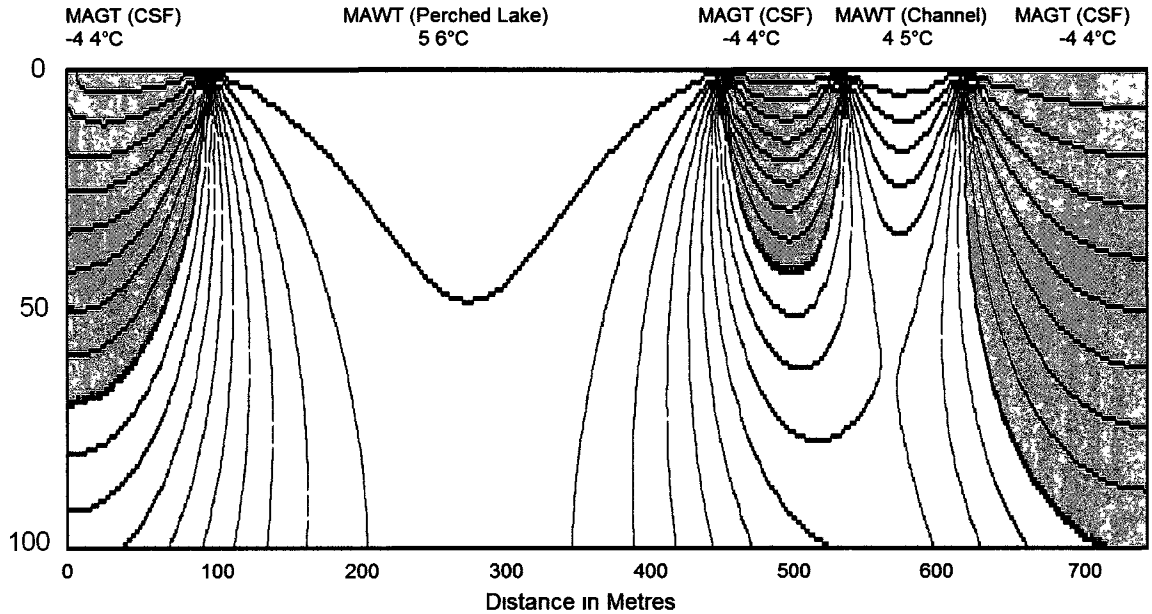

Figure 5.10. Output of steady-state run of Temp/W model using geometry corresponding to south to north (left to right) transect across NRC Lake and the adjacent channel. MAWT and MAGT values specified in figure. Left axis shows depth in metres. Isolines shown at 0.5°C intervals. Dark and light fill represent permafrost and unfrozen ground, respectively.

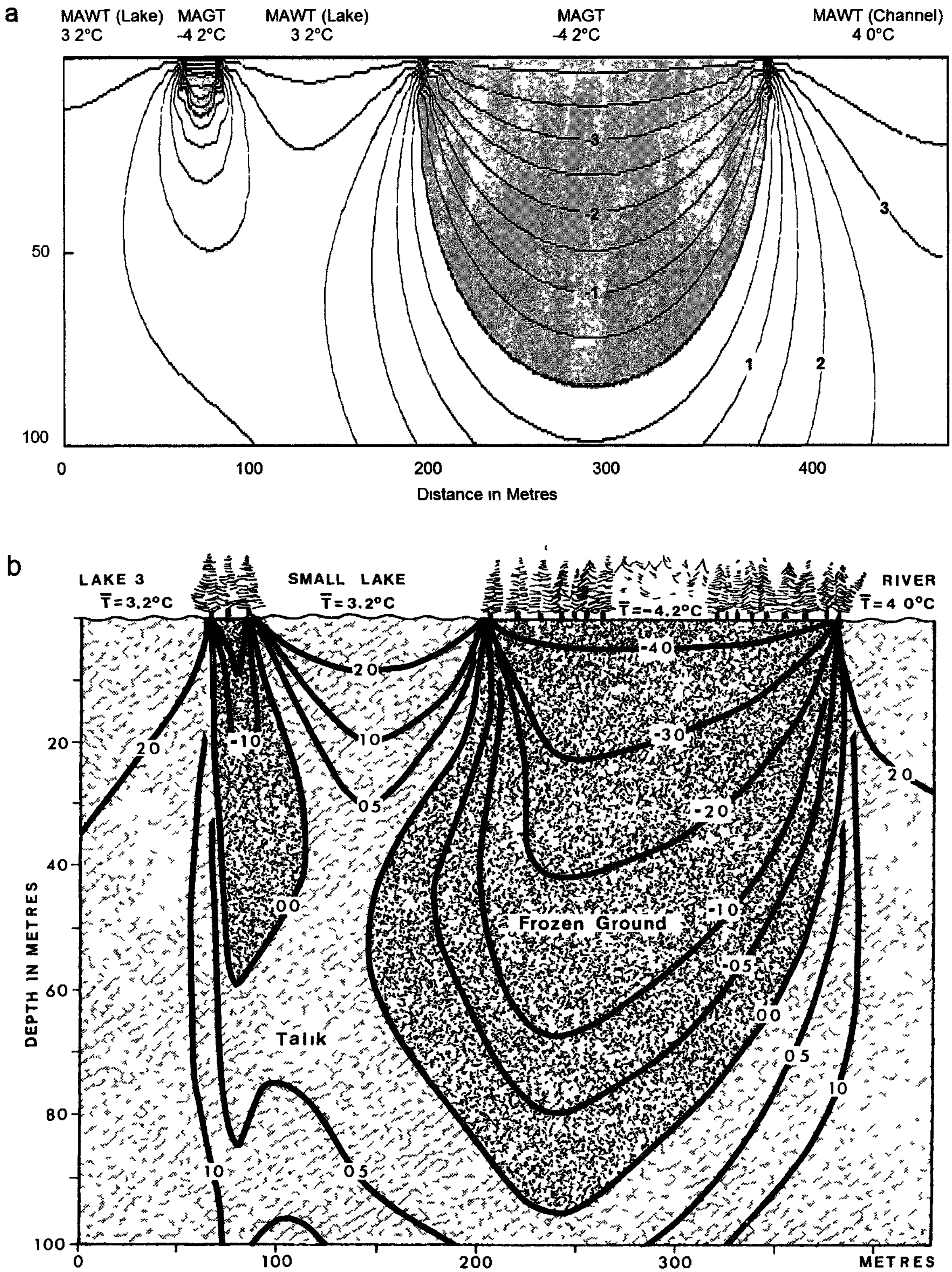

Figure 5.11. Output (a) of steady-state run of Temp/W model using surface geometry and mean temperatures from Fig. 2.13 (reproduced for comparison as part b). MAWT and MAGT values specified in figure. Left axis shows depth in metres. Dark and light fill represent permafrost and unfrozen ground, respectively.

the difference between Fig. 5.11 and Fig. 2.13 (reproduced for reference beneath Fig. 5.11). Both use the same input geometry and mean temperatures, however Fig. 2.13 is a cross section of 3-dimensional model output (Smith, 1976) and reveals narrowing of a through talik beneath a small lake. For this reason, it is possible that through talik area beneath small delta lakes has been overestimated.

Another potential contributor to the overestimate of through talik area is bathymetry-imposed reductions, during winter, in the surface area of basal conditions described by water bodies' MAWTs. Water level reductions and the formation of thick ice cover may reduce long-term mean lake and channel areas to values beneath those expected using GIS datasets based on NTS data from aerial photos taken primarily in summer. As discussed, however, well-distributed snow cover on potentially drained connected lake beds may maintain the effective area and spatial consistency of the thermal disturbances they represent. The thermal influences of snow accumulation along shorelines (Smith, 1976) or thermokarst expansion of lakes since the aerial photographs were taken may also modify effective lake or channel surface area and hence through talik area.

Transient through taliks, which lag shifting channels (Smith, 1976), are assumed to differ insignificantly in surface area from those taliks expected to occur beneath channels in their present configuration under steady-state conditions. This assumption must be made as the delta is a highly dynamic environment. As such, a high-resolution examination of channel migration and lake evolution would be required to produce estimates of current configurations of transient through taliks.

It is assumed that all channels in the Mackenzie Delta wide enough to support through taliks (width >23.6 m and >62.6 m in forest and tundra regions respectively: 'Observed MAWT', Table 5.4) are represented by polygon features rather than line features in the CanVec GIS shapefiles. Line features were not included in analyses. Examination of the channel polygon network in a GIS does reveal channel portions beneath these critical widths, however this may not be apparent in Fig. 5.7 due to x-axis resolution.

5.8 Influence of Climate Change

Figure 5.12 illustrates Inuvik mean annual air temperature since 1926. Rates of air temperature increase for 1970–2006 at Inuvik are 1.1°C per decade for winter (Dec, Jan, Feb), 0.5°C per decade for spring (Mar, Apr, May), 0.1°C per decade for summer (Jun, Jul, Aug), and 0.6°C for autumn (Burn and Kokelj, 2009). Kanigan et al. (2008) concluded that lake bottoms may respond more slowly than subaerial ground temperatures to climate warming, as they remain covered by ice and snow during winter. The most important mechanism of thermal regime change for Mackenzie Delta water bodies may therefore be a reduction in the duration of ice cover. In the case of perched lakes, ice cover may form later in autumn as a result of increased air temperatures. Ice cover may not persist as long in spring, due to increased air temperatures and reduced late winter ice thickness resulting from delayed formation and relatively mild winter temperatures. Ice cover may be lost earlier in spring from channels and connected lakes if the timing of Mackenzie and Peel basin snowmelt results in an earlier spring flood. If lake or channel basal temperatures observed during the open-water period were to persist for an additional two weeks, at the expense of two weeks of ice cover, MAWT is estimated to increase in perched lakes, connected lakes, and channels by 0.2, 0.3, and 0.4°C, respectively, as shown in Table 5.8. If such increases were consistent among all

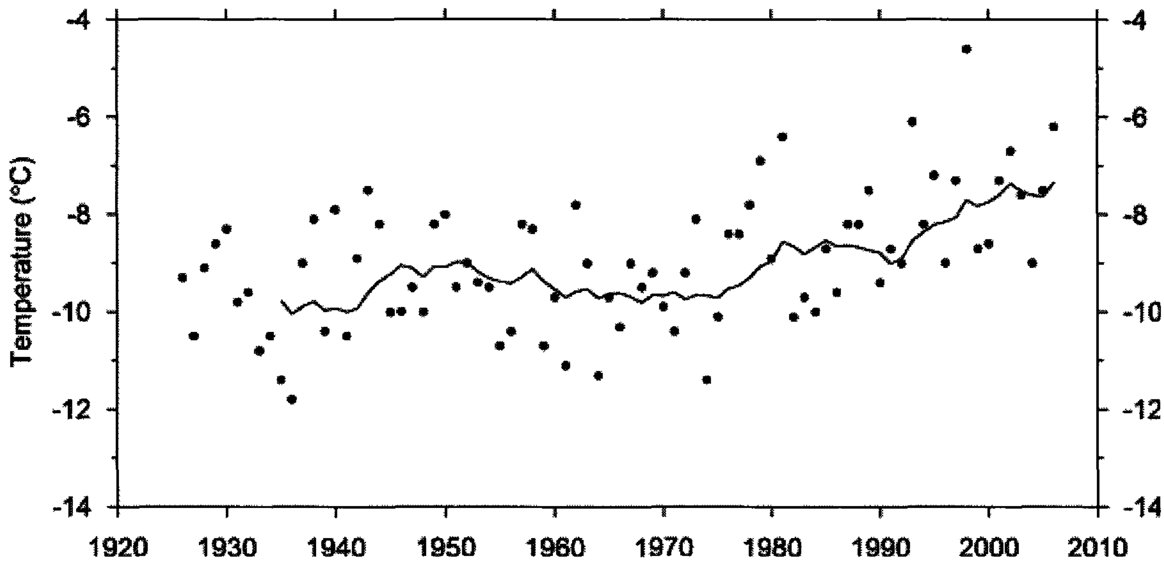

Figure 5.12. Annual mean air temperature at Inuvik, 1926–2006. Data are from Inuvik for 1957–2006 and a composite series based on data collected at Aklavik for 1926–1957. The running mean air temperature series for the previous 10 years is plotted as a line for 1935–2006. Data are from Environment Canada and are available at http://www.climate.weatheroffice.gc.ca/ climateData/canada_e.html. Figure is from Burn and Kokelj, 2009.

Table 5.8. Estimates of MAWT change resulting from a two-week extension of the open-water period (OWP), using mean basal water temperatures (MWT) for the period of ice-cover (ICP) and OWP, June 2009–June 2010, among instrumented Mackenzie Delta water bodies. ICP and OWP dates, given in italics, are determined for each water body type using the temperature series given in Figs. 5.4 and 5.5. All temperatures are given in °C. ICP and OWP length (L) are given in days (d).

Water Body Type	Obs. MAWT	ICP, OWP	MWT	Length (d)	Est. MAWT[1], ICP + 14 d	Change from Obs. MAWT
Perched Lakes	5.6	*1 Oct—26 May* *27 May—30 Sept*	2.6 11.1	239, 126	5.8	0.2
Con. Lakes	3.4	*15 Oct—26 May* *27 May—14 Oct*	-0.6 9.5	223, 142	3.7	0.3
Channels	4.6	*15 Oct—15 May* *16 May—14 Oct*	0.3 10.5	212, 153	5.0	0.4

[1] MAWT is estimated as $[(L_{ICP} - 14)*(MWT_{ICP}) + (L_{OWP} + 14)*(MWT_{OWP})] / 365$

water bodies throughout the delta and changes in MAGT are not considered, resulting equilibrium through talik count and total area are calculated as 30,826 and 4,688 km^2, respectively. These represent modest increases, as current through talik count and total area are estimated as 28,774 and 4,686 km^2, respectively, as shown in Figure 5.8. These variables are insensitive to climate change. This stems from the expectation that most climatic warming will occur in winter, when lakes will continue to develop an ice cover.

5.9 Conclusion

Estimates of MAWT based on one year of measurement may not be representative of long-term MAWT, despite the limited departure of 2009–2010 mean monthly air temperature (Fig. 3.1) and 2009 East Channel water levels (Fig. 3.2) from climate normal and mean values, respectively. The 2009–2010 study period may be less representative of long-term precipitation than temperature and water level. Available records from 2005 onward indicate the extent of MAWT variability at NRC Lake: from 5.1°C (2008) to 6.8°C (2009). The key findings of this examination of MAWT in Mackenzie Delta water bodies pertaining to spatial relations, however, are less sensitive to the length of the sampling period. Spatial variability in MAWT is low in the delta, with a difference of 0.7°C between the average MAWT of forest and tundra water bodies. MAWT in channels is nearly uniform throughout the delta. The greatest variability occurs among lakes on the basis of connectivity and ecological region. Perched lake MAWT is approximately 2.5°C greater than that of connected lakes within the forested region of the delta. While sample size is limited north of treeline, the MAWT values for the two lake types in tundra are more closely aligned.

Estimates of MAWT, based on MSWT, were 3.4°C and 4.1°C for lakes and channels, respectively, as developed in section 4.5. Average MAWT was determined as 3.4°C, 4.6°C, and 5.5°C among connected lakes, channels, and perched lakes, respectively. Connected lake and channel MAWT estimates, based on summer measurements, were therefore accurate to within 0.5°C.

Under the documented mean annual ground and water thermal regimes of the Mackenzie Delta, the size distribution of its lakes and channels suggests a total through talik area of 4,686 km^2, or 35% of the delta area. This is 95% of the delta lake area (3,518 km^2) and nearly the entire 1,360 km^2 network of channels.

CHAPTER 6: SUMMARY AND CONCLUSIONS

6.1 Summary of Results

For the 2009–2010 period, the main findings of this research are as follows:

1) Average MAWT among all studied Mackenzie Delta water bodies was 4.5°C.
2) Spatial variability in mean basal water temperature was greater during summer (7.0°C) than annually (4.0°C).
3) Average MAWT of water bodies north and south of treeline was 4.0°C and 4.7°C, respectively. There is no statistically significant difference between these groups.
4) Average MAWT among connected lakes and channels differed by no more than 1.5°C across treeline.
5) Average perched lake MAWT differed by no more than 3.0°C across treeline.
6) Average MAWTs for all perched lakes, channels, and connected lakes were 5.5°C, 4.6°C, and 3.4°C respectively. Average MAWT for all lakes was 4.5°C.
7) MAWTs differed significantly between perched and connected lakes.
8) Spatial variability in MAWT was lower among channel sites than lakes.
9) An inverse relation was apparent between channel MAWT and latitude.
10) Water bodies' temporal temperature fluctuations, including peak temperature, were closely synchronized during summer.
11) Through taliks were predicted to occur beneath 35% of the delta area. This is nearly the entire channel network, and 60% of delta lakes (95% of delta lake area).
12) MSWT of channels and connected lakes permitted MAWT estimates whose error was $\leq$0.5°C.

6.2 Conclusion

The work of Smith (1976) revealed the heterogeneous nature of permafrost, due to the abundance of through taliks, within a local study region of the delta. This research supports those findings on an extensive scale, using mean annual basal temperatures determined for Mackenzie Delta water bodies in a study period where summer air temperatures were similar to climate normals. This thesis suggests that the annual thermal regime of water bodies, which supports those talik conditions, is similar and reasonably uniform throughout the delta. The suggested prevalence and modelled configuration of through taliks reinforce the findings that Mackenzie Delta permafrost is generally less than 100 m thick (Johnston and Brown, 1965), and that its MAGTs are generally greater than those of adjacent uplands (Mackay 1974; Burgess and Smith, 2000; Burn and Kokelj, 2009). It supports the concept of an abrupt change in permafrost conditions at the interface of the delta and adjacent uplands (Brown, 1966b).

The permafrost conditions of the Mackenzie Delta, which may be characterized by lateral discontinuity due to the effects of water bodies, must be well understood prior to the implementation of resource development projects.

6.3 Future Research Opportunities

Two particularly interesting opportunities exist for further research into the thermal regime of delta water bodies. Water level, which was not monitored in this study, might be logged concurrently with basal temperature at study lakes and channels. This could yield valuable relations between the thermal regime of delta water bodies and the already well-investigated delta flood regime, and help place hydrological variability during short-term study periods in context with respect to long-term normals. Secondly, the examination of winter imagery from spaceborne radar systems may yield estimates of the number of lakes with and without bottom-fast ice (Duguay and Lafleur, 2003). Relations between the winter thermal regime of instrumented lakes and the nature of their ice depth suggested by radar images could enable improved MAWT predictions for imaged, uninstrumented lakes. It may also help determine more representative mean annual surface geometries to be associated with MAWT values, given bathymetry-imposed wintertime reductions in unfrozen lake area due to drawdown and thick ice cover.

REFERENCES

Allen DM, Michel FA, Judge AS. 1988. The permafrost regime in the Mackenzie Delta, Beaufort Sea region, N.W.T. and its significance to the reconstruction of the palaeoclimatic history. Journal of Quaternary Science 3: 3–13.

Bigras SC. 1990. Hydrological regime of lakes in the Mackenzie Delta, Northwest Territories, Canada. Arctic and Alpine Research 22: 163–174.

Brewer MC. 1958. The thermal regime of an Arctic lake. Transactions, American Geophysical Union, 39: 278–284.

Brosten TR, Bradford JH, McNamara JP, Zarnetske JP, Gooseff MN, Bowden WB. 2006. Profiles of temporal thaw depths beneath two Arctic stream types using ground-penetrating radar. Permafrost and Periglacial Processes 17: 341–355.

Brown WG, Johnson GH, Brown RJE. 1964. Comparison of observed and calculated ground temperatures with permafrost distribution under a northern lake. Canadian Geotechnical Journal 1: 147–154.

Brown RJE. 1966a. Relation between mean annual air and ground temperatures in the permafrost region of Canada. In Proceedings: Permafrost International Conference. National Academy of Sciences-National Research Council: Washington, DC; 241–246.

Brown RJE. 1966b. Occurrence of permafrost at an Arctic lake. Nature 211: 952–953.

Burgess MM, Smith SL. 2000. Shallow ground temperatures. In The Physical Environment of the Mackenzie Valley, Northwest Territories: a Base Line for the Assessment of Environmental Change, Dyke LD, Brooks GR (eds). Geological Survey of Canada, Bulletin 547, p. 89–103

Burn CR. 1995. The hydrologic regime of Mackenzie River and connection of ''no-closure'' lakes to distributary channels in the Mackenzie Delta, Northwest Territories. Canadian Journal of Earth Sciences 32: 926–937.

Burn CR. 2002. Tundra lakes and permafrost, Richards Island, western Arctic coast, Canada. Canadian Journal of Earth Sciences 39: 1281–1298.

Burn CR. 2003. Lake-bottom thermal regime in thermokarst terrain near Mayo, Yukon Territory, Canada. In Proceedings, 9th International Conference on Permafrost, June 29- July 3, 2008 Fairbanks Alaska, Vol. 1: Kane DL, Hinkel KM (eds). Institute of Northern Engineering, University of Alaska Fairbanks: Fairbanks, AK; 113–118.

Burn CR. 2005. Lake-bottom thermal regimes, western Arctic coast, Canada. Permafrost and Periglacial Processes 16: 355–367.

Burn CR, Kokelj SV. 2009. The environment and permafrost of the Mackenzie Delta area. Permafrost and Periglacial Processes 20: 83–105.

Burn CR, Parameswaran VR, Kutny L, Boyle L. 1998. Electrical potentials measured during growth of lake ice, Mackenzie delta area, N.W.T., Canada. In Proceedings of the 7th International Conference on Permafrost, Yellowknife, N.W.T., 23-27 June 1998, Lewkowicz AG, Allard M (eds). Université Laval: Québec, Nordicanna 57; 101–106.

Cott, PA. 2007. Fisheries related impacts of water withdrawal from ice-covered lakes. M.Sc. Thesis, University of Guelph.

Caissie D. 2006. The thermal regime of rivers: a review. Freshwater Biol. 51: 1389–1406.

Duguay CR, Lafleur PM. 2003. Determining depth and ice thickness of shallow sub-Arctic lakes using space-borne optical and SAR data. International Journal of Remote Sensing 24: 475-489.

Duk-Rodkin A, Lemmen DS. 2000. Glacial history of the Mackenzie region. In The Physical Environment of the Mackenzie Valley, Northwest Territories: a Base Line for the Assessment of Environmental Change, Dyke LD, Brooks GR (eds). Geological Survey of Canada, Bulletin 547, p. 11–20.

Dyke LD. 2000. Shoreline permafrost along the Mackenzie River. In The Physical Environment of the Mackenzie Valley, Northwest Territories: A Base Line for the Assessment of Environmental Change, Bulletin 547, Dyke LD, Brooks GR (eds). Geological Survey of Canada: Ottawa; 143–151.

Ebdon D. 1985. Statistics in geography: second edition. Blackwell, New York.

Emmerton CA, Lesack LFW, Marsh P. 2007. Lake abundance, potential water storage, and habitat distribution in the Mackenzie delta, western Canadian Arctic. Water Resources Research 43:14 pp.

Environment Canada. National Climate Data and Information Archive. 2009. http://www.climate.weatheroffice.ec.gc.ca/climateData/canada_e.html

Environmental Systems Research Institute. 2008. ArcScripts – Minimum Bounding Rectangle (MBR) Analysis tools. http://arcscripts.esri.com/details.asp?dbid=15502

Fee EJ, Hecky RE, Guildford SJ, Anema C, Mathew D, Hallard K. 1988. Phytoplankton primary production and related limnological data for lakes and channels in the Mackenzie Delta and lakes on the Tuktoyaktuk Peninsula, N.W.T. Canadian Technical Report of Fisheries and Aquatic Sciences 1614, 62 pp.

Gill D. 1972. The point-bar environment in the Mackenzie Delta. Canadian Journal of Earth Sciences 9: 1382-1393.

Goulding HL, Prowse TD, Beltaos S. 2009. Spatial and temporal patterns of break-up and ice-jam flooding in the Mackenzie Delta, NWT. Hydrological Processes 23: 2654–2670.

Johnston GH, Brown RJE. 1964. Some observations on permafrost distribution at a lake in the Mackenzie Delta, N.W.T., Canada. Arctic 17: 163-175.

Johnston GH, Brown RJE. 1965. Stratigraphy of the Mackenzie River Delta, Northwest Territories, Canada. Geological Society of America Bulletin 76: 103–112.

Kanigan JCN, Burn CR, Kokelj SV. 2008. Permafrost response to climate warming south of treeline, Mackenzie delta, Northwest Territories, Canada. In Proceedings, 9th International Conference on Permafrost, June 29- July 3, 2008 Fairbanks Alaska, Vol. 1: Kane DL, Hinkel KM (eds). Institute of Northern Engineering, University of Alaska Fairbanks: Fairbanks, AK; 901–908.

Kanigan JCN, Burn CR, Kokelj SV. 2009. Ground temperatures in permafrost south of treeline, Mackenzie delta, Northwest Territories. Permafrost and Periglacial Processes 20: 127–139.

Kokelj SV, Burn CR. 2005. Near-surface ground ice in sediments of the Mackenzie Delta, Northwest Territories, Canada. Permafrost and Periglacial Processes 16: 291–303.

Kokelj SV, Lantz TC, Kanigan J, Smith SL, Coutts R. 2009. Origin and polycyclic behaviour of tundra thaw slumps, Mackenzie Delta region, Northwest Territories, Canada. Permafrost and Periglacial Processes 20 (2): 173–184.

Lachenbruch AH. 1957. Three-dimensional Heat Conduction Beneath Heated Buildings. U.S. Geological Survey Bulletin 1052-B. U.S. Geological Survey.

Lachenbruch A, Brewer MC, Greene GW, Marshall BV. 1962. Temperature in permafrost. In Temperature: Its Measurement and Control in Science and Industry, Vol. 3. Reinhold Publishing Company, New York, 791–803.

Lesack, LFW, Marsh P, Hecky RE. 1998. Spatial and temporal dynamics of major solute chemistry among Mackenzie Delta lakes. Limnology and Oceanography 43: 1530–1543.

Mackay JR. 1963. The Mackenzie delta area, N.W.T. Department of Mines and Technical Surveys, Geographical Branch, Memoir 8.

Mackay JR. 1967. Permafrost depths, Lower Mackenzie Valley, Northwest Territories. Arctic 20: 21–26.

Mackay JR. 1970. Disturbances to the tundra and forest tundra of the western Arctic. Canadian Geotechnical Journal 7: 420–432.

Mackay JR. 1974. Seismic shot holes and ground temperatures, Mackenzie delta area, Northwest Territories. In Report of Activities, Part A, Paper 74-1A. Geological Survey of Canada: Ottawa; 389–390.

Mackay JR. 1992. Lake stability in an ice-rich permafrost environment: examples from the western Arctic coast. In Aquatic Ecosystems in Semi-Arid Regions: Implications for Resource Management. Robarts RD, Bothwell ML (eds). National Hydrology Research Institute Series 7, Environment Canada, Saskatoon.

Mackay JR. 1997. A full-scale field experiment (1978-1995) on the growth of permafrost by means of lake drainage, western Arctic coast: a discussion of the method and some results. Canadian Journal of Earth Sciences 34: 17–33.

Mackenzie River Basin Committee. 1981. Mackenzie River Basin Study Report. Governments of Alberta, British Columbia, Saskatchewan, and Canada, Ottawa, Ontario. 201 pp.

Marsh P. 1998. Lakes and water in the Mackenzie Delta. Scientific Report No. 6, Aurora Research Institute, Inuvik, NWT. 12 pp.

Marsh P, Bigras SC. 1988. Evaporation from Mackenzie delta lakes, N.W.T., Canada. Arctic and Alpine Research 20: 220–229.

Marsh P, Hey M. 1989. The flooding hydrology of Mackenzie Delta lakes near Inuvik, N.W.T., Canada. Arctic 42: 41–49.

Marsh P, Lesack LFW. 1996. The hydrologic regime of perched lakes in the Mackenzie Delta: potential responses to climate change. Limnology and Oceanography 41: 849–856.

Marsh P, Schmidt T. 1993. Influence of a Beaufort Sea storm surge on channel levels in the Mackenzie Delta. Arctic 46: 35–41.

Natural Resources Canada. 2009. GeoGratis Download Directory. http://geogratis.cgdi.gc.ca/geogratis/en/download/topographic.html

Nguyen T-N, Burn CR, King DJ, Smith SL. 2009. Estimating the extent of near-surface permafrost using remote sensing, Mackenzie delta, Northwest Territories. Permafrost and Periglacial Processes 20: 141–153.

Pelletier, BR (editor). 1987. Marine Science Atlas of the Beaufort Sea: Geology and Geophysics. Geological Survey of Canada Miscellaneous Report 40.

Permafrost Subcommittee, Associate Committee on Geotechnical Research. 1988. Glossary of Permafrost and Related Ground-Ice Terms. National Research Council of Canada.

Ritchie JC. 1985. Late-Quaternary climatic and vegetational change in the Lower Mackenzie Basin, northwest Canada. Ecology 66: 612–621.

Smith MW. 1975. Microclimatic influences on ground temperatures and permafrost distribution, Mackenzie Delta, Northwest Territories. Canadian Journal of Earth Sciences 12: 1421–1438.

Smith MW. 1976. Permafrost in the Mackenzie Delta, Northwest Territories, Paper 75–28. Geological Survey of Canada: Ottawa.

Smith SL, Burgess MM. 2002. A digital database of permafrost thickness in Canada, Geological Survey of Canada Open File 4173.

Squires MM, Lesack LFW, Huebert D. 2002. The influence of water transparency on the distribution and abundance of macrophytes among lakes of the Mackenzie Delta, western Canadian Arctic. Freshwater Biology 47: 2123–2135.

Squires MM, Lesack LFW, Hecky RE, Guildford SJ, Ramlal P, Higgins SN. 2009. Primary production and carbon dioxide metabolic balance of a lake-rich Arctic river floodplain: partitioning of phytoplankton, epipelon, macrophyte, and epiphyton production among lakes on the Mackenzie Delta. Ecosystems 12: 853–872.

Triola MF, Goodman WM, Law R. 1999. Elementary Statistics: First Canadian Edition. Addison-Wesley.

Water Survey of Canada. 2009. http://www.wsc.ec.gc.ca/hydat/H2O/index_e.cfm

Webb BW, Hannah DM, Moore RD, Brown LE, Nobilis F. 2008. Recent advances in stream and river temperature research. Hydrological Processes 22: 902–918.

Welch HE, Bergmann MA. 1985. Water circulation in small Arctic lakes in winter. Canadian Journal of Fisheries and Aquatic Sciences 42: 506–520.

Werenskiold W. 1953. The extent of frozen ground under the sea bottom and glacier beds. Journal of Glaciology 2: 197–200.

Williams PJ. 1968. Ice distribution in permafrost profiles. Canadian Journal of Earth Sciences 5: 1381-1386.

Williams PJ, Smith MW. 1989. The Frozen Earth: Fundamentals of Geocryology. Cambridge University Press.

APPENDIX A: THERMISTOR CALIBRATION

T = If *R*<2252, 99.99;
If *R*<2814, *B*/((LOG(*R*/2252)+*B*/298.15)) -273.15;
If *R*<3539, *B*/((LOG(*R*/2814)+*B*/293.15)) -273.15;
If *R*<4483, *B*/((LOG(*R* /3539)+*B*/288.15)) -273.15;
If *R*<5720, *B*/((LOG(*R*/4483)+*B*/283.15)) -273.15;
If *R*<7355, *B*/((LOG(*R*/5720)+*B*/278.15)) -273.15;
If *R*<9533, *B*/((LOG(*R*/7355)+*B*/273.15)) -273.15;
Else, 99.99

where:

T = water temperature (°C) obtained using thermistor cable and multimeter;

R = adjusted thermistor reading (Ω);

B = If *R*<2252, 99.99;
If *R*<2814, (LOG(2252/2814))/((1/298.15)-(1/293.15));
If *R*<3539, (LOG(2814/3539))/((1/293.15)-(1/288.15));
If *R*<4483, (LOG(3539/4483))/((1/288.15)-(1/283.15));
If *R*<5720, (LOG(4483/5720))/((1/283.15)-(1/278.15));
If *R*<7355, (LOG(5720/7355))/((1/278.15)-(1/273.15));
If *R*<9533, (LOG(7355/9533))/((1/273.15)-(1/268.15));
Else, 99.99

APPENDIX B: VERIFICATION OF TEMPERATURE LOGGER CALIBRATION

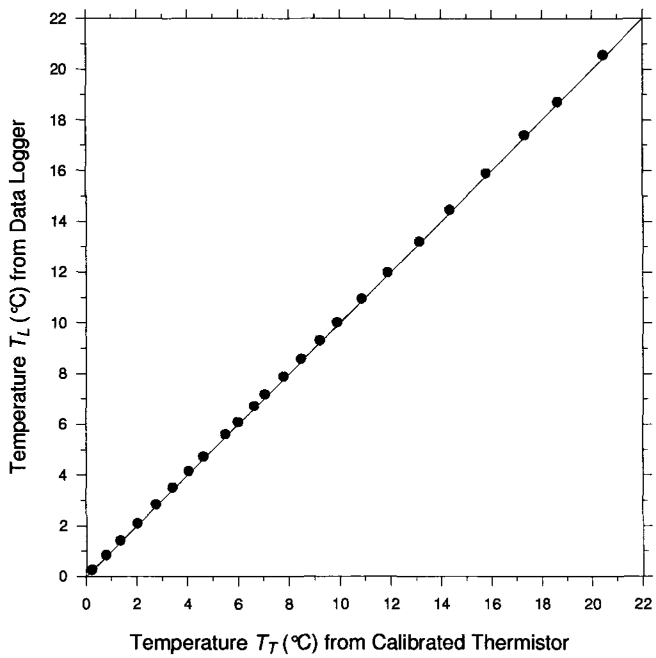

Figure B-1. Relation between standard temperature T_T and measurements by Lake 1 data logger in laboratory ice bath.

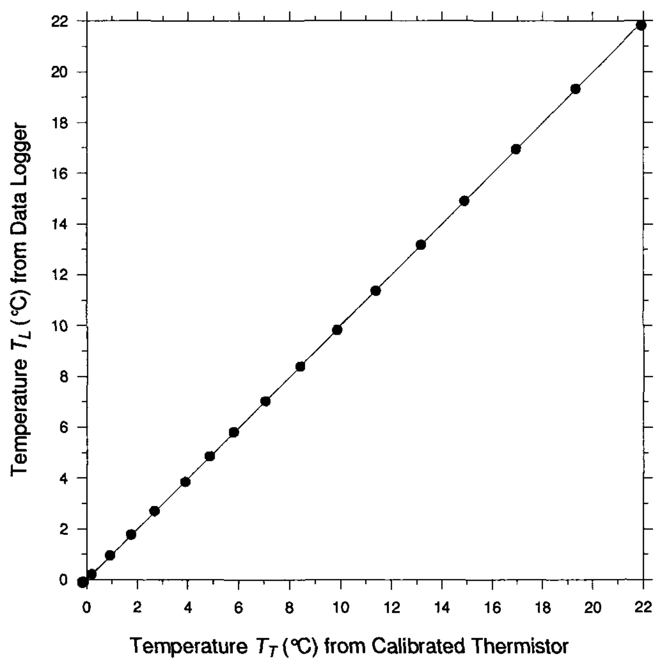

Figure B-2. Relation between standard temperature T_T and measurements by Lake 2 data logger in laboratory ice bath.

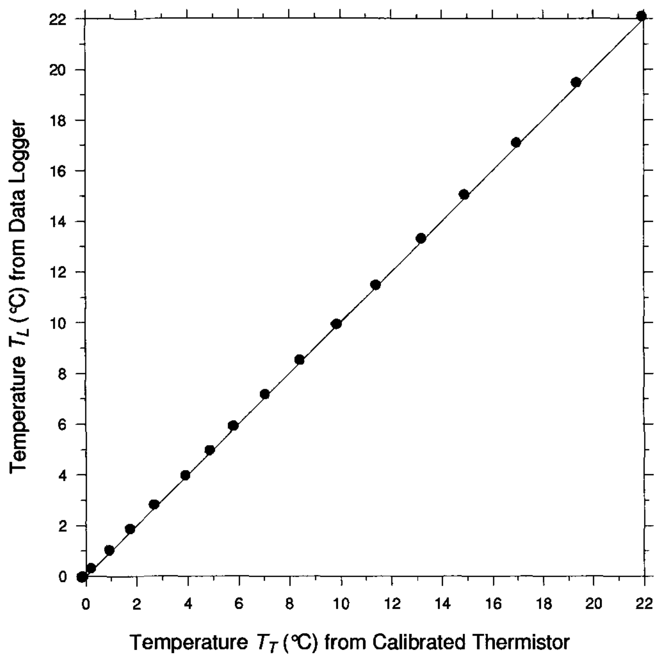

Figure B-3. Relation between standard temperature T_T and measurements by Lake 4 (Myers) data logger in laboratory ice bath.

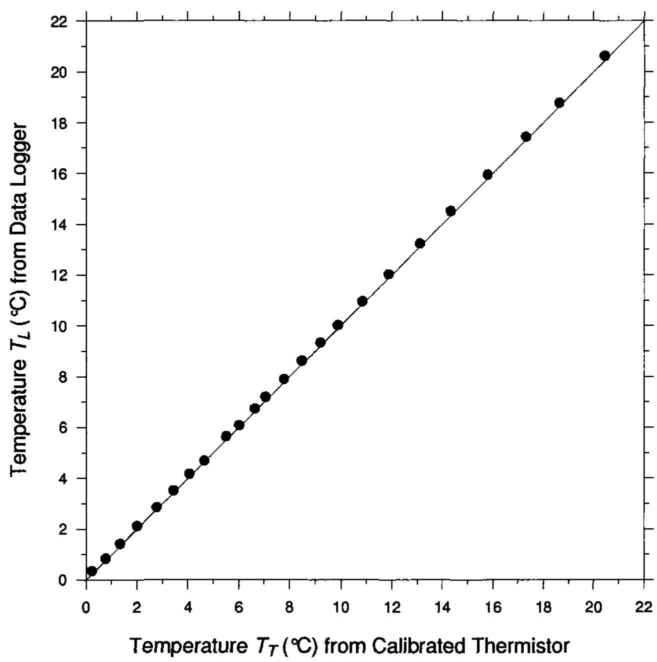

Figure B-4. Relation between standard temperature T_T and measurements by Lake 5 (South) data logger in laboratory ice bath.

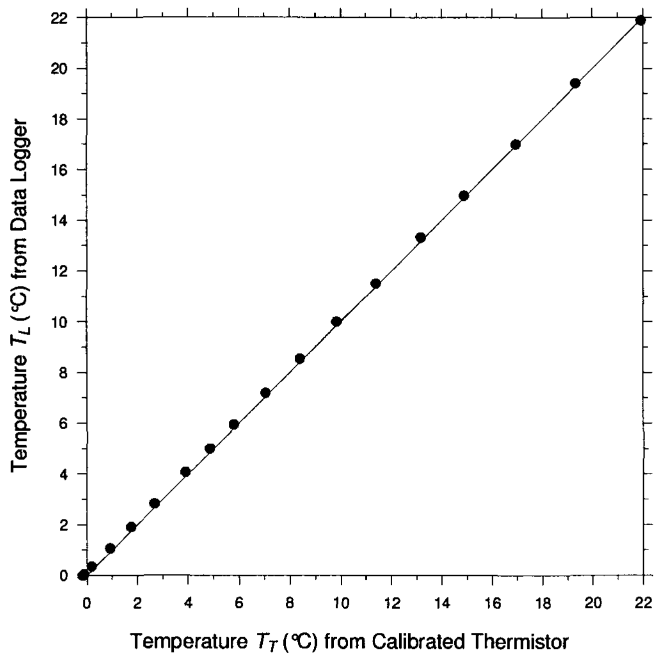

Figure B-5. Relation between standard temperature T_T and measurements by Lake 6 data logger in laboratory ice bath.

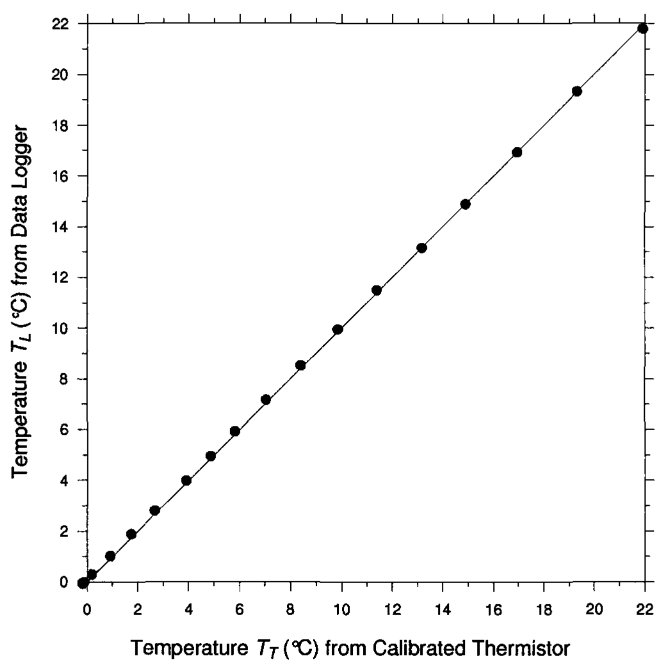

Figure B-6. Relation between standard temperature T_T and measurements by Lake 7 data logger in laboratory ice bath.

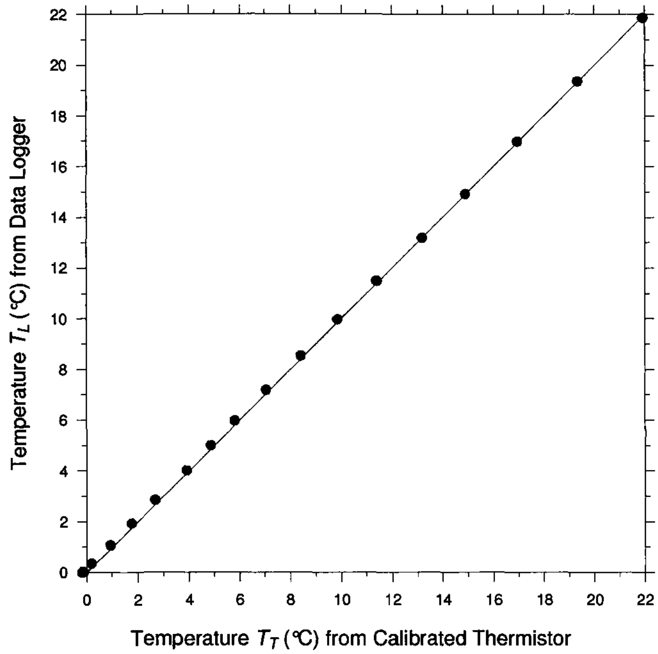

Figure B-7. Relation between standard temperature T_T and measurements by Lake 9 data logger in laboratory ice bath.

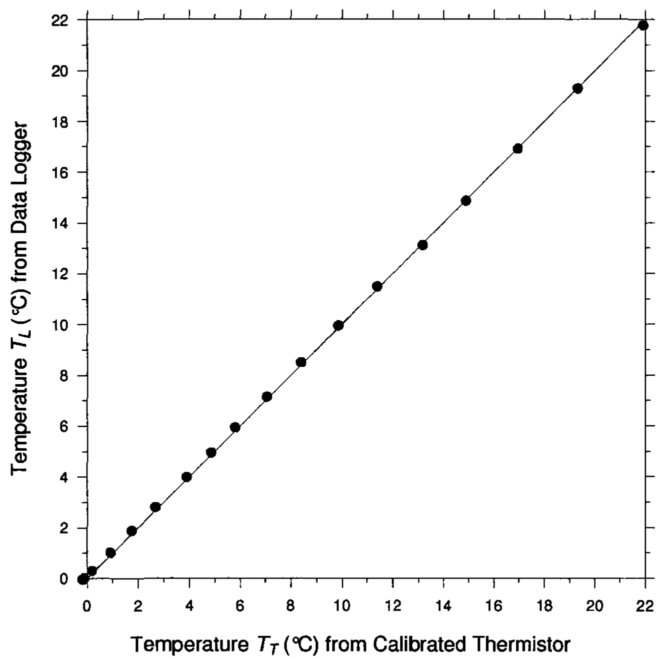

Figure B-8. Relation between standard temperature T_T and measurements by Lake 10 data logger in laboratory ice bath.

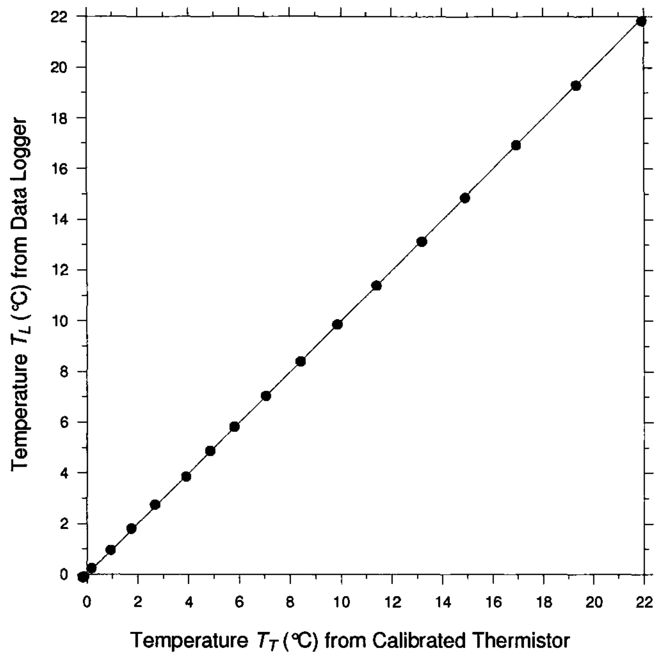

Figure B-9. Relation between standard temperature T_T and measurements by Lake 11 data logger in laboratory ice bath.

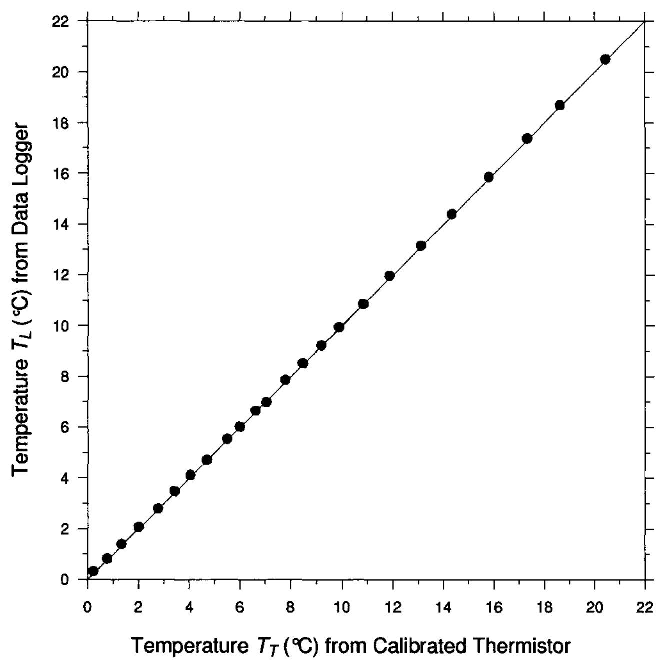

Figure B-10. Relation between standard temperature T_T and measurements by Lake 12 data logger in laboratory ice bath

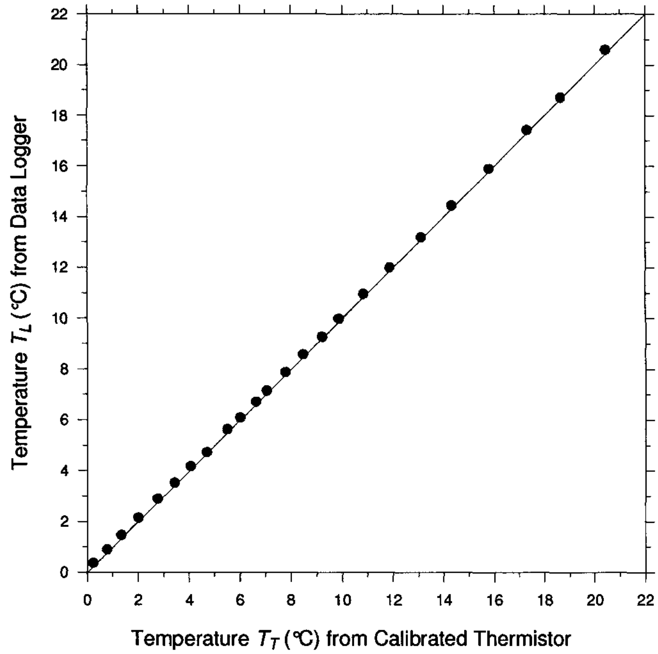

Figure B-11. Relation between standard temperature T_T and measurements by Lake 14 data logger in laboratory ice bath.

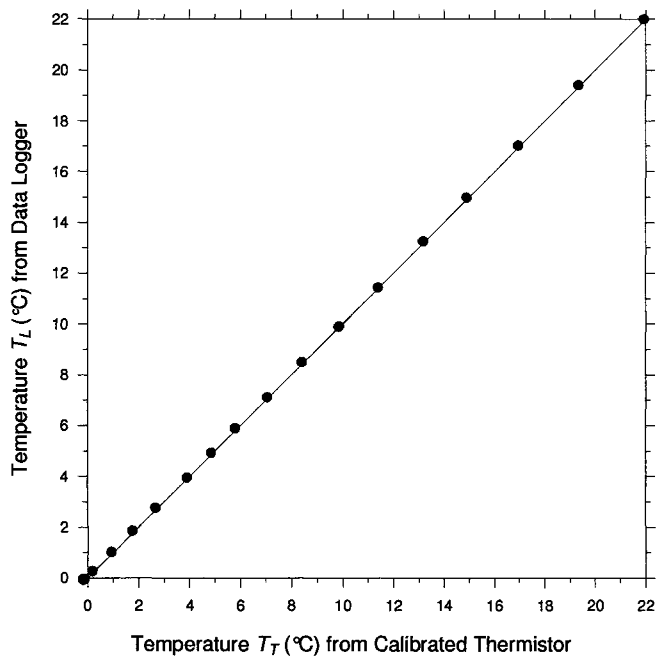

Figure B-12. Relation between standard temperature T_T and measurements by Lake 15 data logger in laboratory ice bath.

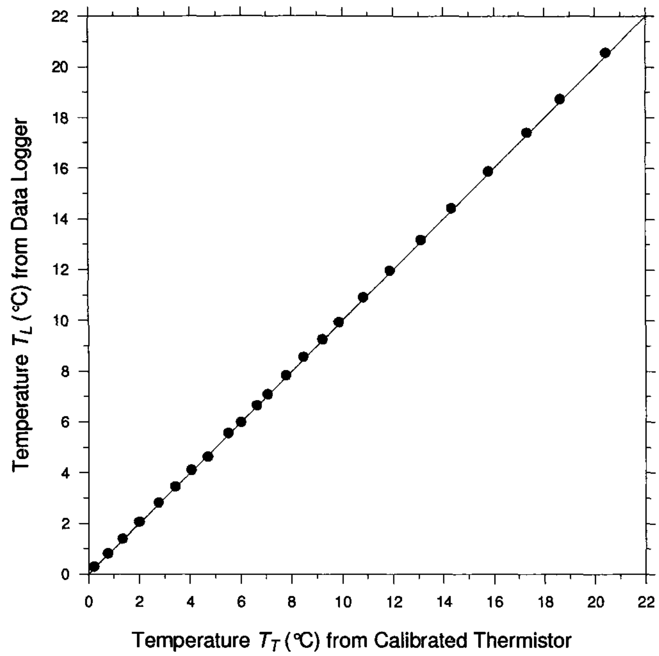

Figure B-13. Relation between standard temperature T_T and measurements by Lake 16 data logger in laboratory ice bath.

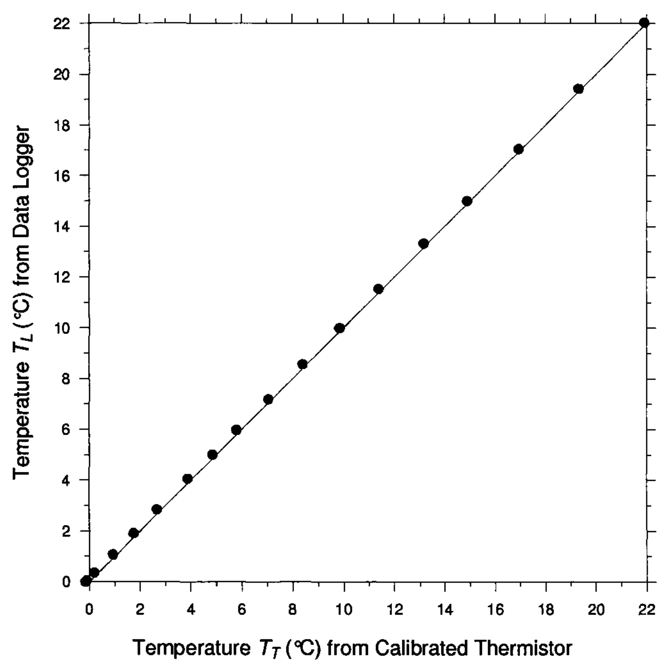

Figure B-14. Relation between standard temperature T_T and measurements by Channel E data logger in laboratory ice bath.

APPENDIX C: STATISTICAL TESTS

C-1: MAWT Across Treeline

a) b)

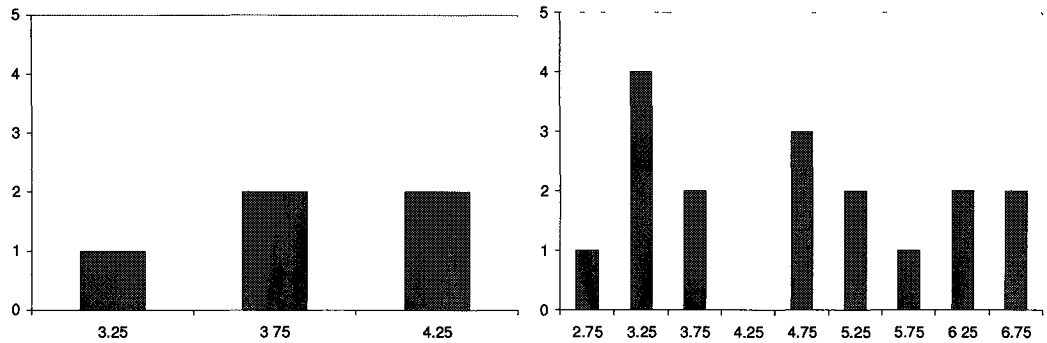

Figure C-1. Histograms of MAWT among water bodies in (a) tundra and (b) forest regions of the Mackenzie Delta. Sample sizes for (a) and (b) are 5 and 17, respectively. Values on x-axes (°C) are central values of 0.5°C temperature ranges.

As shown in Fig. C-1, the distribution of measured MAWT for water bodies in the forested region of the Mackenzie Delta is not normal. Nonparametric methods are thus required for testing hypotheses about MAWT differences between these two groups.

Table C-1. Mann-Whitney Test Statistics (Ebdon, 1985)

Forest (y) Tundra (x)	MAWT (°C)	Rank (r_y or r_x^*)
y	6.807	22
y	6.544	21
y	6.417	20
y	6.280	19
y	5.792	18
y	5.449	17
y	5.229	16
y	4.807	15
y	4.601	14
y	4.573	13
x	4.459	12*
x	4.346	11*
y	3.945	10
x	3.909	9*
y	3.861	8
x	3.574	7*
x	3.464	6*
y	3.450	5
y	3.314	4
y	3.070	3
y	3.054	2
y	2.797	1

$n_x = 5$

$n_y = 17$

$\sum r_y = 208$

$\sum r_x = 45$

$U_x = n_x n_y + ((n_x(n_x + 1))/2 - \sum r_x$

$= 55$

$U_y = n_x n_y + ((n_y(n_y + 1))/2 - \sum r_y$

$= 30$

$U_{crit} = 20$ (when $n_x = 5$, $n_y = 17$)

C-2: MAWT Between Channels and Lakes

a) b)

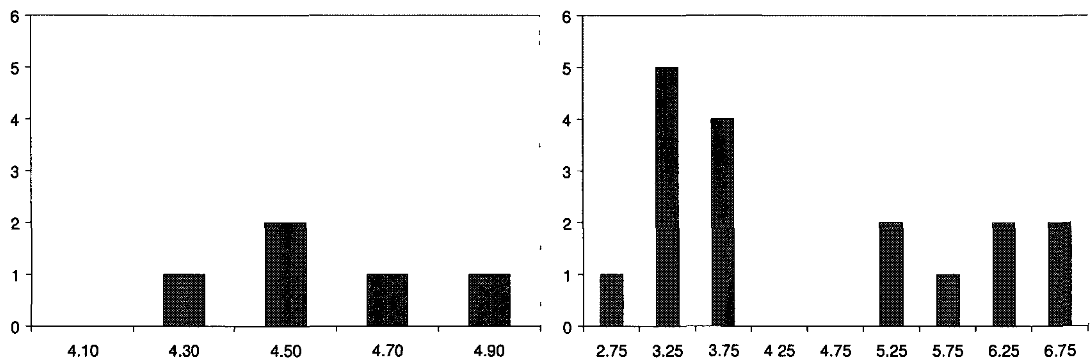

Figure C-2. Histograms of MAWT among (a) channels and (b) lakes in the Mackenzie Delta. Sample sizes for (a) and (b) are 5 and 17, respectively. Values on x-axes (°C) are central values of temperature ranges. These ranges are 0.2°C and 0.5°C for channels and lakes, respectively.

As shown in Fig. C-2, the distribution of measured MAWT for lakes in the Mackenzie Delta is not normal. Nonparametric methods are thus required for the testing of hypotheses about MAWT differences between these two groups. Nonparametric methods should also be used if statements are to be made about the statistical significance of the difference between the two groups' variances.

C-3: MAWT Between Perched and Connected Lakes

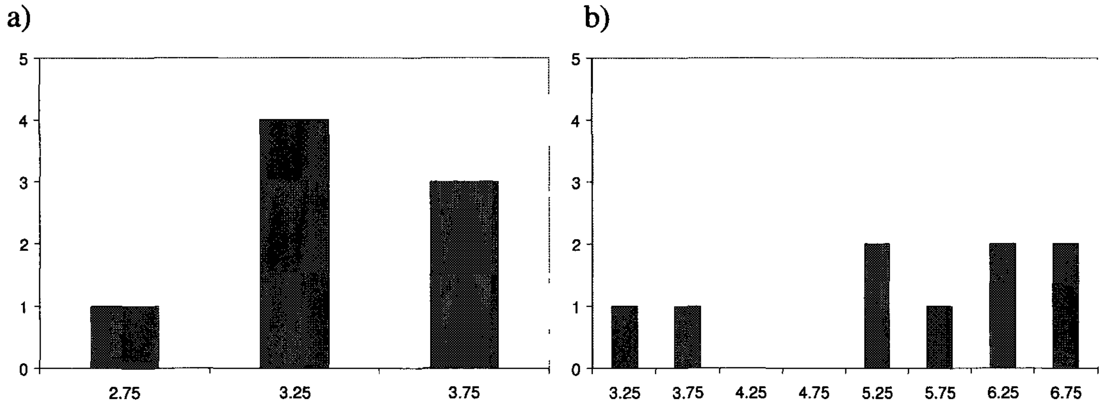

Figure C-3. Histograms of MAWT among (a) connected and (b) perched lakes in the Mackenzie Delta. Samples sizes for (a) and (b) are 8 and 9, respectively. Values on x-axes (°C) are central values of 0.5°C temperature ranges. Note that lowest and second-lowest MAWT values among perched lakes belong to Lakes 15 and 7, respectively.

As shown in Fig. C-3, the distribution of measured MAWT for perched lakes in the Mackenzie Delta is not normal. Nonparametric methods are thus required for the testing of hypotheses about MAWT differences between these two groups.

APPENDIX D: SCENARIOS FOR STEADY-STATE GROUND TEMPERATURE FIELD

Scenario 1: Perched Lake in CSF Vegetation Community

Shown as Fig. 5.9 in section 5.7.

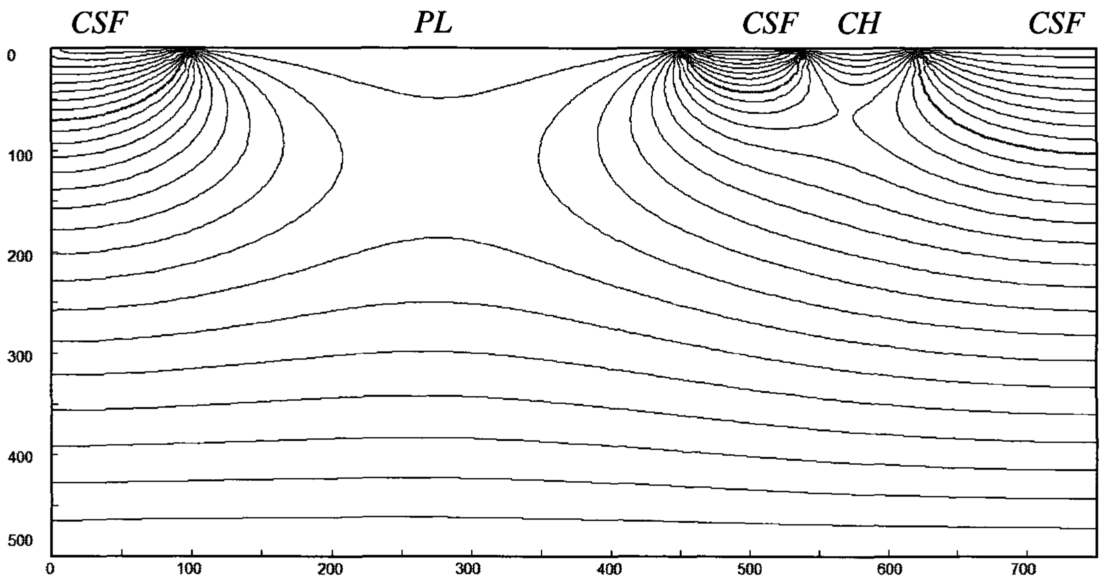

Figure D-1. Scenario 1 – Temp/W© output showing predicted ground temperature field beneath perched lake *PL* (MAWT 5.6°C) and channel *CH* (MAWT 4.5°C) in a closed spruce feathermoss *CSF* environment (MAGT = -4.4°C). Depth and distance (m) are shown on left and bottom axes, respectively. Bold isolines indicate 0°C.

Scenario 2: Connected Lake in CSF Vegetation Community

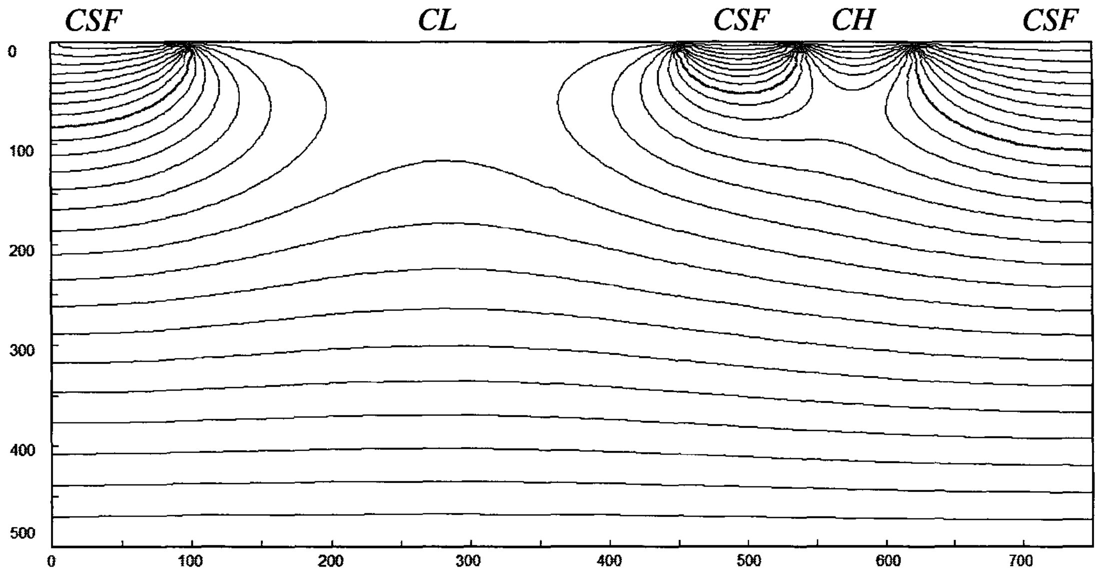

Figure D-2. Scenario 2 – Temp/W© output showing predicted ground temperature field beneath connected lake *CL* (MAWT 3.4°C) and channel *CH* (MAWT 4.5°C) in a closed spruce feathermoss *CSF* environment (MAGT = -4.4°C). Depth and distance (m) are shown on left and bottom axes, respectively. Bold isolines indicate 0°C.

Scenario 3: Perched Lake in SCL Vegetation Community

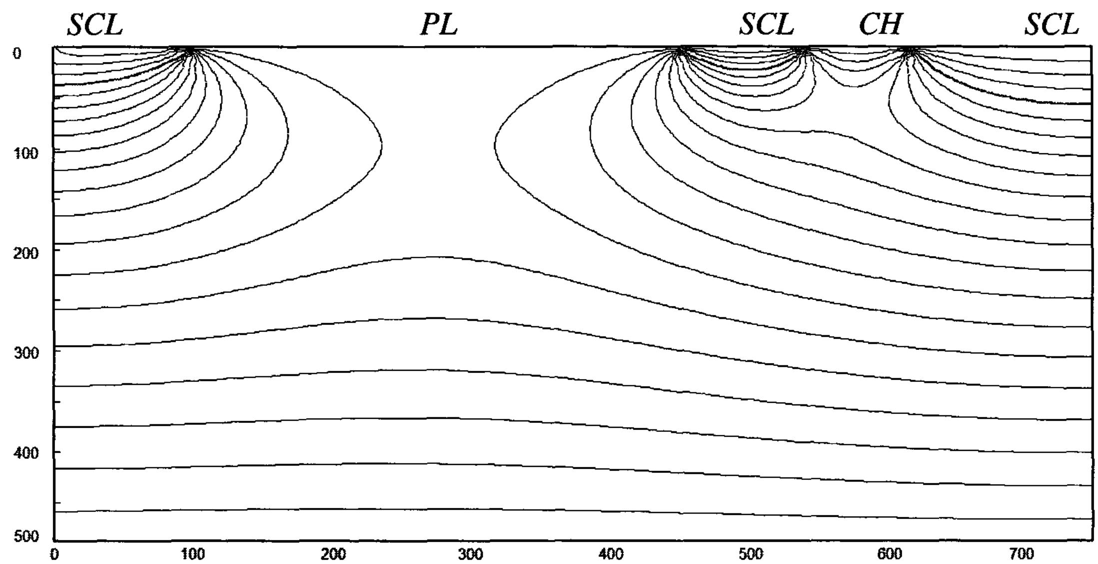

Figure D-3. Scenario 3 – Temp/W© output showing predicted ground temperature field beneath perched lake *PL* (MAWT 5.6°C) and channel *CH* (MAWT 4.5°C) in an open-canopy spruce/crowberry-lichen *SCL* environment (MAGT = -2°C). Depth and distance (m) are shown on left and bottom axes, respectively. Bold isolines indicate 0°C.

Scenario 4: Connected Lake in SCL Vegetation Community

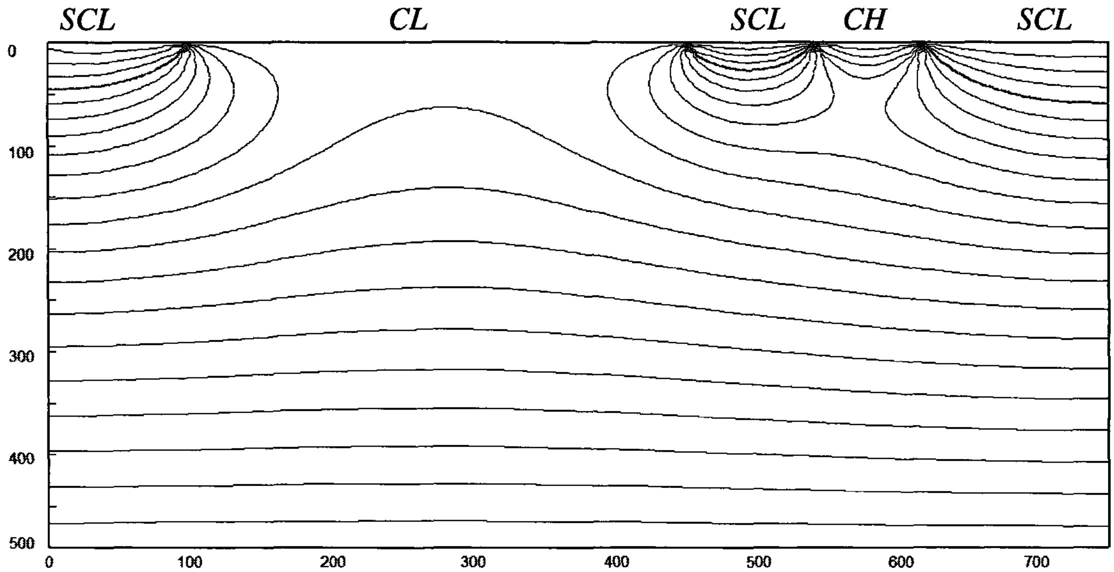

Figure D-4. Scenario 4 – Temp/W© output showing predicted ground temperature field beneath connected lake *CL* (MAWT 3.4°C) and channel *CH* (MAWT 4.5°C) in an open-canopy spruce/crowberry-lichen *SCL* environment (MAGT = -2°C). Depth and distance (m) are shown on left and bottom axes, respectively. Bold isolines indicate 0°C.

Scenario 5: Perched Lake in Southern Delta Environment -- 1

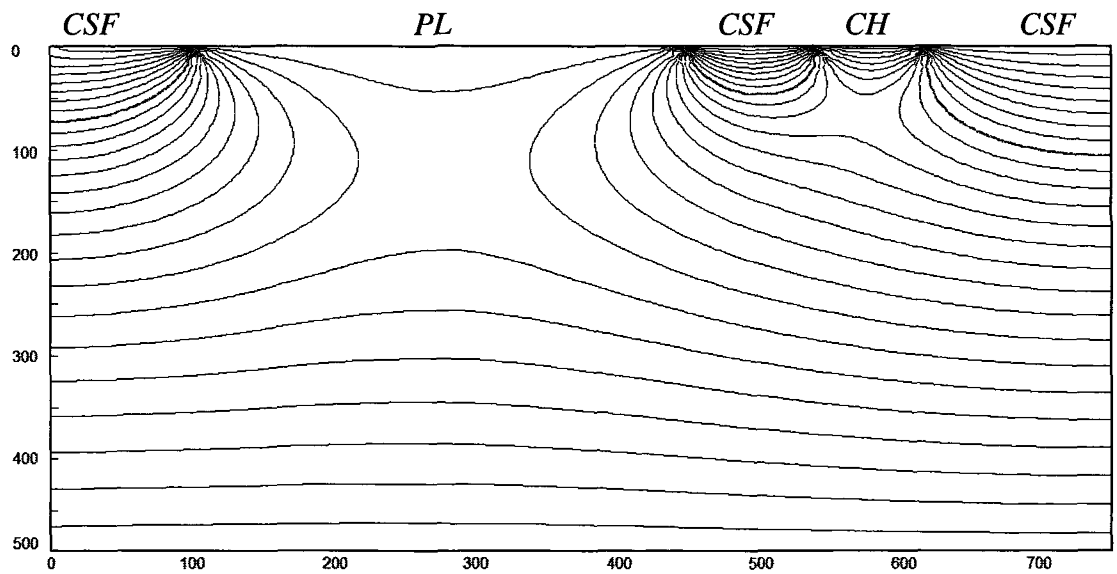

Figure D-5. Scenario 5 – Temp/W© output showing predicted ground temperature field beneath perched lake *PL* (MAWT 5.6°C) and channel *CH* of MAWT expected for the southern Mackenzie Delta (4.7°C), in a *CSF* environment (MAGT = -4.4°C). Depth and distance (m) are shown on left and bottom axes, respectively. Bold isolines indicate 0°C.

Scenario 6: Perched Lake in Southern Delta Environment – 2

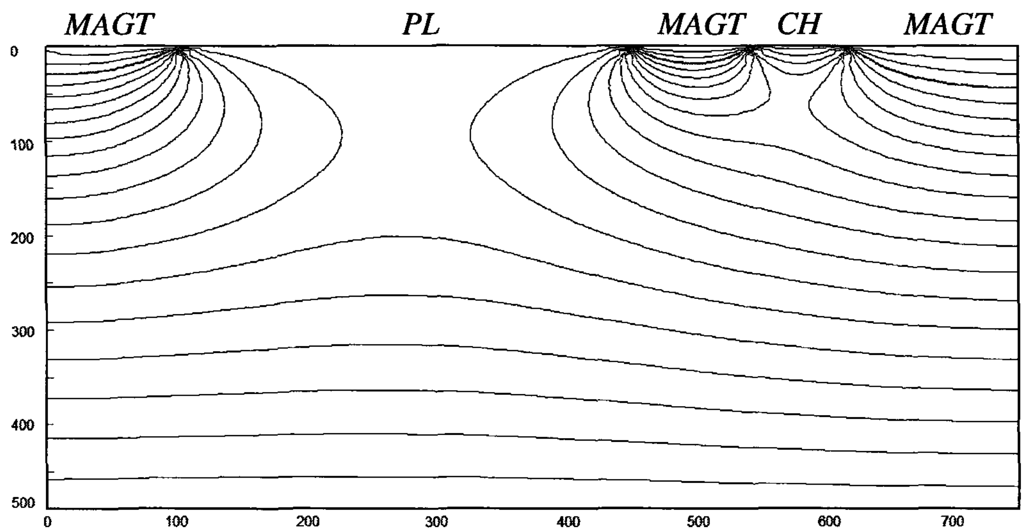

Figure D-6. Scenario 6 – Temp/W© output showing predicted ground temperature field beneath perched lake *PL* (MAWT 5.6°C), where mean annual basal temperature for channel *CH* and mean annual ground temperature are those expected for the southern Mackenzie Delta (4.7°C and -1.5°C , respectively). Depth and distance (m) are shown on left and bottom axes, respectively. Bold isolines indicate 0°C.

Scenario 7: Connected Lake in Northern Delta Environment

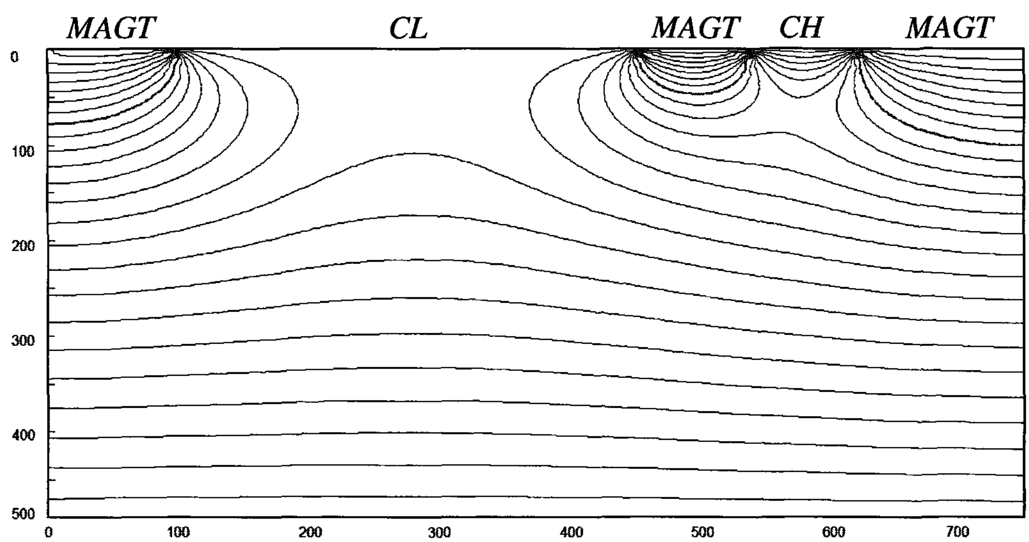

Figure D-7. Scenario 7 – Temp/W© output showing predicted ground temperature field beneath connected lake *CL* (MAWT 5.6°C), where mean annual basal temperature for channel *CH* and mean annual ground temperature are those expected for the northern Mackenzie Delta (4.3°C and -4.0°C , respectively). Depth and distance (m) are shown on left and bottom axes, respectively. Bold isolines indicate 0°C.